Politecnico di Torino

Politecnico di Torino

Master's Degree
in Aerospace Engineering

April 2026

Impact of Input Uncertainties on Thermo-elastic Performance Parameters

Supervisors:
Prof. Alfonso PAGANI

Candidate:
Emanuele LAGORIO

Company Supervisors:
Eng. Savino DE PALO
Eng. Vincenzo MARESCHI

Abstract

This thesis focuses on the implementation and application of ESA's Thermo-Elastic Verification (TEV) software for the thermo-elastic analysis of satellite structures, with particular emphasis on the assessment of a space telescope's performance parameters through uncertainty propagation. The objective of the study is to identify the design parameters that have the greatest impact on system performance and, consequently, to determine the most critical uncertainties affecting the overall satellite performance.

A coupled thermal-structural approach is used to perform the thermo-elastic analysis. ESATAN-TMS, which calculates the temperature fields using the lumped parameter method, is first used to analyze the system's thermal behavior. The pySinas tool is then used to map these temperature fields onto a structural finite element model created in NASTRAN. This allows for the evaluation of thermo-elastic responses, which are here meant to be the performance parameters pertinent to the space telescope.

The process of propagating uncertainty involves defining a set of important design variables for which tabulated uncertainties are taken into account. Each design variable is perturbed by taking into account an upper and a lower bound around the nominal value using the Univariate Reduced Quadrature (URQ) approach. This allows the impact of individual uncertainties on the thermo-elastic performance parameters to be evaluated. The SIMULIA Isight software automates the thermo-elastic analysis process, enabling the execution of all necessary analysis runs and the methodical evaluation of each uncertainty's effect on system performance.

The findings support the identification of the most important design parameters and contribute to a more reliable and knowledgeable satellite design process by offering a quantitative assessment of the sensitivity of the telescope performance to thermal–structural uncertainties.

Contents

List of Figures

Acronyms

ACD Analysis Case Data.

AOT One At a Time.

BDF Bulk data file.

CPPT Centre-Point Prescribed Temperature Method.

CTE Coefficient of Thermal Expansion.

DOE Design of Experiments.

ECSS European Cooperation for Space Standardization.

ESA European Space Agency.

ESTEC European Space Research and Technology Centre.

FE Finite Element.

FEM Finite Element Method.

GGM geometric mathematical mode.

GI Geometrical Interpolation Method.

GRID Grid point.

GUI Graphical User Interface.

LPM Lumped Parameter Method.

MLI Multilayer Insulation.

MPC Multi-point constraints.

PAT Prescribed Average Temperature Method.

PDF Probability density function.

PEM Rosenblueth'sPoint Estimate Method.

PWT Patch-Wise Temperature Method.

RF Radio Frequency.

SEA Statistical Error Analysis.

SPC Single-point constraints.

STOP Structural-Thermal-Optical Performance.

TEMP Temperature.

TETM Thermo-Elastic transfer matrix.

TEV Thermo-Elastic Verification.

TTM thermal mathematical mode.

URQ Univariate Reduced Quadrature.

Chapter 1

Introduction

1.1 Background and Motivation

The aerospace industry is at a pivotal moment as launch costs continue to plummet and small satellite platforms become increasingly standardized. These two trends have greatly facilitated the democratization of space and have led to an explosion of scientific and Earth observation missions using small, low-cost spacecraft. In fact, small satellite platforms are increasingly being used for applications that in the past were the domain of large, expensive missions.

This shift has resulted in a focus on overall system performance rather than just structural survivability. For example, precision payloads like optical instruments and space telescopes demand extremely high levels of pointing accuracy, stability, and alignment for the entire duration of the spacecraft's life. Even slight changes from the ideal setup can cause a dramatic decrease in the payload's performance, particularly in cases where very high resolution or very long exposure times are required.

Space thermal environment significantly affects the performance of a spacecraft. A spacecraft experiences complicated and changing thermal conditions such as eclipses in the orbit, changes in solar illumination, and planetary radiation, which in turn cause temperature gradients within the structure. These thermal changes lead to deformations of the structure that, while often really small in size, can greatly influence the functional behaviour of very high-precision systems. Therefore, thermo-elastic disturbances are the major source of low-frequency, quasi-static deformations that have a direct influence on the pointing accuracy and the optical performance of the newest space missions. This is especially true for small satellite platforms that have to operate under strict mass, cost, and margin limitations.

1.2 Thermal and Structural Analyses in Space Systems

Thermal and structural analyses have been two major components in spacecraft development which, until now, have been performed as almost independent activities, each with its own objectives within the design and verification process. The separation between them is due to different physical phenomena that the two disciplines deal with and also from the independent evolution of tools and methods specifically tailored for particular engineering needs [12].
Spacecraft thermal analysis has been utilized mainly for interpreting the space thermal environment and controlling the thermal management system. The main concern of thermal analysis is that during the whole mission life, the temperature of all spacecraft components should be within their allowance limits. Steady-state and transient temperature distributions, heat fluxes, and thermal balances under various operation and environmental conditions such as orbital eclipses, solar illumination changes, planetary radiation, and internal power dissipation are the typical subjects of thermal analyses. Hence, the principal results of thermal simulations are temperature fields, heat flows, and thermal margins that are component survivability and thermal control performance assessment tools [12].
Meanwhile, structural analysis has, by and large, focused on ensuring the mechanical safety of the spacecraft. The main goal of structural verification is to demonstrate that the structure is capable of resisting the mechanical loads encountered during the launch and in-orbit without failure or permanent damage. Structural analyses usually involve static load cases, modal analyses, sine and random vibration analyses, and shock evaluations. The main results of these analyses comprise stresses, strains, safety factors, natural frequencies, and mode shapes, which are employed to check agreements with strength, stiffness, and dynamic requirements set by launch vehicles as well as mission constraints [13].
Thermal and structural analyses have each, when taken in isolation, been able to meet their verification targets successfully. The decoupled method has been more than enough whenever the main focus was on the survival of the components and the overall structural strength. However, this kind of separation automatically overlooks the coupling of thermal and mechanical behaviour. One of the ways in which, temperature gradients and time-varying thermal conditions can lead to deformations in the structure that are not accounted for when thermal and structural analyses are done separately [14].
As spacecraft missions have continually pushed their objectives to be more performance-oriented, particularly when it comes to having very precise pay-

loads, the disadvantages of this conventional method have become more and more clear [14].
Space missions in the past have shown that it is quite limiting to consider thermal and structural analyses as separated disciplines. The launch of the Hubble Space Telescope is perhaps one of the most famous and educational case studies in this respect. Very soon after it was launched, Hubble had problems with its pointing stability as well as image jitter, and therefore the quality of the scientific observations deteriorated [15].
These issues were eventually resolved by redesigning the spacecraft's solar arrays. The arrays had been subjected to cyclic thermal loading as the telescope switched from sunlight to eclipse during its orbit. The temperature changes brought about thermo-elastic deformations of the solar array support structures, which in turn resulted in quick mechanical movements, known as thermal snap. Even though the size of these deformations was quite small, their impact, due to the rapid vibrations, was transmitted through the spacecraft structure, and in the end, the pointing stability of the telescope was compromised [15].
At the design stage, thermal analyses had accurately predicted the temperature changes that the solar arrays would be subjected to, and structural analyses had verified their mechanical strength and stiffness. However, the coupled thermo-elastic response and its effect on system-level performance were not sufficiently predicted. The interaction of thermal gradients and structural flexibility, along with the consequent dynamic effects on pointing accuracy, were downplayed because of the absence of an integrated analysis approach. This case was a clear demonstration that meeting thermal and structural requirements separately may not always lead to satisfactory system-level performance, especially for missions involving high-precision optical payloads [15].
The Hubble Space Telescope and other missions have taught us that we must change our way of thinking and not rely solely on the traditional decoupled analysis paradigm. Thermal and structural analyses that are performed separately inherently ignore thermo, mechanical coupling effects, which can be very significant in determining the actual behaviour of a spacecraft under real operating conditions. It is not just that temperature fields represent a thermal verification output, they also serve as mechanical loads that generate stresses, cause deformations, and, in some cases, lead to dynamic disturbances [15].

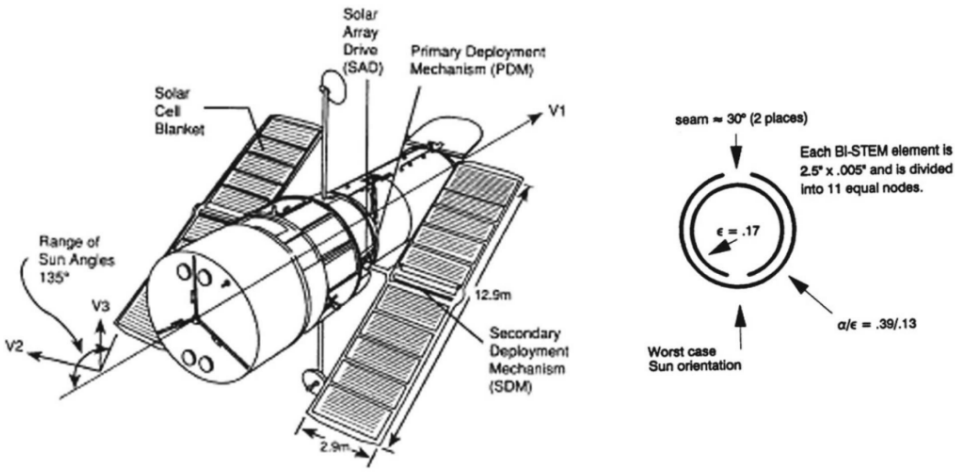

Figure 1.1: Thermo-elastic deformation on Hubble [1].

Thermo-elastic analysis was developed as a tool to overcome these drawbacks. It is a technique that directly links the thermal behaviour of a structure with its mechanical response. In this combined method, temperature fields from thermal analysis are passed down to the structural finite element models, and thus thermal loads are considered. The structural analysis that follows reveals the thermo-elastic behaviour in terms of displacements, strains, stresses, and forces. Of these results, displacements and deformations are, in most cases, the most significant parameters for the overall system performance level, especially for optical and radio-frequency payloads where alignment and stability are essential [15].

1.3 Thermo-elastic Verification

To address the challenge described in the previous paragraph, The European Space Agency has come up with the Thermo-Elastic Verification (TEV) methodology, which is different from just calculating thermo-elastic responses. TEV brings together the disciplines of thermal, structural, system, and performance engineering into one verification process of the impact of thermally induced deformations on instrument performance. Thus, TEV is a concerted multidisciplinary initiative in which different experts collaborate to make sure that the thermo-elastic effects are under control and do not harm the mission at any time.
Within the European space industry numerous ESA projects have significantly contributed to gaining extensive experience with thermo-elastic phenomena over a wide range of spacecraft configurations and stability require-

ments. As a result of the rising complexity and novelty of space instruments, the direct utilization of previous experience is often restricted, thus the need for systematic and structured verification approaches becomes indispensable. Current ECSS standards and handbooks are a source of good requirements and best practices for products at the component level; however, they are generally focused on thermal and structural analyses from a single-discipline point of view and do not completely address their interaction in the framework of performance verification. Thus, TEV guidelines highlight a process that can help engineers identify the main thermo-elastic deformation mechanisms and the structural areas that have the greatest impact on performance degradation or stress generation.
Instead of prescribing detailed modelling steps or establishing strict analysis workflows, the TEV approach puts the main emphasis on understanding-based verification. The methodology is intended to direct engineers towards modelling only those parts of the structure and thermal conditions that are most important in determining the thermo-elastic response. With this intention, the resources can be properly allocated thus avoiding unnecessary refinement of model regions that have no or only very little influence on the performance predictions. The decision to carry out the modelling and analysis activities is based on various primary factors:

- The performance margins relative to the required performance
- The contribution of the individual parts of the structure to the degradation of the performances
- The uncertainties in the individual parts and their impact on the degradation of the performances

1.4 Stages of the TEV process

The TEV process is composed of four main stages [2]:

- **Identification**: This preliminary phase is a necessary part of determining the performance parameters to be verified and the deformation mechanisms that may affect them. This phase needs a reference design, or a baseline model, developed in a way that enables a thorough understanding of the thermal and structural responses to be investigated in later phases. The determination of the performance parameters is obtained by the interaction between the performance groups, thermal, and structural [3].

Figure 1.2: TEV process [2].

- **Modelling**: This phase is intended to identify all significant deformation mechanisms and to verify the robustness of the adopted modelling strategy. The objective of this stage is to construct thermal and structural models that [3]:
  - Are capable of predicting the behavior of the performance parameters;
  - Can relate the performance parameters to quantifiable physical quantities, such as stress;
  - Can model deformation mechanisms that may critically affect the responses of the performance parameters and their associated features;
  - Employ a sufficiently refined mesh to accurately capture the relevant physical phenomena;
  - Are validated to ensure mathematical correctness and reliability of the results.

  To avoid inconsistencies between models, the FEM, thermal, and structural models must be properly aligned to ensure that configuration is consistent and errors are minimal from different structure representations.

- **Classification**: In this stage, the goal is to find the critical thermal cases, in addition to the thermal, mechanical, and thermo-mechanical design parameters, for maintaining sufficient margins on the parameters. The model used is the same developed in the previous stage for simulating the deformation mechanisms. The classification is performed on the basis of [3]:

  - The initially estimated margin for each performance parameter in the nominal model;
  - The relative influence of a model feature on the response of a performance parameter;
  - The uncertainty in the performance parameter responses resulting from uncertainties in the model features.

  The aim is to verify that the thermal and structural models are adequate. Should the models prove insufficient, it may be necessary to implement design modifications.

- **Final verification**: This represents the final stage where the models are considered 'fit for purpose,' symbolically translating the fact that the models are now able to be used for all applicable cases so that the desired performance parameter values could be determined. For the consideration of any uncertainties in the parameter values of the thermal and mechanics properties, safety factors or stochastic methods could be employed [3].

1.5 Uncertainty in the TEV process

During the TEV process, addressing uncertainties goes hand in hand with the classification step in which the suitability of the thermal and structural models is evaluated against the level of confidence needed in the performance parameters predicted. Here, it is not enough only to assess the system's nominal responses; it is also crucial to grasp how uncertainties in the modelling of various features influence the performance parameters. Such understanding is critical for deciding if the models are "fit for purpose" or if further refinement is necessary to make the predictions more reliable [3].
Uncertainties considered during this stage may stem from various sources. On one hand, there are modelling uncertainties that can be reduced by improving the numerical representation of the system, for example by increasing the mesh resolution, refining the geometric description of the structure, or adopting more advanced material models, such as moving from isotropic to orthotropic formulations. On the other hand, there are uncertainties related to material properties, manufacturing tolerances, and assembly conditions, which are not directly controllable by the model developers. Sometimes the characterization of such uncertainties can be greatly facilitated by conducting targeted experimental campaigns, while in other cases the knowledge of

the variability area remains only partial [3].
Only in a few instances, the uncertainty related to a particular characteristic, like a material or surface property, is known and given in the form of stochastic data, e.g. mean values, standard deviations, and probability distributions. When such data exist, they can serve to determine the uncertainty in the performance parameters' response, thus allowing what is called an uncertainty impact assessment. In this scenario, the alteration applied to the feature comes from its statistical properties, and metrics like the standard deviation can be utilized to specify typical variations from the nominal value. Yet, in numerous practical situations, the uncertainty is not properly defined. Therefore, in these cases, the feature's variation is generally expressed as a percentage of the nominal value or as an absolute offset, without a direct link to a probabilistic description of the uncertainty [3].
To properly take into account these uncertainties, the TEV approach suggests that one should see to what extent different model regions or features contribute to the change of the performance parameters as well as the impact of their uncertainties. This method allows determining the degree of dependence of the performance parameters on specific model parts, and how the uncertainty in those parts affects the overall output. The joint details on contributions and uncertainties offer an in-depth insight into the causes of performance decline, and thus, they stand as the primary input to the classification step, helping to identifying the most critical areas and directing additional model improvement work [3].

1.6 Approaches to cover the uncertainties

In the realm of uncertainty assessment, it is common for two main approaches to be taken to consider how uncertainties can affect engineering analyses, such as thermo-elastic problems. The safest and most common approach is the use of safety factors, which form a standard structural verification practice, e.g. in ECSS standards. This method essentially involves assuming uncertainties by applying over-conservative margins to the design parameters in order to make sure that the system is operating within the limits of acceptability under the worst-case scenario assumptions.
The safety factor, representing the cumulative effect of the different steps of the thermo-elastic analysis process, can be expressed as follows [3]:

$$K_{\mathrm{TE}} = K_{\mathrm{MT}}\, K_{\mathrm{ET}}\, K_{\mathrm{MAP}}\, K_{\mathrm{MS}} \tag{1.1}$$

Where K_{MT} is the thermal model factor, K_{ET} is a thermal environment factor, K_{MAP} is a safety factor for the temperature mapping process and K_{MS}

is the safety factor for structural thermo-elastic model [3].
Another more sophisticated alternative is the use of stochastic methods that take into account the variability of the input parameters more explicitly and propagate this variability through the analysis to determine how it affects the response of the outputs. These techniques make it possible to gain a deeper level of understanding of the system behaviour, revealing which parameters have the greatest impact on the performance and how the results are influenced by the uncertainties. In thermo-elastic verification, this type of data can serve as a supplement to the categorization method, giving a more quantitative evaluation of the factors causing the performance degradation.
Compared with the use of safety factors, stochastic methods provide a greater depth of insight and allow for a more realistic modeling of uncertainties. However, this greater level of detail entails more computational effort and a more complicated analysis setup, since a number of simulations are usually necessary to assess the propagation of uncertainties. Thus, the choice of the most suitable method is a matter of balancing the need for accuracy against the availability of computational resources [3].

1.7 Stochastic methods for uncertainty analysis

After this general overview, it should be pointed out that deterministic AOT methods still stand as one of the most popular choices for uncertainty analysis in the engineering practice of today. Essentially, these techniques consist of changing only one input parameter at a time from its nominal value and all other parameters are kept fixed, in order to understand the effect of that particular parameter on the system response. In the context of space engineering, three major AOT methods are generally recognized and practiced:

- **Statistical Error Analysis (SEA)** The SEA approach draws from sensitivity analysis notion, which locates the impact of the uncertain input parameters on the chosen performance outputs by means of the sensitivity coefficients. These coefficients are the partial derivatives of the performance parameters over the input variables and they give a first-hand account of what happens to the system response when each parameter is altered. The value of the performance parameters P_i can be defined as [16]:
$$P_i = P_i(x_1, x_2, \ldots, x_k) \tag{1.2}$$
The sensitivity coefficients are obtained as: $\frac{\partial P_i}{\partial x_k}$

In addition, the integration of these sensitivity coefficients and the hypothesis of input parameters uncertainties ($w_k x$) at a certain confidence level allows for the quantification of the total uncertainty in relation to each performance parameter. The uncertainty of the performance parameters for that same level of confidence can be expressed as [16]:

$$w_{P_i} = \left[\left(\frac{\partial P_i(x_1, \ldots, x_k)}{\partial x_1} w_{x_1} \right)^2 + \ldots + \left(\frac{\partial P_i(x_1, \ldots, x_k)}{\partial x_k} w_{x_k} \right)^2 \right]^{1/2} \tag{1.3}$$

The final SEA uncertainty is calculated from the root mean square of the various contributions, the final uncertainty for each performance parameter is straightforwardly traceable to the contributions of the input parameters [16].

- **Rosenblueth'sPoint Estimate Method (PEM)** This method was originally conceived to address some of the drawbacks of linear sensitivity-based techniques by giving a more accurate estimation of output uncertainty while not increasing the computational cost by much. The PEM method is especially interesting in the field of engineering where the system response is only slightly non-linear and first-order methods such Stat Error Analysis may not sufficiently represent the behavior of the system [17]. The Rosenblueth method takes the idea of determining the system response by evaluating the output at a few points, but those points have to be very carefully chosen in the space of the input parameters. For each uncertain input parameter, two values are considered, usually, the positive and negative deviations around the nominal value. These deviations are selected in accordance with the probability distribution of the input parameter, which, in most cases, is a normal distribution. Therefore, for each uncertain input parameter, the performance parameter is first assessed at its nominal value and then at positive and negative perturbations corresponding to one standard deviation from the mean [17].

$$P_{ji}^{+} = P_j(\mu_1, \mu_2, \ldots, \mu_i + \sigma_i, \ldots, \mu_n) \tag{1.4}$$

$$P_j^{0} = P_j(\mu_1, \mu_2, \ldots, \mu_n) \tag{1.5}$$

$$P_{ji}^{-} = P_j(\mu_1, \mu_2, \ldots, \mu_i - \sigma_i, \ldots, \mu_n) \tag{1.6}$$

Based on the evaluation of the performance parameter at the positive and negative perturbations of each uncertain input, the Rosenblueth

method allows the estimation of the mean value, variance coefficients, and relative sensitivities of the system response [17]:

$$\begin{aligned} P_{ji} &= \frac{P_{ji}^{+} + P_{ji}^{-}}{2} \\ V_{ji} &= \frac{P_{ji}^{+} - P_{ji}^{-}}{P_{ji}^{+} + P_{ji}^{-}} \\ 1 + V_{P_j}^2 &= \prod_{i=1}^{n} \left(1 + V_{ji}^2\right) \\ S_{ji} &= \frac{V_{ji}}{V_{P_j}} \end{aligned} \tag{1.7}$$

One of the major benefits of Rosenblueths Point Estimate Method is its potential to partly represent the non-linearity in the dependency of system response on input parameters. Because the performance parameters are assessed at the upper and lower limits of each uncertain variable, the technique can recognize the asymmetries in the response, which would be overlooked if only linear approximations were used. This feature makes PEM a more reliable method than SEA when the thermo-elastic response of the structure does not strictly follow the linear behaviour [17]. Nevertheless, Rosenblueth's approach is not without its flaws. In the same vein as other OAT methods, it does not take into consideration the combined effect of several uncertain parameters as each variable is changed individually while the rest are kept at their nominal values. Furthermore, the correctness of the method relies on the presumption that the selected point estimates properly represent the underlying probability distributions. If, on the whole, the system behavior is highly non-linear or strongly influenced by parameter interactions, the uncertainty assessments derived from PEM might still be lacking [17].

- **Univariate Reduced Quadrature (URQ)** The core concept of the URQ technique is to estimate the statistical moments of a performance parameter by testing the system response at a few judiciously chosen points around the nominal design point. The model is run at three levels for each uncertain input parameter: the nominal, and two additional values representing positive and negative deviations which are defined based on the probability distribution that is assumed. Different from simpler OAT methods, URQ mode of operation takes into

account the role of the nominal point thereby enhancing the accuracy of the estimated mean and variance [18].

$$P_{ji}^{+} = P_j(\mu_1, \ldots, \mu_i + \Delta_i, \ldots, \mu_n) \tag{1.8}$$
$$P_{j}^{0} = P_j(\mu_1, \ldots, \mu_n) \tag{1.9}$$
$$P_{ji}^{-} = P_j(\mu_1, \ldots, \mu_i - \Delta_i, \ldots, \mu_n) \tag{1.10}$$

In the context of the Univariate Reduced Quadrature method, the role of each evaluation point in the calculation of the statistical moments is determined by a collection of weighting coefficients. These depend on the selected quadrature points and are formally defined as follows [18]:

$$w_0 = 1 + \sum_{i=1}^{n} \frac{1}{h_i^{+} h_i^{-}} \tag{1.11}$$
$$w_i = \frac{1}{h_i^{+} - h_i^{-}} \tag{1.12}$$
$$w_i^{+} = \frac{(h_{p,i}^{+})^2 - h_i^{+} h_i^{-} - 1}{h_i^{+} - h_i^{-}} \tag{1.13}$$
$$w_i^{-} = \frac{(h_{p,i}^{-})^2 - h_i^{+} h_i^{-} - 1}{h_i^{+} - h_i^{-}} \tag{1.14}$$
$$w_i^{\pm} = \frac{2}{\left(h_i^{+} - h_i^{-}\right)^2} \tag{1.15}$$

The weighting coefficients depend on the selected quadrature points h_i^{+} and h_i^{-}, which are defined as [18]:

$$h_i^{\pm} = \frac{\nu_i}{2} \pm \sqrt{\Gamma_i - \frac{3\nu_i^2}{4}} \tag{1.16}$$

Based on the defined weighting coefficients and quadrature points, the Univariate Reduced Quadrature method allows the estimation of the mean value and the variance of the performance parameter as follows [18]:

$$\mu_{P_j} = W_0 P_j^0 + \sum_{i=1}^{n} W_i \left(\frac{P_{ji}^{+}}{h_i^{+}} - \frac{P_{ji}^{-}}{h_i^{-}} \right) \tag{1.17}$$
$$\sigma_{P_j}^2 = \sum_{i=1}^{n} \left[W_i^{+} \left(\frac{P_{ji}^{+} - P_j^0}{h_i^{+}} \right)^2 + W_i^{-} \left(\frac{P_{ji}^{-} - P_j^0}{h_i^{-}} \right)^2 + W_i^{\pm} \frac{(P_{ji}^{+} - P_j^0)(P_{ji}^{-} - P_j^0)}{h_i^{+} h_i^{-}} \right] \tag{1.18}$$

One of the most significant benefits of the URQ method is that it can effectively represent moderate non-linearities in the system response while maintaining computational efficiency. Because the technique involves only a limited number of deterministic model evaluations per uncertain parameter, it is extremely convenient for use cases needing computationally intensive analyses, such as coupled thermo-elastic simulations of space structures. Besides, the formulation of the URQ provides an unambiguous measure of the influence of each uncertain parameter on the total variability of the performance metrics, thus aiding sensitivity analysis and design decision-making [18].

Within the scope of this thesis, the URQ method has been chosen as the main tool for uncertainty evaluation in thermo-elastic analyses. It is quite a good fit for space optical systems analysis since several design parameters can affect thermo-elastic deformations and, therefore, the system performance. Connecting URQ with an automated analysis workflow, the method allows a thorough examination of how main design uncertainties affect thermo-elastic performance parameters, thus facilitating a more knowledgeable and performance-oriented design approach.

Chapter 2

Fundamentals of Thermoelasticity, TEV and Thermal Modelling

2.1 Heat Transfer Mechanisms

The heat transfer is defined as: "Heat transfer (or heat) is thermal energy in transit due to a spatial temperature difference" [2]. Heat transfer models can be classifed as follow:

- **Conduction**: Conduction is the mode of the heat transfer for stationary solid or fluid medium. Energy is transferred within solids from regions at higher temperature to regions at lower temperature through their mutual interactions. The heat flow vector q by conduction per unit area is expressed by Fourier's law as follow [2]:

$$\mathbf{q} = -k\nabla T \tag{2.1}$$

- **Contact Conductance**: The heat flow across the interface between two contacting surfaces per unit temperature difference is measured by contact conductance. It is dependent upon the contact pressure, flatness, and roughness of the surface. From a modeling standpoint, contact conductance can be thought of as classical conduction with an extra, non-zero thermal resistance at the interface that takes into account the temperature discontinuity brought on by imperfect contact. The heat transfer Q(W) over a thermal contact can be described as [2]:

$$\dot{Q} = h_c\, A\, (T_1 - T_2) = \frac{T_1 - T_2}{R_c} \tag{2.2}$$

- **Convection**: Convection occurs between a surface and a moving fluid when they are at different temperatures. Heat is transferred from one place to another by movement of fluids. The process is described by Newton's law of heat transfer [2].

  $$\dot{Q} = h\, T = h\, A\, (T_f - T_s) \tag{2.3}$$

  In this case $(T_f - T_s)$ is the temperature difference between solid and fluid, the parameter h is the convective heat transfer coefficient and it's value is typically tabulated.

- **Thermal Radiation Heat Transfer**: "Thermal radiation is a mode of heat transfer between two surfaces at different temperatures by means of electromagnetic waves that do not need medium to propagate. Even better, these waves are most efficiently propagated in vacuum" [2]. The heat flux for an ideal blackbody (ε=1), that is, a surface with unit emissivity, is given by:

  $$q_b = \sigma T_s^4 \tag{2.4}$$

  This equation represents the maximum thermal radiation that a surface can emit at a given temperature T_s. The emitted power by a real surface or grey surface per unit area is [2]:

  $$\dot{Q}_e = \varepsilon\, \sigma\, T_s^4 \tag{2.5}$$

  Where ε is a radiative property of the surface referred to as emissivity with $0 \leq \varepsilon \leq 1$

2.2 Thermoelasticity

"Thermoelasticity extends classical elasticity theory. In this area, structural changes and stress states come from mechanical and thermal loads. Thermoelastic analysis allows us to predict how a satellite responds to temperature changes. Depending on how the thermal and mechanical fields interact, we can conduct thermoelastic analysis in a coupled or uncoupled way [19].

- **Coupled thermoelastic analysis**: "This is the most general case, where the equations governing the system describe the mutual interaction between the satellite's mechanical and thermal behaviour. This

interaction is formulated within the first law of thermodynamics and is captured by the heat conduction equation, which accounts for the mutual interaction between the two fields" [19].

- **Uncoupled thermoelastic analysis**: "The purely mechanical deformation field does not appear in the heat conduction equation. As a result, the temperature field is no longer linked to elastic deformation" [19].

2.3 Coupled thermoelastic analysis

The two main unknown variables of the problem are displacement and temperature, and their interaction calls for a mathematical formulation that can represent the coupling between the mechanical and thermal fields. The analysis is carried out in the framework of small displacement and small rotation, assuming linear elastic behavior. As a result, plastic effects are not considered, including irreversible material deformations linked to entropy production. The formulation is [19]:

$$\begin{bmatrix} [K_{uu}] & [K_{u\theta}] \\ [K_{\theta u}] & [K_{\theta\theta}] \end{bmatrix} \begin{Bmatrix} \{u\} \\ \{\theta\} \end{Bmatrix} = \begin{Bmatrix} \{F\} \\ \{0\} \end{Bmatrix} \tag{2.6}$$

2.4 Uncoupled thermoelastic analysis

The mechanical effects have no effect on the heat conduction equation; the mechanical and thermal stress components are independent of one another. The formulation is [19]:

$$\{K\}\{u\} = \{T\} + \{F\} \tag{2.7}$$

In this case, K is the stiffness matrix, u is the displacement vector, F is the external force vector that corresponds to the mechanical loads applied to the system, and T is the equivalent vector of concentrated nodal loads defined as "energetically equivalent to the virtual variation of the work performed by a temperature change within the body on the nodal displacements." [19]

2.5 Thermo-elastic verification

The aim of TEV is the reduction of stresses and deformation produced due to thermal loads on a structure. This is due to interaction analysis, which

results from structural as well as thermal analysis. The final goal is the proper functioning of critical components, including optical/RF components [3].
At the present time, there is no ECSS standard for the thermo-elastic verification process (TEV); nevertheless, it has widespread use within the space field. In related literature, there are guidelines set by the ESA for the purpose of compiling it as a future official ECSS standard.
In the TEV guidelines, “feature” is defined as "any aspect of the mathematical or physical model or design that might have some influence on the response of the system to the thermal-elastic effects" [3]. The objective of spacecraft design is to maximize its performance capabilities, in accordance with the space environment and component degradation, which are measured through a set of parameters called "performance parameters".
Before running any thermal and structural analyses, it is necessary to recognize the sorts of structural deformations that could negatively impact performance and how the respective performance measure depends on the pertinent physical phenomena. Thermo-elastic deformations, in particular, depend on those factors such as [3]:

- Temperature field
- CTE
- State of constraints, so the interaction between stiffness constraints and thermally imposed deformation

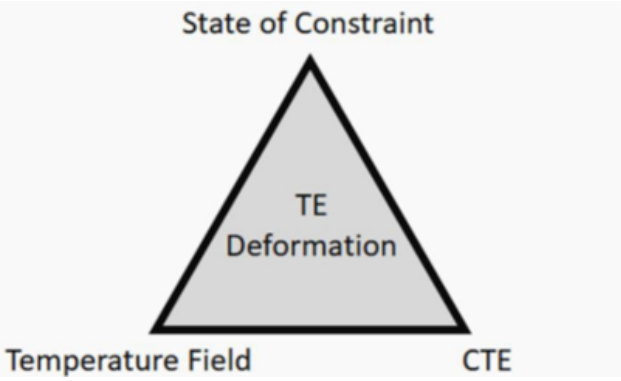

Figure 2.1: aspects of thermo-elastic [3].

2.6 Thermo-Elastic Deformation Mechanisms

Since thermo-elastic deformations have been known to depend on the coefficient of thermal expansion, the temperature distribution, and structural constraints, it makes sense to study how these factors affect deformation behavior. The CTE is a material property that sets how much thermal strain occurs when temperature changes. If a structure experiences equal temperature shifts and can move freely, the thermal strain spreads evenly and scales with T. In such cases, the structure expands or contracts uniformly, moving all points in the same direction without altering internal angles or relative positions. No internal forces or twisting occurs as a result.
When the temperature across a structure isn't the same everywhere, thermal strain changes from place to place because parts of it face different heat levels. Each section expands differently due to these varying temperatures, leading to uneven movements that can cause bending, twisting, or shape shifts even without outside forces pushing or pulling. As various parts grow at different rates, they shift relative to one another and rotate in response. When the structure has fixed points or limits on movement, the normal expansion expected from the materials coefficient of thermal expansion and temperature patterns cannot happen freely. This mismatch between what the material wants to do and what is physically blocked leads to internal stresses and extra deformation. In practical engineering applications, especially in sensitive optical equipment, the final shape change usually comes from all three factors working together. The overall behavior depends on whether the system responds mainly with uniform growth, uneven bending, or warping caused by physical restrictions.

2.7 CTE

"The CTE, is defined as being the change in engineering strain due to a unit increase of the temperature" [2]. It is a material property that is relevant for the thermoelastic behaviour of a material. For cases in which the coefficient of thermal expansion (CTE) is not constant over the considered temperature range, the secant coefficient of thermal expansion is used and defined as follows [2]:

$$\alpha_s(T) = \frac{1}{T - T_{\text{ref}}} \int_{T_{\text{ref}}}^{T} \alpha(\xi)\, \mathrm{d}\xi \;\approx\; \frac{\varepsilon_t(T) - \varepsilon_t(T_{\text{ref}})}{T - T_{\text{ref}}}. \tag{2.8}$$

In this case, T_{ref} is the reference temperatures, $\varepsilon_t(T)$ is the the thermal engineering strain. In the secant CTE is lin earised between the reference temperature T_{ref} and the current temperature T. When $\varepsilon_t(T)$ is assumed to be a continuous function, the coefficient of thermal expansion T_{ref} can be expressed as [2]:

$$\alpha(T) = \frac{\mathrm{d}\varepsilon_t(T)}{\mathrm{d}T} \tag{2.9}$$

If CTE in constant over the full temperature rage of interest, $\varepsilon_t(T)$ is a linear function of T, therefore it is possible to use incremental ratios. In this case the one-dimensional elongation can be written as [2]:

$$\Delta L = L_{\text{ref}}\, \varepsilon_t(T) = L_{\text{ref}}\, \alpha\, T = L_{\text{ref}}\, \alpha\, (T - T_{\text{ref}})\,. \tag{2.10}$$

2.8 Constitutive Laws of Linear Thermoelasticity

In the termoelasticity, the components of the strain tensor ε_{ij} is calculated as the sum of elastic deformations ε_{ij}^e and thermal deformations ε_{ij}^T [2].

$$\varepsilon_{ij} = \varepsilon_{ij}^e + \varepsilon_{ij}^T \tag{2.11}$$

The thermal strain for isotropic materials can be written as [2]:

$$\varepsilon_{ij}^T = \alpha\, (T - T_{\text{ref}})\, \delta_{ij} = \alpha\, T\, \delta_{ij} \tag{2.12}$$

The elastic strain tensor is calculated using the generalized Hooke's law. By summing the elastic and thermal strain tensors the formulation of total strain tensor is obtained, this equation is called the constitutive law of the linear thermoelasticity. Solving it for the stress tensor σ_{ij} gives [2]:

$$\sigma_{ij} = 2G \left[\varepsilon_{ij} + \frac{\nu}{1-2\nu} \left(\varepsilon_{kk} - \frac{1+\nu}{\nu}\, \alpha\, \Delta T \right) \delta_{ij} \right] \tag{2.13}$$

The preceding equation may be expressed in the following compact form [2]:

$$\boldsymbol{\sigma} = [\mathbf{D}]\,\boldsymbol{\varepsilon} - \beta\,\Delta T\,\mathbf{a} \tag{2.14}$$

In this case, $[\mathbf{D}]$ is the matrix of elastic constans, β is the thermal stress modulus.

2.9 Stages of thermo-Elastic Analysis

The two primary goals of thermoelastic analysis are to confirm the structural strength and, in cases where instrument performance may be impacted by deformations, to identify the deformation responses that should be utilized for performance verification. The primary steps of the thermoelastic analysis process are depicted in the following figure [2]:

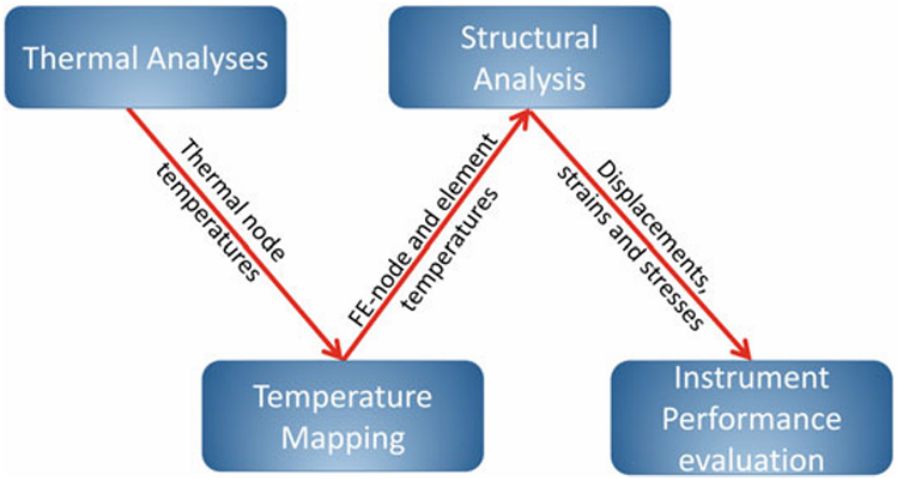

Figure 2.2: Thermoelastic analysis process [2].

The thermal node temperatures are used to represent the temperature fields calculated by thermal analysis, which are subsequently mapped onto the structural finite element model. This mapping procedure takes into consideration the conversion of data formats as well as the variations in solution techniques between the structural analysis (which mostly uses the finite element method, or FEM) and the thermal analysis (which is frequently based on the lumped parameter method). It's also crucial to remember that temperature fields frequently change over time, so in order to properly capture their temporal evolution, the mapping process needs to be applied at several time steps [2].

The finite element model is used to simulate the loading for the structure, which is made up of the temperature fields. The thermoelastic responses in the form of displacements, strains, stresses, and forces are generated by the structural analysis. The deformations, or displacements, which include three linear translations and three angular rotations, are frequently the most important for the instrument's or spacecraft's performance. Therefore, the displacements are given so that their effect on the instrument's or spacecraft's performance can be assessed. "The main theme of the suggestions is that the thermal and structural analysis needs to be considered as one integral analysis process". [2].

Chapter 3

Thermal Analysis with ESATAN-TMS

3.1 Lumped Parameter Method

The thermal analysis is the initial stage of a thermoelastic analysis. This was performed using the ESATAN-TMS software, which is based on the lumped parameter method. this tool enables the modeling of individual components as single thermal nodes, with all of their thermal properties lumped at those nodes. The thermal model is normally divided into two models with a different function in the thermal analysis [2]:

- **The geometric mathematical model GGM**: The main purpose of the Geometric Mathematical Model (GMM), which describes the geometry of the spacecraft or component under thermal analysis, is to produce the radiative data needed to solve the thermal problem. This model is used to assess radiative couplings, or radiative interactions between thermal nodes. The radiative heat fluxes acting on the spacecraft in orbit are also calculated using the GMM. These fluxes vary throughout the orbit as a result of changes in the spacecraft's orientation with respect to the solar radiation and the planetary surface normal [2].

- **The thermal mathematical model TTM**: The Thermal Mathematical Model (TMM) is a thermal network composed of nodes interconnected by conductors that represent conductive, radiative, and convective couplings. It is employed to solve the thermal system and to determine the resulting temperature fields and heat fluxes within the structure [2].

3.2 Thermal Analysis

Depending on the thermal conditions and the study's goals, different ways of analysis can be considered. More specifically, thermal analyses are divided into steady, state and transient analyses, which are focused on different aspects of the thermal behavior of the system [2].

- **Steady State Analysis**: A steady, state thermal analysis is concerned with finding the temperature distribution of a system at thermal equilibrium conditions. At this state, the temperatures of all thermal nodes are stable and do not change with time, and thus the temperature field's time variation is disregarded. Consequently, thermal capacitances and transient effects are left out, and the governing equations become a set of algebraic energy balance equations for each thermal node only. The answer is reached through the iteration process until the nodal temperatures converge [2].

- **Transient Analysis**: The thermal lumped parameter network model can also be employed for transient thermal analyses. A transient analysis provides the possibility to follow the time variations of the responses when changes in the environment occur. Obviously, the changing environment leads to a temperature field changing with time along with the position in the orbit. Moreover, the thermoelastic deformation, as a result, is also time, dependent [2].

3.3 Thermal model

The satellite taken into account for the thermoelastic study is made of a titanium structural framework, which is used to support two mirrors, one smaller than the other, both made of Zerodur. Besides, the system comprises an optical bench and a detector of honeycomb material. The whole satellite is wrapped with a MLI layer to offer thermal protection. The figure below reveals the thermal model used for the study.

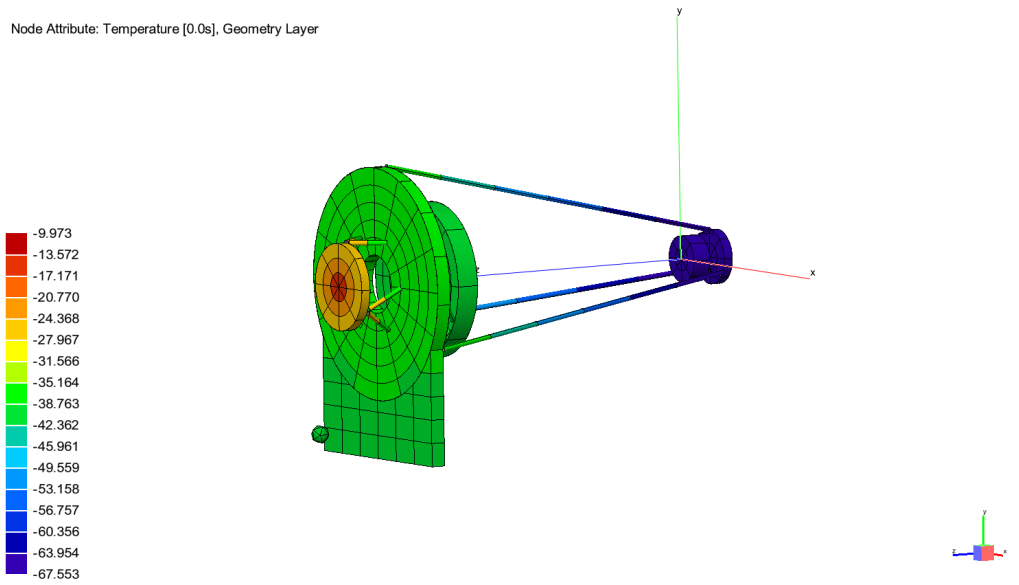

Figure 3.1: Thermal model

The thermal analysis performed with ESATAN-TMS involves the sequential execution of a Radiative Case followed by an Analysis Case:

- **Radiative case**: Radiative case in ESATAN-TMS is the main instrument to calculate the heat transfer by radiation among the system elements and between the spacecraft and surrounding space. This step utilizes the Geometric Mathematical Model, which is a representation of the spacecraft's surfaces in terms of shape and reflectivity. The Radiative Case calculates the view factors that determine the radiation coupling between thermal nodes and the environmental heat fluxes such as direct solar radiation, planetary albedo and planetary infrared emission and all information about orbit. These factors rely on the geometrical features, surface optical properties and orbital parameters of the spacecraft and thus have to be recalculated whenever any of these inputs change [2]. For the satellite considered in the analysis, an orbit at 550 km altitude with zero eccentricity and an inclination of 97.4° was selected.

  The main heat fluxes to be considered are shown in the following figure.

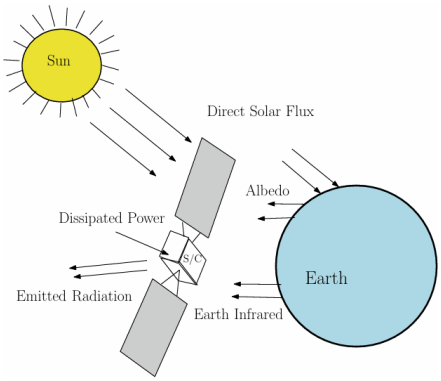

Figure 3.2: Space Thermal environment. [2]

- **Analysis case**: The thermal solution of the system is carried out by the Analysis Case using the Thermal Mathematical Model, which is a model of the spacecraft as a thermal network of nodes connected by conductive and radiative paths. Here, the radiative couplings calculated in the Radiative Case are combined with linear conductors, internal heat dissipation, and boundary conditions to solve the energy balance equations. Depending on the type of analysis chosen, the Analysis Case decides the temperature distribution in steady, state or the transient thermal response of the system. The temperature fields obtained become the main output of the thermal analysis and are usually employed as input for further thermoelastic simulations [2]. Thermoelastic analysis tool use is TEV. The output from the thermal analysis required is an Excel .csv file which contains the temperature of each thermal node at equilibrium conditions. As explained above, this document represents the real temperature field which will be multiplied by the TETM to get the thermoelastic displacements.

3.4 Thermal Analysis process

The ESATAN-TMS analysis workflow is organized into a series of clear steps. Each step focuses on a specific part of the thermal problem. The following sections explain these steps in detail. They outline the role of each phase in the overall thermal analysis process and highlight their importance for the thermo-elastic assessment.

- **analysis file** The thermal analysis process in ESATAN-TMS starts

with defining the analysis file. This file provides the mathematical description of the thermal system to be simulated. It forms the basis of the thermal model and includes all the information needed to describe how the spacecraft or subsystem behaves thermally. Typically, users create this analysis file using a text editor, which allows them to clearly define the elements that make up the thermal network. Inside this file, the thermal system is modeled as a network of distinct thermal nodes connected by conductors. Each thermal node represents a specific area of the structure where thermal properties like mass, heat capacity, and temperature are concentrated. Heat transfer between nodes occurs through conductive, radiative, or convective conductors, which model the physical paths that heat takes within the system. This lumped parameter representation provides an efficient way to approximate the thermal behavior while keeping the computational effort reasonable [4]. In addition to nodes and conductors, the analysis file includes boundary conditions. These boundary conditions represent external influences on the thermal system, such as environmental heat fluxes, imposed temperatures, or heat sinks. They play a key role in defining how the spacecraft interacts with its surrounding environment and in determining the thermal loads the structure experiences under operational conditions. The result of this modeling stage is a text-based analysis file, often called an ACD file. It serves as the base for all later stages of the thermal analysis process in ESATAN-TMS, allowing for the radiative and thermal simulations needed to calculate the temperature distribution of the system [4].

- **Preprocessor and model validation** After the thermal analysis file has been generated, the following step in the ESATAN-TMS workflow is to feed this file to the preprocessor module. The preprocessor's primary function is to interpret the text-based analysis file and to build the corresponding TTM, while also carrying out a detailed check of its structure and logical coherence before any numerical solution is attempted [4]. As part of this validation step, the preprocessor ensures that the entire thermal network is correctly defined and adequately connected. This encompasses verifying the existence and completeness of thermal nodes, the proper definition of conductive and radiative conductors, and the consistency of the specified boundary conditions. The preprocessor automatically detects and reports any issues with the model, such as disconnected nodes, missing conductors, or incorrectly defined thermal links, at this point. It is a very crucial step to guarantee that the thermal model stands for the real physical system that the

modeler has in mind and that numerical instabilities or wrong results are not produced in the following analyses [4]. Along with the checking of logical consistency of the thermal network, the preprocessor internally performs some checks related to data formatting and parameter ranges. By identifying errors and discrepancies at the very beginning, this component substantially contributes to the model robustness and reliability, especially when it comes to complicated spacecraft thermal models [4]. After the Thermal Mathematical Model has been verified, the preprocessor changes the initial text-based analysis file into a binary file format. This binary format is particularly suitable for numerical processing and is basically a compact and efficient version of the validated thermal model. The produced file is the direct input for solver modules used at the analysis final stage, thus making feasible the running of radiative and thermal simulations necessary for the calculation of the system temperature distribution [4].

- **Fortran code** When a verified thermal model has been saved in the ESATAN-TMS database, the subsequent step of the analysis workflow is the creation of the numerical solver through the Fortran Generator module. This module is what translates the Thermal Mathematical Model into executable source code that carries out the thermal simulation [4]. ESATAN-TMS uses Fortran as the programming language for the solution stage mainly because of its very high computational efficiency and the fact that it has been used for a very long time in scientific and engineering applications. Fortran is especially suitable for large numerical problems that require matrix operations and iterative solvers, which are the key methods used in the thermal analyses of spacecraft systems. Employing this language guarantees dependable and efficient runs of both steady-state and transient thermal simulations [4]. During this step, the Fortran Generator runs on its own producing source code that succinctly expresses the mathematical model of the thermal problem. Thus, the heat transfer equations together with the energy balance equations at each thermal node of the system are included. The obtained code describes heat transfer by conduction, radiation, and convection as per the thermal network, and also accounts for the boundary conditions and external heat sources given in the analysis file [4]. Besides the main Fortran source code, there is a collection of header files, commonly named MODEL. h, which are also produced. These header files declare the functions, variables, and data structures needed by the thermal libraries utilized by ESATAN-TMS at the solution stage. The source code and header files together

constitute a full numerical portrayal of the verified thermal model that is ready for compiling and running at the next simulation phase. The benefit of this automated code generation step is that it guarantees the user, specified thermal model matches the numerical solver perfectly and at the same time it reduces the possibility of mistakes in manual implementation [4]. After the Fortran source code is created it is converted to an executable program by a Fortran compiler like gfortran. While compiling, the code is converted to instructions that the computer understands and it is also combined with the thermal libraries from ESATAN-TMS. These libraries hold numerical routines that are needed to solve the heat transfer and energy balance equations as per the thermal model [4]. By doing this, an executable program is generated which completely represents the thermal system and incorporates all the numerical methods required for the performance of thermal calculations. Subsequently, this executable may be run to compute the thermal model in the presence of given boundary conditions thereby providing the temperature distributions for further thermo-elastic analyses [4].

- **Output generation** The last operation in the thermal analysis chain basically entails running the thermal simulation through the executable that was produced previously. This operation is carried out by the Model Solution Program, which takes the thermal state of the system as a starting point and, subsequently, handles the numerical solution of the thermal problem. Before the solver is run, the program assigns starting temperatures to thermal nodes and sets the values of relevant thermal entities so that the simulation begins from a physically consistent state [4]. In accordance with the nature of the analysis, either steady-state or transient, the solver determines temperatures in the system at equilibrium or over time steps. At each step, temperatures and heat fluxes are updated on the basis of the heat transfer mechanisms as defined by the thermal network model, which comprises among others the conduction and radiation exchanges between nodes. For transient cases, the Crank-Nicholson technique is used for solving the heat conduction differentials. This method of integrating in time from an implicit standpoint offers a good compromise between numerical stability and accuracy, thus, it is especially fitting for space vehicle thermal simulations where temperature changes are slow and gradual [4]. During the solution process the program takes care of the interpolation and application of radiative results as well. This point is very crucial for space applications, where radiative heat transfer is often the main ther-

mal exchange mechanism. Accurate treatment of the radiative terms ensures that the temperature fields obtained correspond well to the real situation of the spacecraft thermal environment interaction [4]. After running the simulation, the results are output in two principal forms. The text, type results are saved in an output (.out) file, which gives a comprehensive description of temperatures at nodes, heat fluxes, and other node and conductor thermal quantities at a granular level. At the same time, binary result files (.TMD) are generated to be used later for post-processing in the ESATAN-TMS Workbench environment. This binary format is specially created for dealing with big datasets and allows for quick and efficient visualization and analysis of the system's thermal performance [4].

The following figure summarizes the main steps of the ESATAN-TMS thermal analysis workflow described in this chapter.

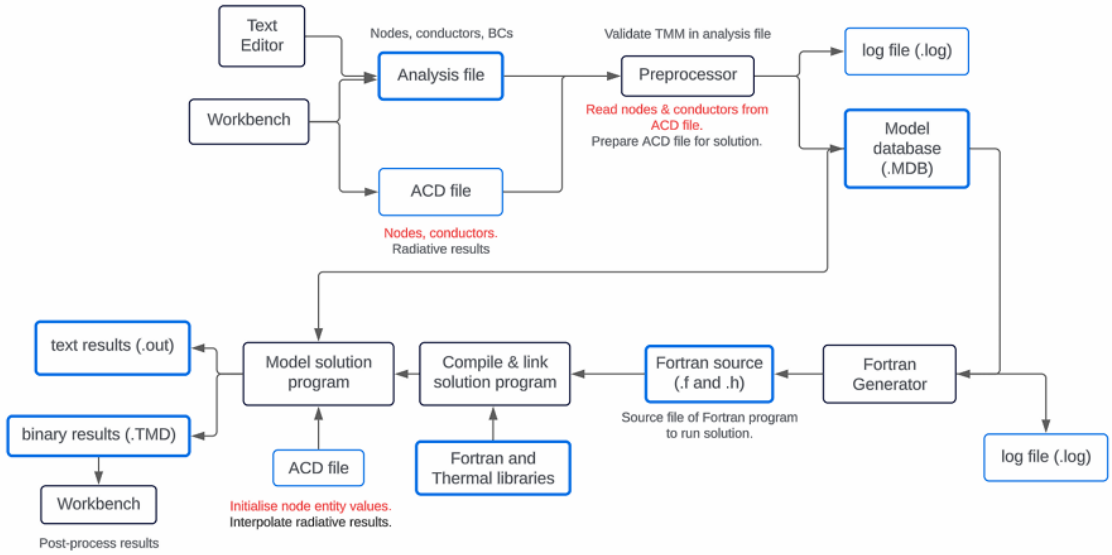

Figure 3.3: ESATAN-TMS Process [4].

Chapter 4

Thermo-elastic Analysis with Pysinas and TEV

Figure 4.1 summarizes the main steps of the thermo-elastic analysis workflow within the TEV framework. The figure shows the interaction between thermal and structural analyses, starting from the establishment of the correspondence between thermal and structural models up to the calculation of thermo-elastic responses. It emphasizes how temperature mapping utilities like pySinas produce the temperature transfer matrix that is used for transferring the thermal results to the structural finite element model, after which structural analyses are carried out to assess thermo-elastic responses induced by thermal loading.

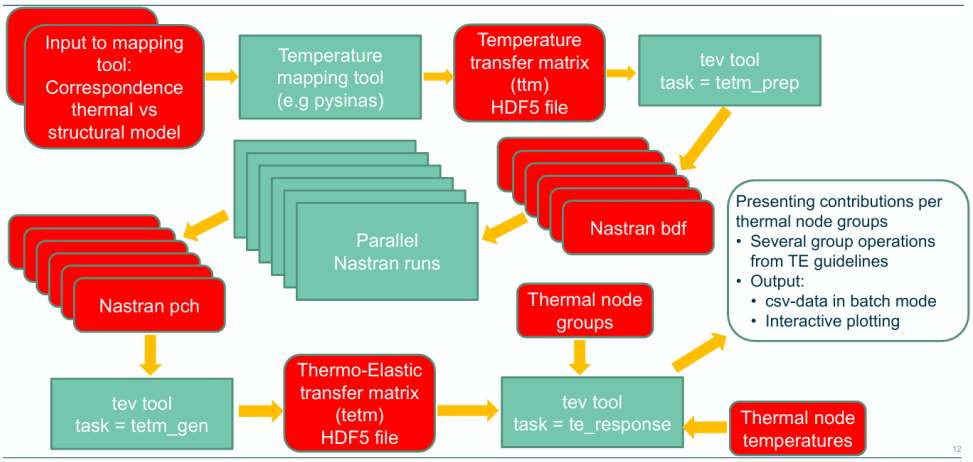

Figure 4.1: TEV workflow [5].

The diagram serves to explain how different tools and files are interconnected and it also sets a stage for the temperature mapping work described later.

4.1 Ttm generation with Pysinas

PySinas is an internal software tool that was initially developed at ESTEC to facilitate thermo-elastic analyses in the context of ESA spacecraft projects. It mainly helps to the transfer of temperature fields obtained by thermal lumped parameter solvers, like ESATAN-TMS, to structural finite element models that are defined in NASTRAN. This temperature distributing step is one of the most important steps in the thermo-elastic analysis chain as it makes the thermal results useable consistently as input loads for structural simulations [7].
PySinas was created out of the need to have a reliable and physically consistent interface between thermal and structural disciplines, which have different modelling approaches and numerical methods. Thermo-analyses usually use lumped parameter models, which means that the spatial discretization is relatively coarse, whereas structural analyses use finite element models with very fine meshes. PySinas has been created to fill this void by granting robust algorithms to associate thermal nodes with structural nodes and elements, thus ensuring the correct transfer of temperature data between the two models [7].
The software is created and kept up to date by ESA engineers with the main purpose to internally support activities at ESTEC and industrial spacecraft projects. It is based on the experience of the previous temperature mapping tool SINAS and implements various features which have been aimed at increasing the flexibility, robustness, and applicability to modern spacecraft models. In particular, PySinas is capable of dealing with complex geometries and different modelling strategies, thus making it a versatile tool for thermo-elastic verification scenarios [7].
PySinas is a fundamental component of the overall thermo-elastic analysis process as it allows the thermal and structural analyses to be integrated in a consistent and automated way. The temperature distributions obtained from ESATAN-TMS are first delivered to the structural FE model and then used to derive thermo-elastic responses such as displacements and deformations that are directly related to system and payload performance. Because of these factors, pySinas is a core tool in the thermo-elastic verification methodology of this thesis [7].

4.2 The simplest temperature mapping method for Thermo-Elastic Analysis

The first step in making a spacecraft both structurally sound and resistant to the harsh environment of space is to combine thermal and mechanical analyses of the spacecraft. This combination is done by transferring the temperature distribution obtained from a thermal analysis to a structural finite element model. Indeed, this step is a crucial part of the thermo-elastic analysis chain because the temperature fields used as loads in the structural calculations cause deformations and stresses. In the literature and practice, many temperature mapping methods have been proposed to achieve the temperature transfer, differing in the level of complexity and accuracy of the modeling [2].
Among these methods, the one most commonly used in industrial and institutional practices, including the European Space Agency, is the Patch-Wise Temperature (PWT) method. The essence of the PWT method is to transfer the temperatures calculated at the nodes of the thermal model directly to the areas of the structural finite element model that correspond to them. In other words, every thermal node is matched to a group of structural nodes or elements, which are then given the same temperature value. Usually, this matching is done by a nearest-neighbour method in which each structural node is connected to the closest thermal node considering geometric distance [20].
The PWT approach captures the essence of the difference between thermal and structural modelling disciplines. Thermal models, especially those derived from lumped-parameter methods, normally use relatively coarse discretisations, with each thermal node corresponding to a large physical area with lumped thermal properties. Structural finite element models, however, are generally made up of much finer meshes in order to precisely capture stresses, deformations, and local structural behaviour. Therefore, within the PWT framework, it is typical for multiple structural nodes or elements to be related to a single thermal node [20].
In terms of realisation, the Patch-Wise Temperature approach has a lot of advantages. Its straightforward nature makes it very robust, fast in execution, and very compatible with automation within complex analysis chains. The mapping method is purely based on geometric operations and does not need interpolation schemes or additional numerical solvers. After the transfer, the temperature distribution is represented in the structural finite element model by a number of discrete regions, or patches, each with a uniform temperature taken from the associated thermal node. This straightforwardness has

been a major factor in the PWT method becoming so widely used in a large number of space projects, where reliability, traceability, and repeatability of the analysis process are critical requirements [20].
On one hand, PWT method still involves certain inherent limitations due to its assumption nature. Since the temperature within each patch is considered to be uniform, there are artificially created temperature discontinuities at the boundaries between neighbouring patches. Such discontinuities do not depict the real physical temperature distribution inside the structure which is generally smooth. In thermo- elastic analyses, these artificial gradients can cause the local predictions of stresses, strains or reaction forces to be overly conservative, especially around zones of high structural stiffness gradients or geometric discontinuities [20].
The extensive reliance on patch, based temperature mapping techniques can be seen in a number of recent European space missions as well. One such example is the ARIEL mission where temperature mapping methods have been explored for the thermal, structural analysis of the payload module. In this context, the temperature distributions obtained from a lumped-parameter thermal model were used as inputs to a structural finite element model to assess the thermo-elastic deformations and their potential consequences on payload performance. The ARIEL scenario exemplifies the practical significance of the PWT method in actual spacecraft scenarios, especially for intricate payload shapes and dense structural meshes, however, it also emphasises the necessity of thoroughly evaluating the assumptions made during the temperature mapping process [6].
Several improved temperature mapping algorithms have been suggested that aim to overcome the drawbacks of the PWT approach. One example is the inclusion of the shapes, sizes, and relative positions of thermal and structural components to get smoother temperature transitions. Nevertheless, such methods usually require more modelling work and computational resources. Therefore, the Patch-Wise Temperature method continues to be the standard solution in numerous real-world applications, thus being a compromise between modelling accuracy and engineering productivity. Hence, it is the fundamental temperature mapping technology used in this study and is also the method implemented in popular mapping tools such as PYSINAS. In the dedicated chapter temperature mapping and thermo-elastic modelling, a more thorough treatment of this technique and its effects on thermo-elastic results is given [2].

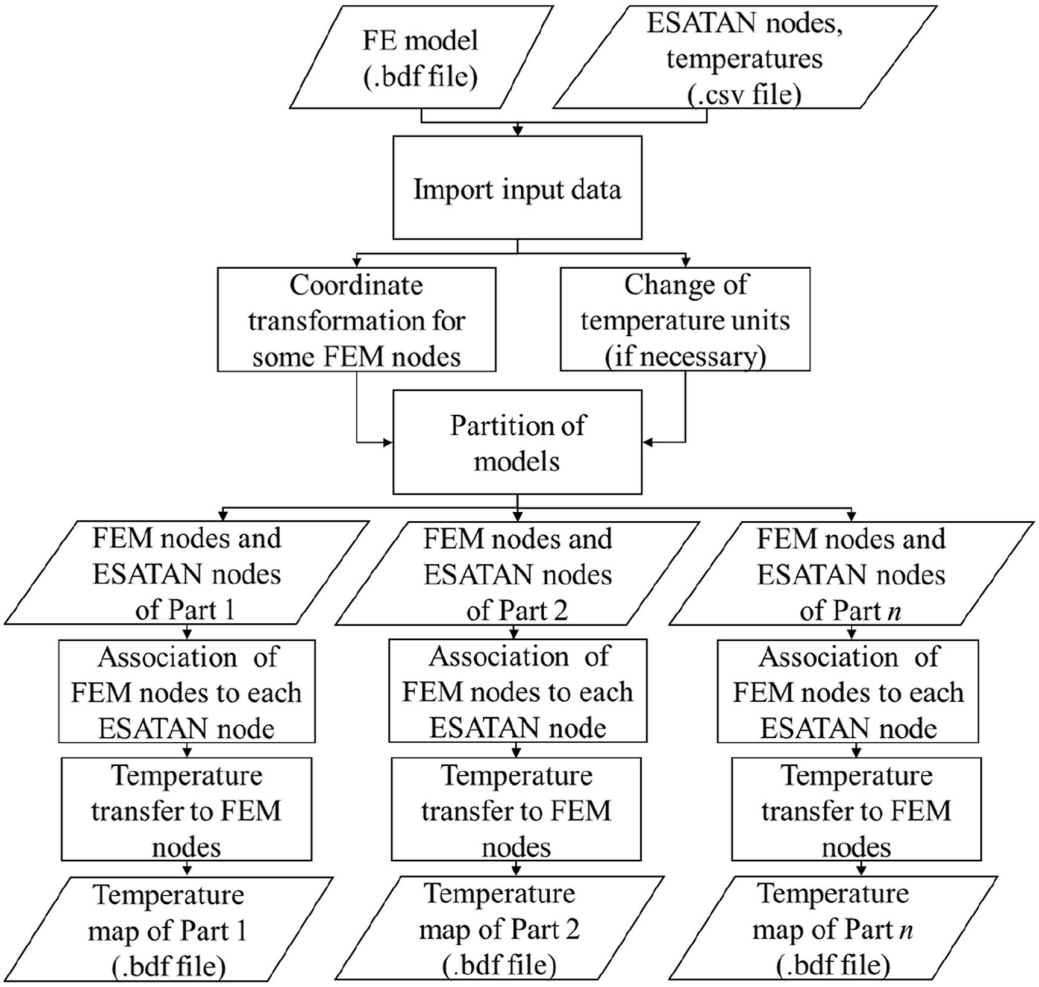

Figure 4.2: Flowchart of the temperature mapping process with the Patch-Wise method. [6].

4.3 State of the Art of Thermo-Elastic Analysis Methods

Although the Patch-Wise Temperature method still stands as the fundamental baseline method in a vast number of practical applications, the intrinsic drawbacks of this method have prompted the rising of more advanced temperature mapping techniques. To be specific, the desire to obtain smoother and more physically representative temperature fields into structural finite element models has been the impetus of the explore for the novel ways that break the traditional patch-based ones. These methods have the objective of

lessening the artificial temperature gaps as well as enhancing the accuracy of thermo-elastic predictions, particularly in the areas where local gradients and structural sensitivities are crucial factors.
Of the choices, two methods are most often considered as the representatives of the present leading edge in temperature mapping for thermo-elastic analysis. These techniques propose various interpolation schemes which allow for a more continuous temperature field depiction on the structural mesh, albeit increased modeling complexity and a greater reliance on algorithmic assumptions. The next parts of the paper briefly summarize these methods, starting with the Geometrical Interpolation approach.

4.3.1 Geometrical Interpolation Method

The Geometrical Interpolation (GI) method is basically a more advanced version of the standard temperature mapping technique in that it tries to produce a smooth temperature distribution on the structural finite element model. In contrast to the Patch, Wise Temperature method, which sets a constant temperature to patches of structural nodes, the GI method tries to represent a continuous temperature field by interpolating thermal data solely based on geometric relationships between nodes [21].
In the GI method the temperature at each thermal node is first mapped to one structural node, which is generally the nearest node in terms of physical distance, i.e. , the closest one. This action creates a network of reference temperature points in the structural model. Afterwards, through an interpolation formula that takes into account only the geometry of the nodes (like distances between nodes and relative spatial positions), the temperature at the other structural nodes is determined. This method does not rely on any extra physical or material data, and the interpolation is only geometrical [21].
One of the main advantages of Geometrical Interpolation is that it can significantly reduce artificial temperature discontinuities which are typical of patch-based mapping techniques. In fact, the GI method by interpolating temperatures on the structural mesh results in smoother temperature gradients, which are, more often than not, representative of the real thermal behaviour of the structure. This feature is very helpful especially in thermo-elastic analyses since sudden temperature jumps can cause locally conservative predictions of stresses or reaction forces that are not the true physical response [21].
The GI technique has been extensively used in a number of research works and applications with a special emphasis on integrated Structural-Thermal-Optical Performance (STOP) analysis processes. In such scenarios, the fidelity of the transferred temperature field is paramount as thermo- elastic

deformations have a direct impact on optical alignment and system, level performance parameters. Hence, the smoother temperature profiles resulting from the GI method can be instrumental in yielding more accurate thermo-elastic trigger predictions and the thermal, structural model correlation can be greatly enhanced [21].
The Geometrical Interpolation method is not without its disadvantages even though it brings several benefits. The main drawback is that the final temperature field is highly dependent on the interpolation algorithm chosen and the input parameters set. The decision regarding interpolation order, weighting functions, or distance metrics can have a major impact on the temperature distribution obtained through mapping. In case these parameters are set arbitrarily or without adequate physical reasoning, the generated temperature maps may not reflect the real thermal behaviour of the structure, hence, the thermo-elastic predictions could be inaccurate [20].
Moreover, the GItechnique being based solely on geometric data, it does not directly consider thermal properties, material discontinuities, or heat transfer paths of the structure. Therefore, the interpolated temperature field may look uniformly-distributed but could be physically, incorrect in the areas where the thermal behaviour is dominated by the material interfaces or local conduction effects. This feature of the model calls for caution when the application of the GI method is considered, especially in the case of spacecraft structures composed of heterogeneous materials and complex thermal layouts [20].
In essence, the Geometrical Interpolation technique is a major step forward from patch-based temperature mapping as it results in smoother and more numerically well, behaved temperature fields. But, its efficiency is highly contingent upon the right choice of interpolation schemes and parameters. Therefore, although the GI method is generally considered a state-of-the-art technique for temperature mapping, using it necessitates a deep knowledge of its pros and cons [21].

4.3.2 Centre-Point Prescribed Temperature (CPPT) Method

The CPPT method is a more sophisticated and physically consistent way of temperature mapping for thermo-elastic analysis. Geometrical methods only use shapes to estimate temperatures, whereas CPPT attempts to refine the temperature distribution on the structural finite element model by conducting extra thermal analyses on the exact finite element mesh used for structural simulations, thus coming up with a more physically consistent

temperature distribution [22].
With CPPT, a structural finite element model is essentially transformed into a thermal finite element model by changing its properties from structural to thermal. The change keeps the original mesh topology, i. e. , nodes and, in most cases, elements, intact while shifting material properties and connectivity to represent heat conduction. Specifically, thermal conductivity parameters are introduced, and suitable joining elements are defined to allow heat conduction throughout the structure. Therefore, the converted model can be utilized to conduct thermal conductive analyses that take advantage of the high spatial resolution of the structural mesh [22].
The parametric boundary conditions for the extra thermal analysis that can be performed come from the lumped parameter thermal model that works at aggregate level. More accurately, the temperature at each thermal node of the lumped parameter model is sent to a respective node of the finite element model, which is usually the one physically closest. These set temperatures serve as boundary conditions for the conductive thermal analysis run on the FEM. Thus, the first stage of temperature transfer in this way is basically the same as that used in geometrical interpolation methods, but then it is followed by a physics-based temperature field adjustment [22].
Essentially, CPPT is an innovative method that, paves the way to a smooth and physically plausible distribution of temperature over the structural finite element model, assuming thermal equilibrium inside the structure. In fact, temperature gradients are a natural consequence of the material properties and conductive paths of the structure, rather than being imposed by arbitrary interpolation methods. Therefore, the CPPT method is essentially different from the Patch-Wise Temperature method, which basically assumes constant temperature regions, and the Geometrical Interpolation method, which is based solely on geometric relationships between nodes [22].
Perhaps one of the major benefits of the CPPT method is the increased accuracy of the temperature maps generated. In fact, since the temperature field is obtained through conductive thermal analysis, it is a better representation of the physical nature of the structure being subjected to thermal load. This is especially important in thermo-elastic analyses, where non-physical temperature gradients may cause non-physical stress concentrations or result in extremely conservative estimates of structural behaviour. Therefore, the CPPT method is considered by many as one of the most precise temperature mapping technologies available nowadays [22].
Nevertheless, this enhanced accuracy is traded for a considerable increase in modelling work. Transforming a structural finite element model into a thermal model entails the structural and thermal engineers working very closely together and having a deep know of both modelling domains. Specifying

correct thermal properties, conductive paths, and boundary conditions on a complicated structural FEM can be very time-consuming and if not done very carefully, it may lead to modelling inconsistencies. This condition is the main limitation of the CPPT approach and has been a barrier to its extensive use in regular industrial practice [22].
Nonetheless, the CPPT technique has been utilized effectively in a number of research works of STOP analyses of space structures. In such cases, the enhanced precision of the temperature distribution became a sufficient reason for the extra modelling work, especially when extremely precise performance metrics were at stake. Therefore, the CPPT method is nowadays frequently regarded as the most advanced solution for temperature mapping in thermo-elastic analysis, in particular, when the utmost degree of physical realism is demanded in the modeling [22].

4.4 Prescribed Average Temperature (PAT) Method

The Prescribed Average Temperature (PAT) method is an innovative and physically consistent temperature mapping technique that stands out as the most advanced one among those commonly used for thermo-elastic analyses based on the coupling between lumped parameter thermal models and structural finite element models. The development of this method has been carried out to enhance the Centre-Point Prescribed Temperature approach after it has been realized that PAT can effectively overcome the main physical limitation of the former and also increase the accuracy of the transferred temperature fields [6].
The Prescribed Average Temperature implementation is a great deal more involved than the Patch-Wise Temperature one. In fact, one can consider the PAT procedure an improvement of the PWT flow in that the simple goal of sharing temperature data from the heat to the structural finite element model is complimented by an extra pathway of analysis.

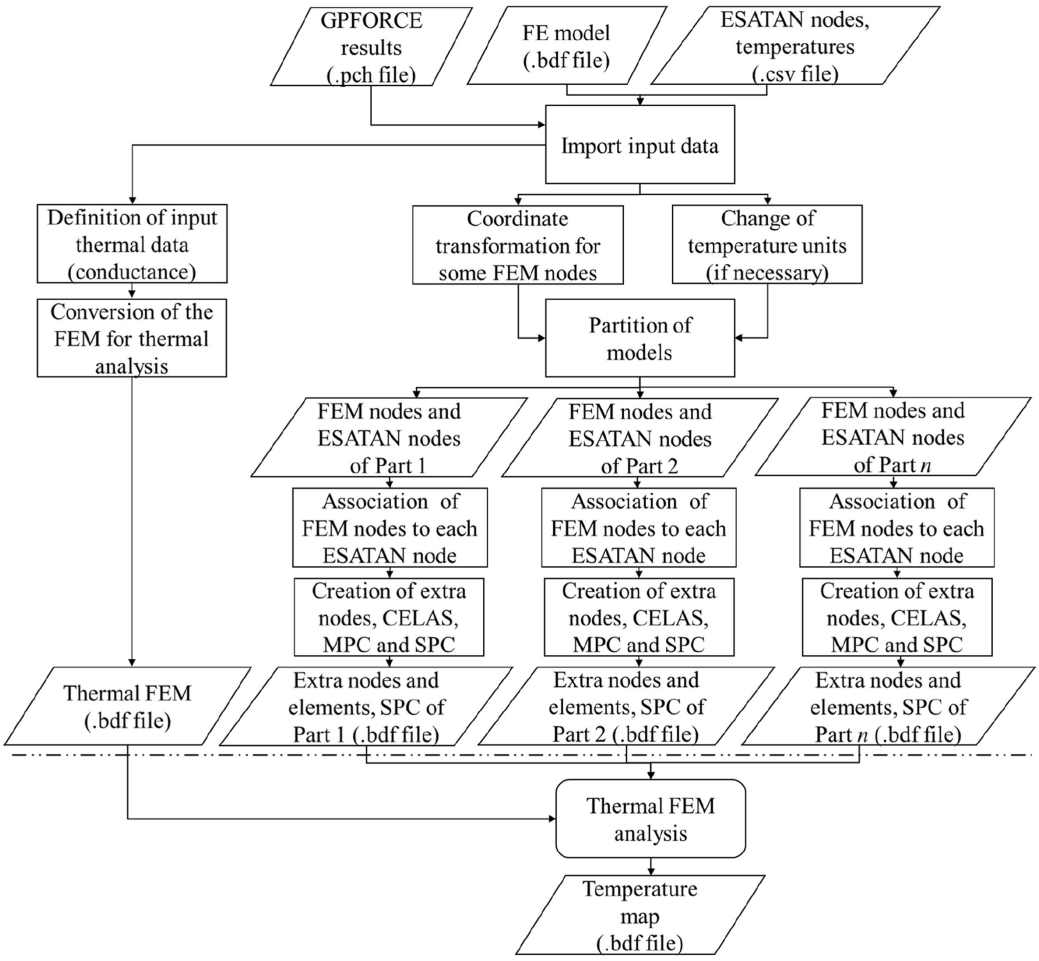

Figure 4.3: Flowchart of the temperature mapping process with the PAT method. [6].

As shown in figure above, besides temperature extraction and transfer from the lumped parameter thermal model, the PAT method also involves the transformation of the structural finite element model into a thermal model. This step makes it possible to carry out a conductive thermal analysis directly on the FEM, which is crucial for adjusting the temperature distribution while at the same time keeping the physical consistency to the average temperatures given by the lumped parameter model. Hence the entire chain of analyses now has additional tasks compared to the PWT method, such as defining thermal material properties on the FEM, setting up conductive connections, and imposing average temperature restrictions over the areas corresponding to each thermal node [6].
The PAT method rests on two key premises. Firstly, a temperature value

obtained at a node of a lumped parameter thermal model should not be interpreted as a temperature at a local point but as the average temperature of the physical domain represented by that thermal node. This is a modelling assumption that is inherent to the lumped parameter modelling paradigm and it is quite consistent with the fact that each thermal node corresponds to an aggregation of the thermal behaviour of a volume or surface. Secondly, the temperature on the structural finite element model can be further detailed by the assumption of a quasi-steady thermal equilibrium in which heat transfer is only through conduction within the structure, thus radiative exchanges are not considered. The refined temperature field in this scenario can be obtained by solving a linear thermal conductive problem on the finite element mesh [23].
Even though this expanded workflow leads to more modelling work and necessitates closer collaboration between thermal and structural analysis, it helps the PAT method to reach a quality of the resulting temperature maps at least as high as that of the PAT approach. Hence, the extra complexity introduced by the flowchart is justified not only by the higher accuracy but also by the greater physical realism of the temperature fields that are used as inputs for the following thermo-elastic analyses [23].
Just like the CPPT method, the PAT approach is based on the conversion of a structural FEM into a thermal model for an additional thermal analysis performed on the finite element model. This conversion keeps the same mesh topology but changes material properties and element definitions to represent conductive heat transfer. The thermal analysis is based on temperature data, which have been transferred from the lumped parameter model. However, the main difference is that the CPPT approach believes that the temperature corresponding to a thermal node is a point- wise value that is applied at a specific FEM node, whereas the PAT method is based on the notion that the average temperature in the finite element region corresponding to each thermal node is forced to be the same as the temperature given by the lumped parameter model [23].
This additional limitation is what makes the PAT approach work its magic. The PAT method manages to maintain the physical interpretation of the LPM by making sure the average temperature of the FEM region is consistent with the temperature of the thermal node. Thus the PAT method keeps the physical significance of the LPM while at the same time it is getting the benefit of the higher spatial resolution of the finite element mesh. The FEM temperature distribution, therefore, is physically meaningful and continuous, without depending on arbitrary interpolation schemes or temperature prescriptions at localised points. Hence, intrinsically, the PAT method is more precise than both types of patch-based methods and pure geometrical

interpolation techniques [23].
The PAT method has been developed and tested in the SINAS software environment which is a temperature mapping tool created over a few decades and tuned for thermo-elastic analyses in the space applications area. SINAS uses a thermal lumped parameter model generated in ESATAN-TMS and a structural finite element model defined in NASTRAN to perform the temperature mapping. An extremely important factor in this implementation is the geometric association between thermal and structural models that reiterates not only nodal positions but also the shapes and extents of the corresponding geometric entities. This kind of procedure, usually called model overlapping, entails determining the areas of intersection between thermal nodes and structural elements [23].
Earlier software versions like SINAS IV had issues that basically restricted the overlapping process of modelling. For instance, the success of such process was very much dependent on how similar the modelling approaches were for the thermal and structural models. Especially, these situations necessitated using elements of the same dimensionality in both models, usually two-dimensional representations, thus, the method could only be applied to cases where the geometric definitions were almost the same. This limitation has totally compromised the present day structural finite element models that are largely made up of three-dimensional elements to obtain the utmost accuracy, especially for Structural-Thermal-Optical Performance analyses, while thermal models still mainly use surface-based geometries [23].
The PAT method in the pysinas software package today has been able to overcome these drawbacks. The renewed tool is capable of handling any mix of geometric representations between lumped parameter models and finite element models, thus, achieving temperature mapping regardless of the level of differences in dimensionality and geometric definition. The technique's improved capacity and the capability of the PAT method have been drastically broadened, thus, it can be used nowadays for spacecraft analyses that involve complicated three-dimensional structural models [23].
Due to its solid physical basis, higher precision, and successful embedding in ESA, supported tools, the Prescribed Average Temperature method is generally considered the state-of-the-art solution for temperature mapping in thermo-elastic analysis coupled with LPM-FEM. Because of its capacity to create realistic temperature distributions over structural finite element models, this method is highly appropriate for ultra-precise applications, in which trustworthy prediction of thermo-elastic deformations is critical for system-level performance validation [23].

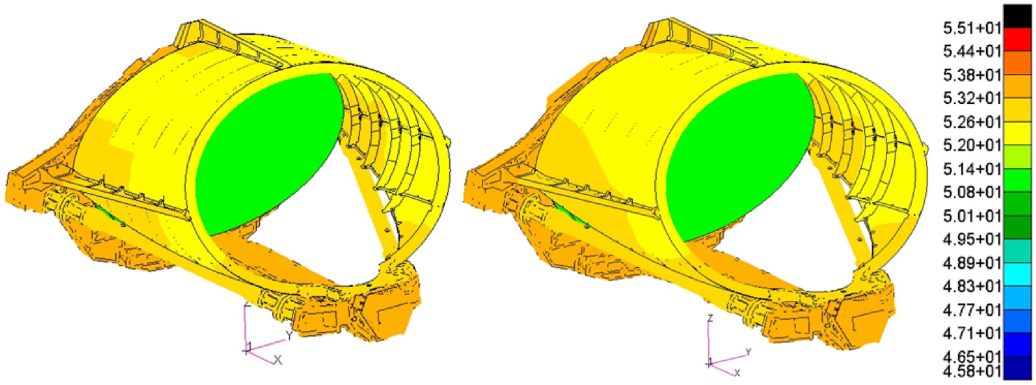

(a) Operational Cold case: PWT (left) and PAT (right)

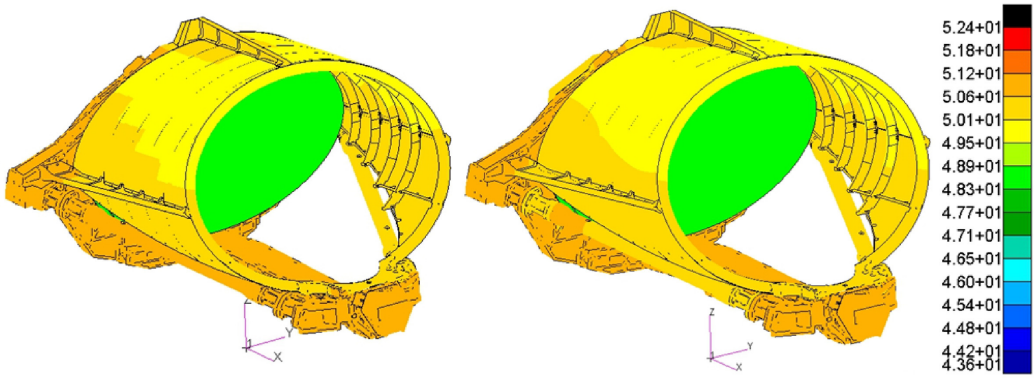

(b) Non-Operational Cold case: PWT (left) and PAT (right)

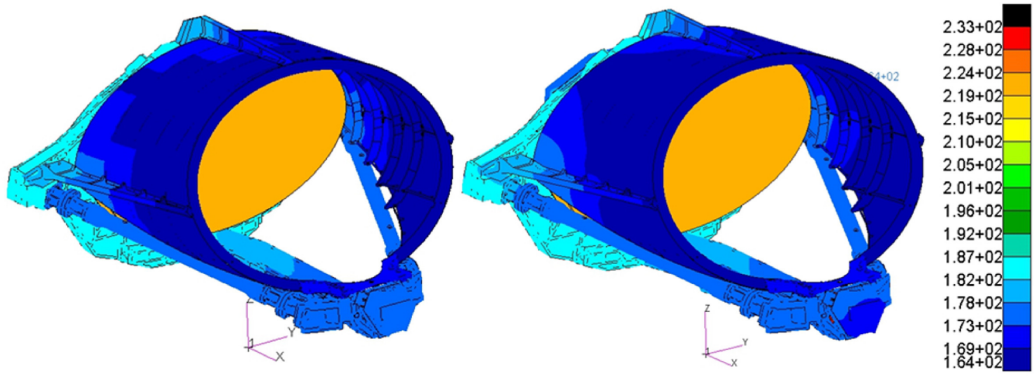

(c) Max Gradient case: PWT (left) and PAT (right)

Figure 4.4: Temperature maps (in Kelvin) transferred to the ARIEL Telescope Assembly FEM. [6].

4.4.1 Format of file-job

The pySinas executable is provided directly within the software installation directory and can be launched from the command line without requiring additional compilation steps. The execution of the tool is performed by invoking the following command from the terminal [7]:

```
<path to bin-dir>\run_pysinas --job=<jobfile name> --log=<logfile name>
```

The command line parameters are [7]:

- –**job** Mandatory parameter that specifies the job file name.
- –**log** Optional parameter to override the default log-file name.

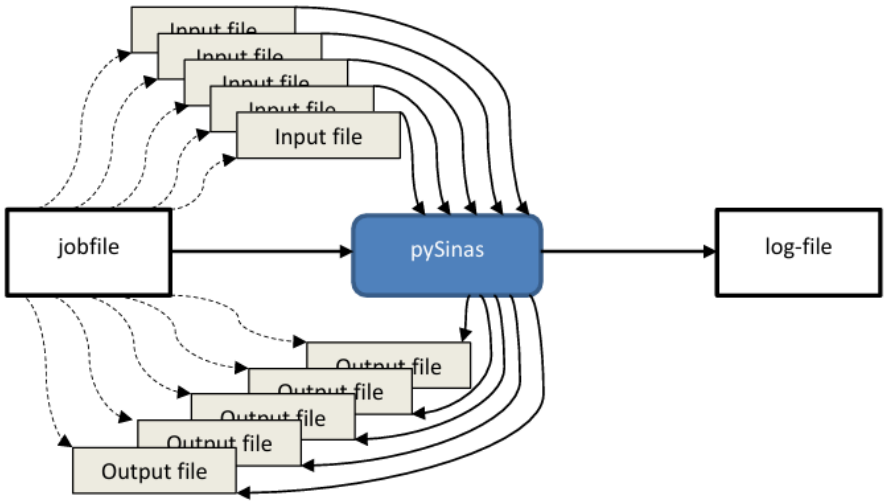

Figure 4.5: General data flow of pySinas [7].

Figure 4.5 shows a general workflow of PySinas and how the jobfile interacts with the input files and the outputs produced. The jobfile is the main piece that controls the whole operation and sets the tasks that PySinas should carry out one by one. Following the directions that the jobfile holds, the software opens the necessary input files among which can be thermal model data, structural finite element models, and auxiliary configuration files [7]. The jobfile is basically an ini-file that is used to organize the information into different sections where each section corresponds to a single task. It is noteworthy that the ini-file architecture allows repetition of non-unique section names. Thus, in the case that such section names are repeated, parameters of the first instance can be extended or replaced by the ones of

later occurrences. Hence, the user should be careful not to duplicate section names so as not to unintentionally overwrite existing parameters [7].
Another important issue is the order in which tasks are executed. PySinas takes up the sections specified in the jobfile in the alphabetical order of their section names, which is not necessarily the order they appear in the file. If there are task dependencies, for example, the output of one task is needed as the input of another, the user should carefully specify the section names to force the right order of execution. Typically, one sets a numbering scheme for the tasks, such as task_01, task_02, which makes sure that the alphabetical order corresponds to the desired workflow [7].
During running, PySinas not only produces the output files that have been requested but also creates a log file containing infos about the execution process, including the operations carried out, any warnings, and errors found. This well-arranged input-output system guarantees the temperature mapping process traceability, reproducibility, and robustness in the context of the overall thermo-elastic analysis workflow [7].

```
[task_01]
; Generation of con-file and sdf-file
; from the bdf file and ovl file
task = matgen
bdf  = mymodel.bdf
ovl  = mymodel.ovl
con  = mymodel_amat.con
sdf  = mymodel_cmat.sdf
[task_02]
task = interpolate
sdf  = mymodel_cmat.sdf
con  = mymodel_amat.con
tdf  = orbit_1.tdf
; set some tighter tolerances
ctl  = tight_tolerance.ctl
gen  = orbit_1_temps
```

Figure 4.6: Example of file log [7].

4.4.2 Task "ttm_gen"

According to the European Guidelines for Thermo-Elastic Verification, TEV process relies largely on the use of a temperature transfer matrix, commonly

referred to as the TTM. This matrix formalizes the connection between the temperatures calculated in the thermal model and the corresponding temperatures which are assigned to the nodes of the structural finite element model as shown in the following expression [7]:

$$\{T_s\} = [M_T]\{T_t\} \tag{4.1}$$

In the equation 4.1, T_t the vector represents the temperatures of the heat nodes. On the other hand, the vector T_s represents the temperature of the nodes of the structural finite element or GRID points. The rectangular matrix $[M\_T]$ called the temperature transfer matrix, specifies the mapping relation between the thermal and structural models. The matrix operation illustrated in equation 4.1 is carried out within the TEV chain and gives the ability to generate the temperature fields mapped on the structural model in a very efficient manner [7].
Basically, each column of the temperature transfer matrix refers to one thermal node and shows the structural temperature field which would result after a unit temperature excitation was applied only to that node. To carry out this method, the temperature of the selected thermal node is set to unity and, at the same time, the temperature of all the other thermal nodes are set to zero. The temperature field obtained on the structural model is then called a unitary temperature field, which may look like the vector presented in the equation 4.2 the unit value is located at the position corresponding to the i-th thermal node, while all other components of the thermal temperature vector are zero. [7].

$$\{l_t^{(i)}\} = \begin{Bmatrix} 0 \\ \vdots \\ 0 \\ 1 \\ 0 \\ \vdots \\ 0 \end{Bmatrix} \tag{4.2}$$

Each vector $\{I_s^{(i)}\}$ represents the temperature field on the structural finite element model that results from a unitary temperature excitation of the th-thermal node, the temperature at this node is set to unity whereas all other thermal nodes' temperatures are set to zero [7].

$$[M_T] = \left[\{I_s^{(1)}\} \quad \cdots \quad \{I_s^{(i-1)}\} \quad \{I_s^{(i)}\} \quad \{I_s^{(i+1)}\} \quad \cdots \quad \{I_s^{(n_t)}\}\right] \tag{4.3}$$

The task 'ttm_gen' computes the vectors $\{I_s^{(i)}\}$, assembles these into a matrix and saves the matrix with corresponding administrative information in the ttm-file. The format of the ttm-file is hdf5.

The approach to compute the matrix $[M_T]$, that is followed by the task 'ttm_gen', is by solving the PAT equation within part of the right hand-side a unit matrix $[I_t^{(i)}]$ representing the vectors with thermal node temperatures [7].

$$\begin{bmatrix} C & A^T \\ A & 0 \end{bmatrix} \begin{bmatrix} M_T \\ Q \end{bmatrix} = \begin{bmatrix} 0 \\ I_t \end{bmatrix} \tag{4.4}$$

4.4.3 Input files

The task 'ttm_gen' uses the following job-file parameters to specify input file names:

Example input with pysinas:

```
[0-ttmgen_01]
task = ttm_gen
bdf = double_walled_panel_model.bdf
ovl = double_walled_panel.ovl
ttm = double_walled_panel_ttm_sparse_01.h5
fieldsperchunk = 4
```

Figure 4.7: ttm_generation task [7].

- **BDF file** NASTRAN (BDF) file is one of the principal input files for PySinas. It contains the definition of the conductive finite element model of the structure. The file is essentially the conductive behaviour of the system through which the conduction matrix for the temperature transfer process can be derived. Depending on the complexity of the model and the adopted modelling strategy, one or more BDF files can be provided [6].
  The BDF file that is used for temperature mapping is not necessarily the original structural finite element model. Rather, it is a conductive thermal finite element model converted from the structural NASTRAN model. The structural model is modified and extended by introducing heat conduction elements and thermal-specific properties to enable the representation of heat conduction to be consistent during the conversion process. Although the structural geometrical description is mostly kept, the thermal model is mainly concerned with the conductive heat transfer paths within the system [6].
  Especially PAT method, this step to change is very important because the same finite element mesh is used to carry out thermal conductive analyses. Here, most of the original features of the structural model,

e.g. nodes, coordinate systems, 2D and 3D elements, are kept unchanged. Additional modelling is however required to make some other entities compatible with thermal analysis. Materials, joints, and rigid elements in particular have to be adjusted not merely to include thermal parameters, chiefly thermal conductivity values, but also to be physically valid given the heat transfer [6].
Table 4.12 lists the NASTRAN entries that need to be changed during this conversion process. These changes are essential to make the finite element model be a conductive one and thus, fit for thermal simulations. By delivering a complete and consistent conductive FEM to the BDF file, PySinas can implement the conduction matrix and hence, accurately generate temperature transfer matrices within the framework of the PAT [6].

Table 1. List of NASTRAN entries modified for thermal analysis.

Category	Structural entries	Thermal entries	Description
Materials	MAT1	MAT4	Entry for isotropic material definition
	MAT8	MAT5	Entry for orthotropic and anisotropic material definition
Element properties	PCOMP	PSHELL	Entry for composite 2D property
	PBARL, PBEAML	PBAR, PBEAM	Entries for 1D bar and beam properties
	PBUSH	PELAS	Entry for property of the joining 1D elements
Elements	CBUSH	CELAS	Entry for the joining 1D elements
Multipoint constraints	RBE2, RBE3, RBAR	MPC or CELAS	Entries for multipoint constraints

Figure 4.8: List of NASTRAN entries modified for thermal analysis [6].

At present, the work involves substituting isotropic structural materials defined by MAT1 cards and characterized by parameters such as Young's modulus and Poisson's ratio with their equivalent isotropic thermal material definitions using MAT4 cards, where thermal con-

ductivity is the main property. In a similar manner, the more complex material definitions that were originally described by MAT8 or MAT9 cards were replaced by MAT5 entries, which allows the definition of orthotropic and anisotropic thermal conductivities [6].
In addition, great care was given to the conversion of joints and connection elements. Shear rigid structural elements that were originally modelled with RBE3 cards were changed into RBE2 elements that pySinas automatically converts to CELAS2 elements by using 'rbe2_conduction' option. This operation is of paramount importance since the method of joining entities determines to a large extent the heat conduction paths of the structure. Because bonding in structural FEMs is usually depicted by combinations of rigid elements, appropriate conversion of these elements to thermally valid connections is not only necessary but also a key attribute of the overall FEM conversion process [6].

- **overlap file** Another important input for pySinas is the overlap file delineating the correspondence between the thermal nodes of the thermal model and the finite elements of the structural finite element model. This file thus has a vital role rested on it for the temperature mapping process as it lays down the geometric connection basis for the thermal node temperatures to be transferred onto the structural mesh in a physically consistent manner [7].
  The overlap file is the map providing exact information on how to point out the structural element or the specific region that relates to each thermal node. Thanks to the established connection, pySinas gets to interpret a thermal node's temperature as a certain component for the temperature distribution of the structural finite element model. This correspondence is an essential part of advanced temperature mapping methods, for example, the PAT method, where the spatial relationship between thermal and structural models is correctly defined as having a direct impact on the accuracy of the resulting temperature transfer matrix [7].
  Overlap data can be given either from a single overlap file or from a list of several overlap files, in line with the model complexity and the modelling strategy chosen. The use of several overlap files permits a modular definition of the thermal, to, structural associations, which can be very helpful for large or very detailed models. The overlap file, by clearly specifying these correspondences, guarantees the mapping process traceability and robustness, thus allowing pySinas to always correctly associate the thermal and structural models in the whole

thermo-elastic analysis workflow [7].

4.5 Preparation of tetm

The thermo-elastic analysis second phase is basically to employ the TEV tool to set up the structural input needed for the computation of thermo- elastic responses. Here, one uses the task tetm_prep to generate the thermo-elastic responses associated with each column of the temperature transfer matrix [8]. The tetm_prep piece of work automatically creates a bunch of input files, based on this formulation, for one or more NASTRAN runs. These files specify the thermal loading conditions corresponding to the individual unitary temperature fields and represent the necessary input for the next computation of the thermo-elastic transfer matrix with the tetm_gen task. The figure below shows how the tetm_prep task takes the temperature transfer matrix file as its main input and prepares the data flow necessary for the structural analyses [8].

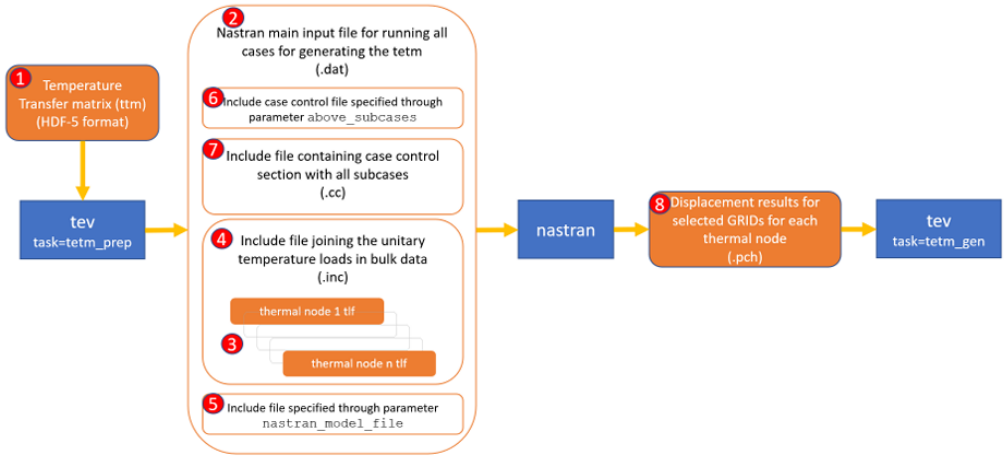

Figure 4.9: Data flow and files generated by the task 'tetm_prep' [8].

The process results in at least one ready to run Nastran input file (File 2) that is referring to several include files [8]:

- **file 3** The temperature load files show the various individual columns of the temperature transfer matrix. One file is equivalent to a vector I_s, defined by equation 4.3, which is a temperature field mapped onto the structural model corresponding to a unit thermal excitation. Such

vectors are saved to separate temperature load files with the .tlf extension, formatted as NASTRAN TEMP cards. TEV tool automatically carries out the production of these files.

```
$ tetm_prep_01.inc
$ file to be included in the bdf for nastran job 01 for generating
$ the thermo-elastic transfer matrix
$
TEMPD*            999999 2.200000000E+01
INCLUDE 'tetm_prep_0001.tlf'
INCLUDE 'tetm_prep_0002.tlf'
INCLUDE 'tetm_prep_0003.tlf'
INCLUDE 'tetm_prep_0004.tlf'
INCLUDE 'tetm_prep_0005.tlf'
INCLUDE 'tetm_prep_0006.tlf'
INCLUDE 'tetm_prep_0007.tlf'
INCLUDE 'tetm_prep_0008.tlf'
INCLUDE 'tetm_prep_0009.tlf'
INCLUDE 'tetm_prep_0010.tlf'
INCLUDE 'tetm_prep_0011.tlf'
INCLUDE 'tetm_prep_0012.tlf'
INCLUDE 'tetm_prep_0013.tlf'
INCLUDE 'tetm_prep_0014.tlf'
INCLUDE 'tetm_prep_0015.tlf'
INCLUDE 'tetm_prep_0016.tlf'
INCLUDE 'tetm_prep_0017.tlf'
INCLUDE 'tetm_prep_0018.tlf'
$ end of generated part of bdf section
```

Figure 4.10: TEMP card example [5].

- **file 4** This file is in NASTRAN bulk data format and it is just a list of INCLUDE statements each pointing to a temperature load file generated in File 3. The idea behind this file is to make sure that every temperature load definition is properly included in the structural analysis. The TEV tool automatically generates this file.
- **file 5** Structural finite element model definition is provided in NASTRAN bulk data format and encompasses the geometry, material properties, element definitions, and the relevant boundary conditions, such as SPCs. The user provides this file, and its name and location are specified via the parameter 'nastran_model_file'.

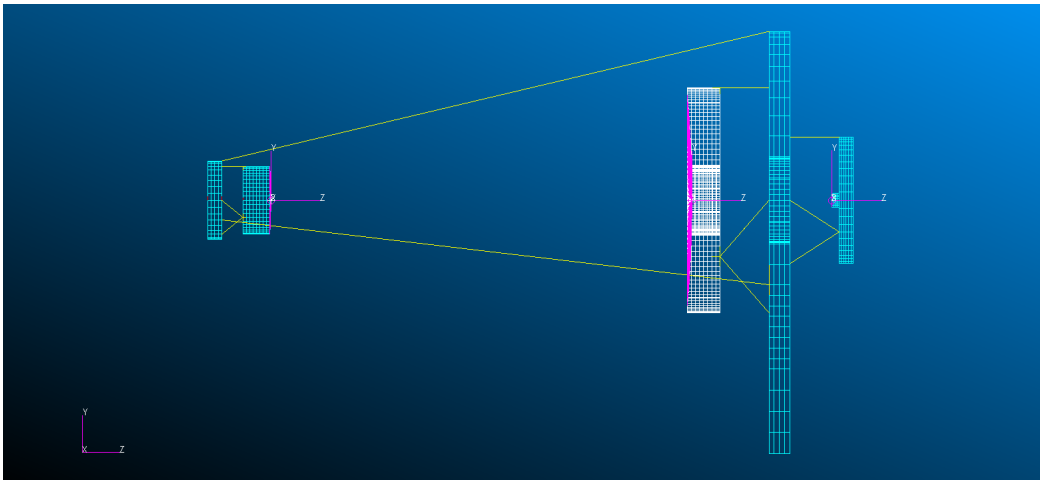

Figure 4.11: Structural model.

- **file 6** This user-defined include file is located just before the subcase definitions and comprises the output set definitions, output requests, and the activation of the relevant SPC sets, MPC sets, and other necessary control parameters. The file name and path are given through the 'above_subcases' parameter.

```
SET 90000 = 171, 200, 339
DISP(PUNCH) = 90000
SPC = 1
```

Figure 4.12: Above_subcase example [5].

- **file 7** This include file comprises the entire case control definitions necessary for setting up one subcase for each column of the temperature transfer matrix, i.e. , equal to the total number of thermal nodes considered. The file is generated automatically by the TEV tool and guarantees that each unitary temperature load is analysed in a separate subcase.

```
[00-tetm_prep]
task=tetm_prep
ttm=../1-ttm_gen/double_walled_panel_ttm_sparse_01.h5
gen_out=../3-nastran_runs/tetm_prep
nparallel_nastran_runs = 1
reference_temperature = 22.
nastran_above_subcases=above_subcases_special.bdf
nastran_model_file = structural_te_model_special.bdf
```

Figure 4.13: 'tetm_prep' task [5].

NASTRAN is used in the next stage of the thermo-elastic analysis to determine the structural response to the thermal loading conditions prepared by the 'tetm_prep task'.
For each subcase, NASTRAN carries out a structural analysis and calculates the displacements of the finite element nodes that result from the load. The displacement results of the nodes mentioned in the 'above_subcases' file are saved in a punch (.pch) file. This file contains the thermo-elastic displacement responses corresponding to each unitary temperature field.
The .pch file thus created is fed to the TEV tool in the next step. Here the thermo-elastic transfer matrix is calculated. This matrix describes the relationship between the mapped temperature fields and the structural displacements produced. Thus, it makes the thermo-elastic response evaluation for any thermal loading conditions quick and easy [8].

```
$TITLE   =                                                                1
$SUBTITLE= THERMAL NODE 111                                               2
$LABEL   =                                                                3
$DISPLACEMENTS                                                            4
$REAL OUTPUT                                                              5
$SUBCASE ID =          1                                                  6
       171    G        -1.711546E-05     -1.803151E-04      4.894987E-06   7
-CONT-                   1.246072E-04     -1.334359E-05     -1.444691E-05   8
       200    G        -1.818307E-05     -1.941235E-04      1.684299E-05   9
-CONT-                   1.089046E-04     -1.214546E-05     -8.865546E-06  10
       339    G        -1.943916E-05     -1.994903E-04      4.886096E-06  11
-CONT-                   1.198595E-04     -1.273352E-05     -1.369831E-05  12
```

Figure 4.14: puch file example [5].

Chapter 5

Implementation of TEV

5.1 tetm_gen task

The primary focus of chapter 5 is on the use of TEV software to generate a thermo-elastic transfer matrix along with other necessary outputs needed for the subsequent stages of the analysis. The initial step of this operation is carried out by the tetm_gen task, which is in charge of transforming the results of the structural analysis into a thermo-elastic transfer matrix [5].
The tetm_gen task requires as input the data produced by the NASTRAN runs that were carried out in the previous stage. These data come in the form of punch files, which at the moment are the only input format recognized by TEV. The displacement information found in the .pch files is transformed and turned into a tetm, which is then saved in a file using the HDF5 format. This format provides an efficient and organized way of storing large datasets and makes it easier to access and manipulate the data later on [5].
Furthermore, TEV is capable of running several NASTRAN simulations concurrently. When that happens, the tetm_gen task can accept multiple .pch files as inputs and merge the results into one tetm.
Figure 5.1 shows the general process related to the tetm_gen task and how it fits into the TEV, based thermo-elastic analysis flow [5].

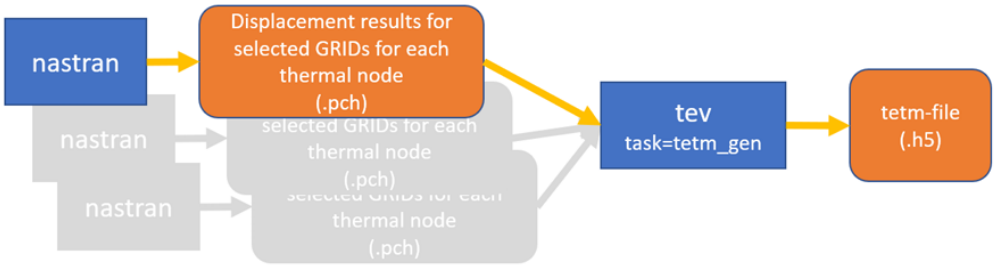

Figure 5.1: Conversion of Nastran output files into the tetm-file [5].

5.2 Thermo-elastic transfer matrix

The thermo-elastic transfer matrix is one of the most effective instruments for rapidly determining the structural responses that result from thermal loads. It is developed based on a number of basic assumptions which need to be fulfilled if the method is to be used. For instance, the structural finite element model for determining the thermo-elastic mechanical responses should not have any non-linearity, and the constitutive properties of the materials should remain constant with temperature. If these parameters are met, the linear superposition principle can be applied, thus the overall thermo-elastic response can be represented as a sum of scaled individual response vectors (each corresponding to a single thermal loading element).
Applying this idea to thermo-elastic problems, one has to remember that: the very origin of the thermo-elastic effect is temperature change, not temperature itself [5].
Structural displacements and interior forces are the results of the space-time changes of temperature relative to the reference thermal condition, at which the structure is considered to be without deformation and internal force. This 'reference condition' is typically called the reference temperature [5].
As a result, the temperatures that refer to the thermal nodes have to be understood as a reference temperature plus a temperature fluctuation relative to that reference. Hence, the thermo-elastic transfer matrix works on temperature increments, converting changes in the thermal field into the corresponding structural responses. This way of representing the problem guarantees that the thermo-elastic displacements calculated are not only physically meaningful but also consistent with the stress-free reference configuration assumed [5].

$$\{T_t\} = \{T_t^{\text{ref}}\} + \{\Delta T_t\} \tag{5.1}$$

Similarly, the temperature field obtained for the structural model, $\{T_s\}$ must also be interpreted as the combination of a reference temperature field and

a temperature variation relative to this reference state.

$$\{T_s\} = \{T_s^{\text{ref}}\} + \{\Delta T_s\} \tag{5.2}$$

Equations 5.3 essentially shows that the thermo-elastic response can be modeled as a linear operator with respect to temperature changes only if the principle of linear superposition is valid, where F is a functional that relates the thermal node temperature to the displacements of structural nodes. Based on this premise, the displacement of a structure due to any random thermal field can be represented as a linear combination of the responses to the corresponding unit temperature variations. This is the foundational principle that justifies the thermo-elastic transfer matrix concept theoretically [5].

$$\begin{aligned} \{u\} &= F(\{\Delta T_t\}) \\ F(c\,\{\Delta T_t\}) &= c\,F(\{\Delta T_t\}) \\ F(\{\Delta T_{t1}\} + \{\Delta T_{t2}\}) &= F(\{\Delta T_{t1}\}) + F(\{\Delta T_{t2}\}) \end{aligned} \tag{5.3}$$

Having established that the principle of linear superposition applies to temperature variations, the mapping of thermal node temperature changes $\{\Delta T_t\}$, defined with respect to the thermal reference temperature field $\{T_t^{\text{ref}}\}$, to the corresponding structural node displacement responses $\{u\}$ can be expressed through the equations 5.4 [5].

$$\{u\} = [\text{TETM}]\,\{\Delta T_t\} \tag{5.4}$$

The components of the displacement vector $\{u\}$ correspond to the thermo-elastic response variables which are, at present, structurally limited to only displacements. An important benefit of the thermo-elastic transfer matrix is that the displacement vector $\{u\}$ needs to contain only those structural node responses which are instrumental in the assessment of instrument performance parameters that measure the deterioration of system performance due to thermo-elastic effects [5].
After the thermo-elastic transfer matrix has been created, it becomes very easy to calculate the thermo-elastic responses for different thermal load cases. If the only change is the temperature field applied to the satellite, the required structural displacements can be directly obtained by the multiplication of the thermo-elastic transfer matrix and the thermal node temperature variation vector, thus a simple matrix-vector operation. This means that there is no need to perform the entire temperature mapping, structural analysis, and post-processing procedure again for each thermal scenario [5].
This feature comes handy especially in situations where thermo-mechanical classification methods at times require the derivation of thermo-elastic responses for numerous thermal cases. Under these circumstances, the tetm

usage drastically diminishes the computational workload and time for analysis, at the same time, guaranteeing the consistency and precision of the results obtained across all these cases [5].

5.3 Performance parameters

Before the thermo-elastic outputs are generated, it is essential to firstly identify the performance parameters that are relevant and which will help in the evaluation of the system behaviour.
In this paper, the system under consideration is a satellite with an optical payload. Hence, the performance parameters picked are those that relate to the telescope's optical alignment and geometrical stability. The main performance indicators selected for determining the correct operation of the device are the relative alignment of the mirrors, this is usually given as the M2 tilt; the lateral displacement of the secondary mirror, which is referred to as M2 de-center; and the variation in the axial distance between the primary and secondary mirrors, known as the M1-M2 distance. These parameters represent the major optical degradation and, thus, are the most critical thermo-elastic response characteristics of the system under consideration [16].

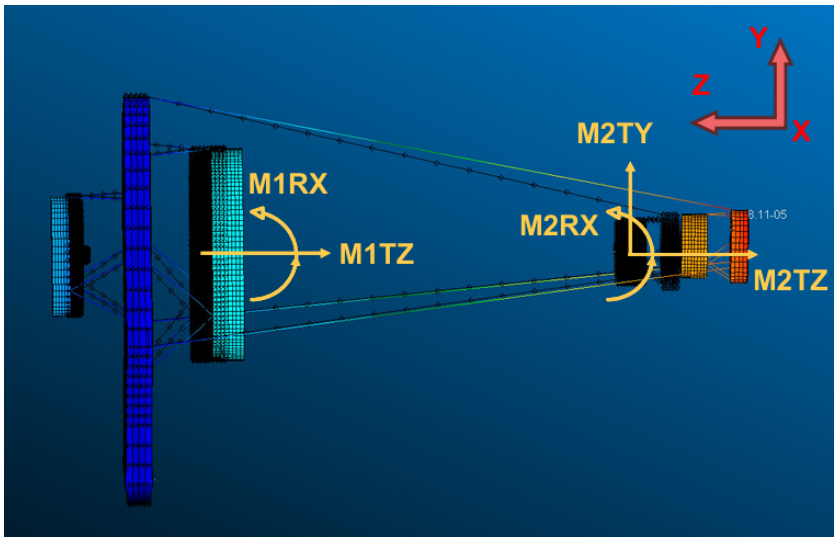

Figure 5.2: Performance parameters.

5.4 TEV output

Besides the calculation of thermo-elastic displacement responses, TEV is a set of tools that provides functionalities which are specifically aimed at the support of model development and validation activities. Refining and assessing the quality of thermal and structural models require a deep understanding of the structure parts that contribute most significantly to the overall thermo-elastic response. Engineers that identify the deformation-driving regions can concentrate their modelling work in such areas and therefore the analysis becomes more predictive [5].
This feature is realised in TEV by the 'te_response' task and it is also available through the GUI. It is essentially a method of dividing the thermal nodes into sets representing different parts of the structure, or subsystems. Each set is associated with a particular spacecraft or instrument segment, thus the total thermo-elastic response can be broken down into contributions from the different structural areas [5].
By dissecting the thermo-elastic reactions linked to each group, TEV facilitates the pinpointing of major contributors to displacement or rotation results. This geographical delineation of the problem is especially helpful in the stages of model correlation, sensitivity analysis, and design optimisation where the need to know the physical source of thermo-elastic deformation is equally important to the need to get their magnitude [5].
According to the thermal node groups that were determined, TEV creates various kinds of temperature variation fields, with each being linked to a particular structural region. The resulting thermo-elastic contribution to the overall structural response from each group is calculated. Besides the option of a regional breakdown, the several temperature field types also make it possible to single out the effect of the specific attributes of the applied thermal field on the resultant thermo-elastic response [5].

- **UnitT** The initial output type is the one that corresponds to a uniform temperature variation of a unit applied to a chosen group of thermal nodes. Moreover, a unit temperature increase is given to all thermal nodes that are part of the group under consideration, and a zero temperature change is imposed on all other thermal nodes of the model.
  The temperature distribution offers a first insight into the inherent capability of each mechanical region to produce thermoelastic response variables. A thorough investigation of the displacement responses that result makes it possible to determine the relative sensitivity of the system to temperature changes in particular areas of the structure [5].
  It is important to emphasize that the relative contribution revealed by

this unit temperature field might not accurately represent the real effect in the actual working conditions. Eventually, the effective contribution of any group is determined by how large and how the real temperature changes, as predicted by thermal analysis, are distributed. A group which, under unit excitation, seems very influential might have only a small impact if actual temperature changes in that region are minimal. Another benefit of this kind of temperature field is that it does not rely on the thermal analysis results. So, it can be a tool for quick sensitivity checks at early design phases even before the entire thermal simulation is ready [5].

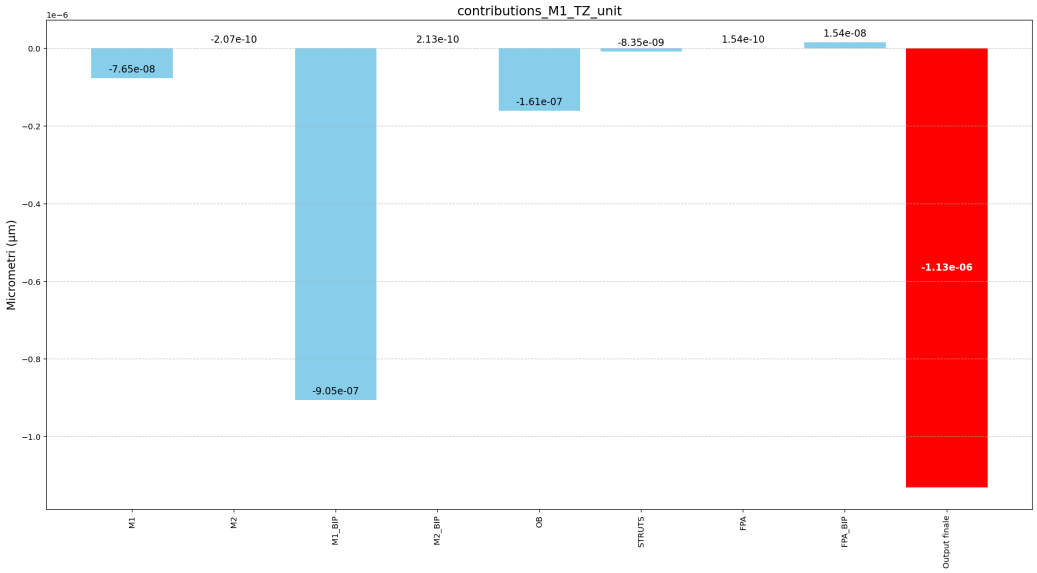

Figure 5.3: UnitT for M1_TZ.

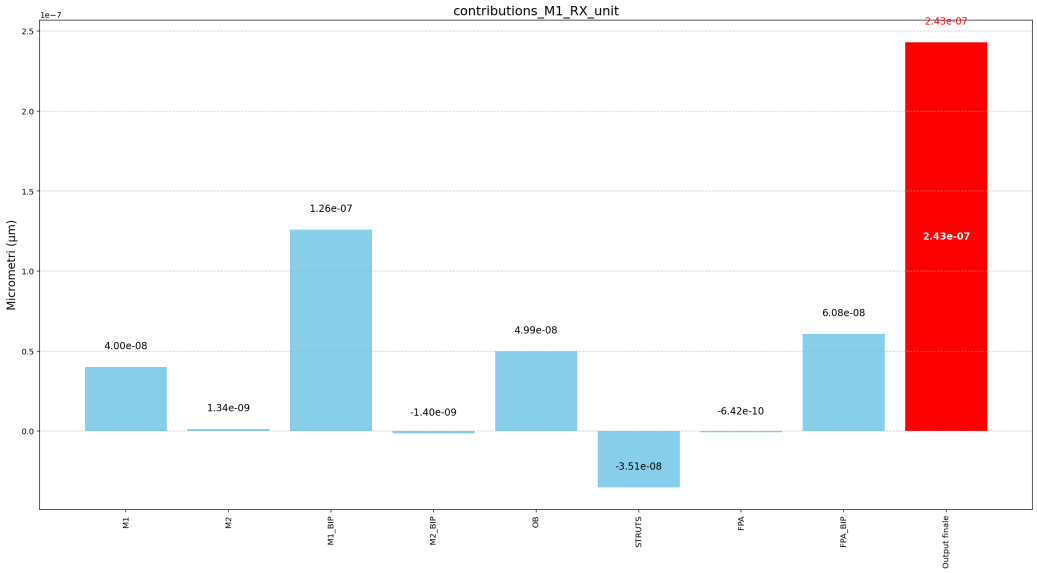

Figure 5.4: UnitT for M1_RX.

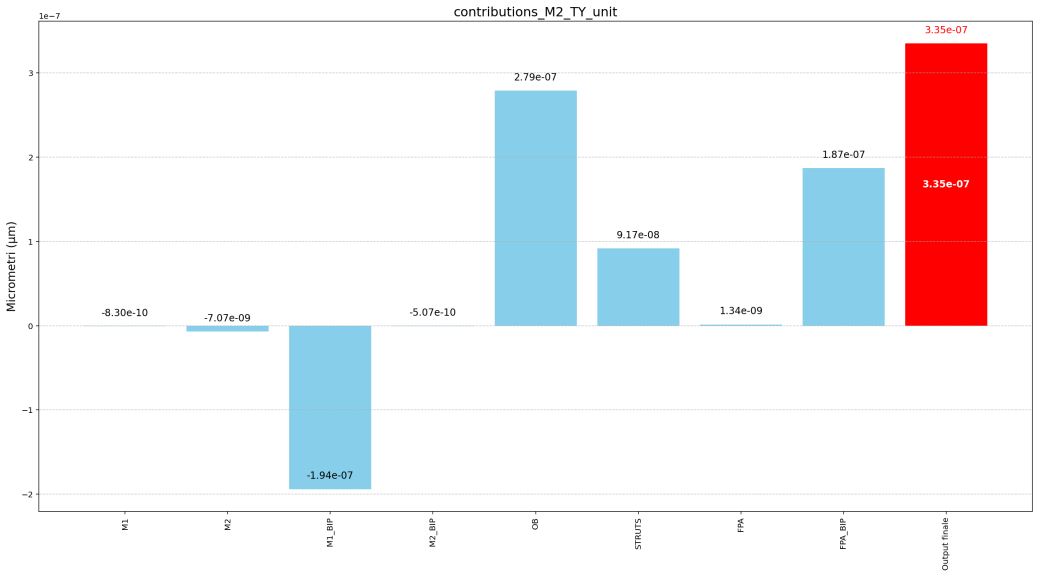

Figure 5.5: UnitT for M2_TY.

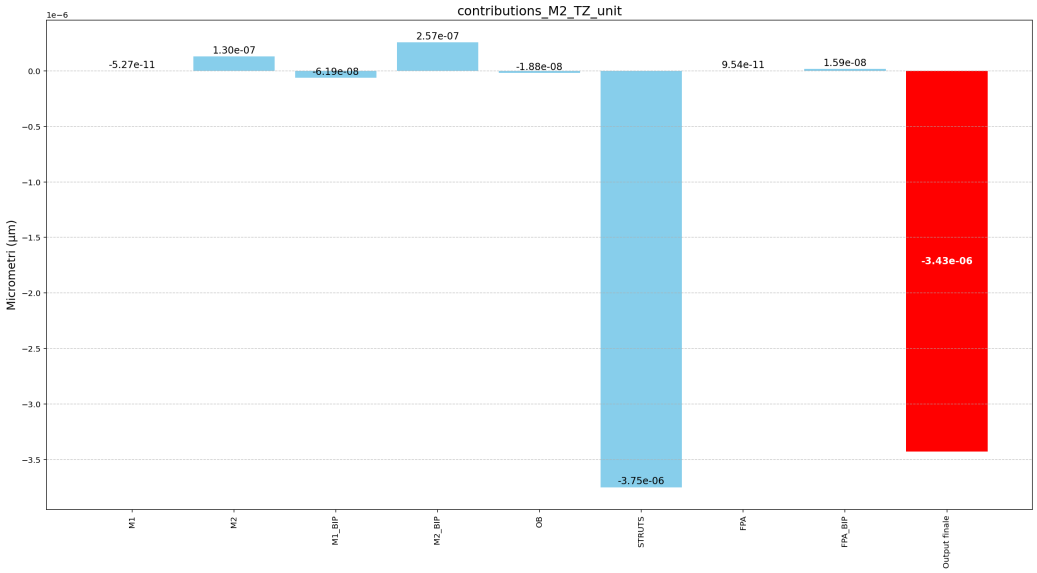

Figure 5.6: UnitT for M2_TZ.

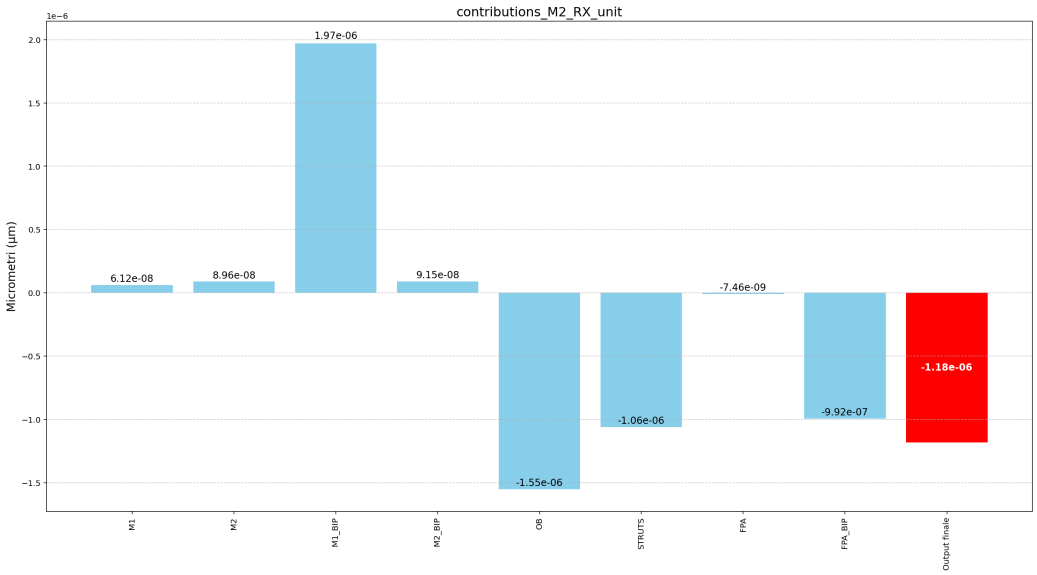

Figure 5.7: UnitT for M2_RX.

The bar charts for the UnitT output illustrate the thermo-elastic response that comes from a one degree unit step temperature change being applied to each thermal node group separately. In other words, a temperature rise of one unit is given to the chosen group and all other

thermal nodes are at zero temperature variation. So, the bars show the inherent ability of each structural region to the considered thermo-elastic response variable. The height of the bar shows the magnitude of the effect that the region would have on the output if it experienced a unit temperature change, and the sign indicates the direction of the displacement. The last bar is the result of adding all the group contributions and it serves as a proof of the linearity assumption, which is at the basis of the thermo-elastic transfer matrix formulation.
Analyzing the outputs results, it appears that, the rotational outputs M1_RX and M2_RX, the biggest contribution is coming from the M1_BIP group, which means that the rotational behaviour is very sensitive to temperature changes in that structure region. On the other hand, regarding the translation along the optical axis of the second mirror (M2_TZ), the most significant contribution comes from the support structure thus essentially determining the out-of-plane displacements. Finally, the lateral translation of second mirror (M2_TY) is essentially affected by the M1_BIP group and the optical bench, thus indicating the mirror interface region, the optical support structure coupling effect.

- **DeltaT** The deltaT operation is essentially the difference in temperature between the measured field of temperatures from the thermal analysis actually carried out with ESATAN-TMS, and that used as the basis of the structure's design. By this process, the temperature variations on the surface are obtained from the temperature changes by which the structure has been directly exposed.
  The temperature changes, therefore, correspond to what the spacecraft has actually undergone and are hence used to calculate the thermo-elastic deformation associated with the thermal loading condition via the tetm. While the UnitT case was a hypothetical scenario, the deltaT output here is indeed the real case under which the structure operates and therefore stands for the physically valid displacement responses that correspond to the predicted thermal environment [5].

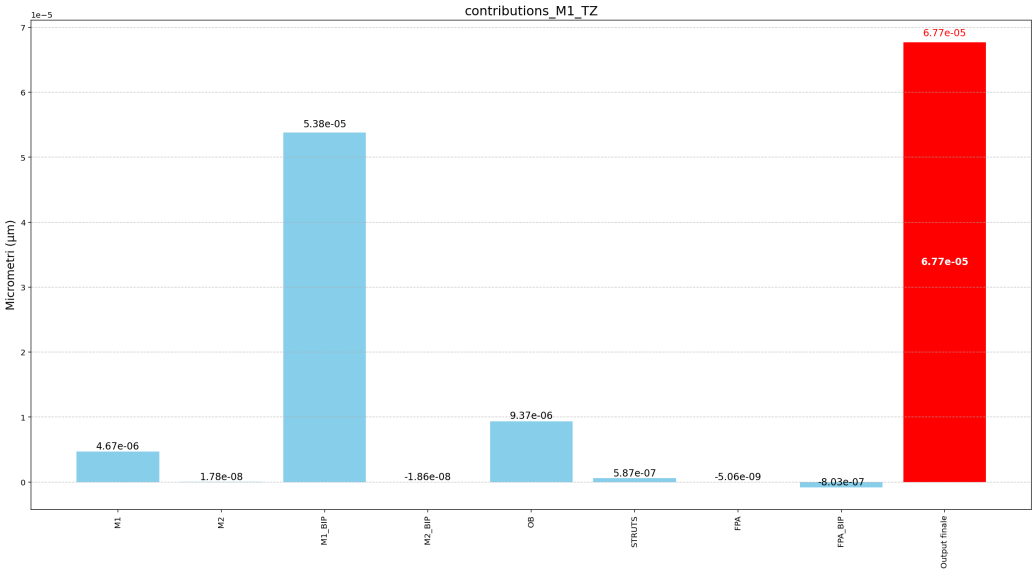

Figure 5.8: DeltaT for M1_TZ.

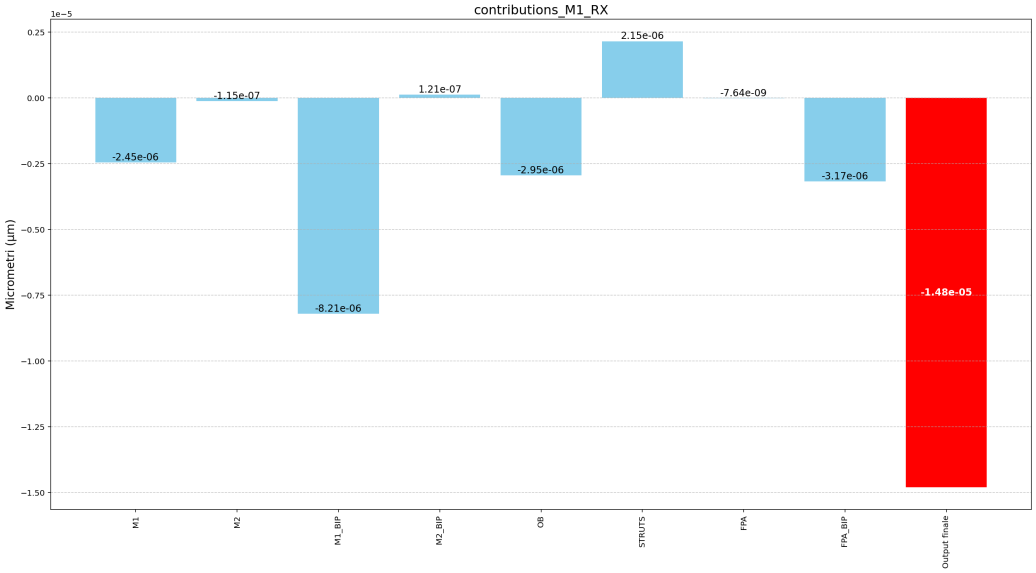

Figure 5.9: DeltaT for M1_RX.

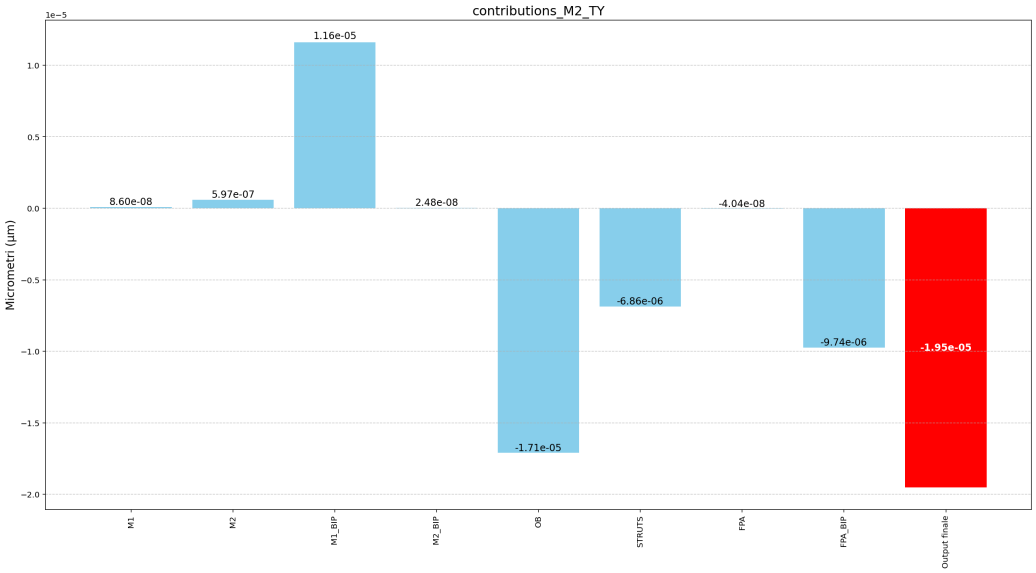

Figure 5.10: DeltaT for M2_TY.

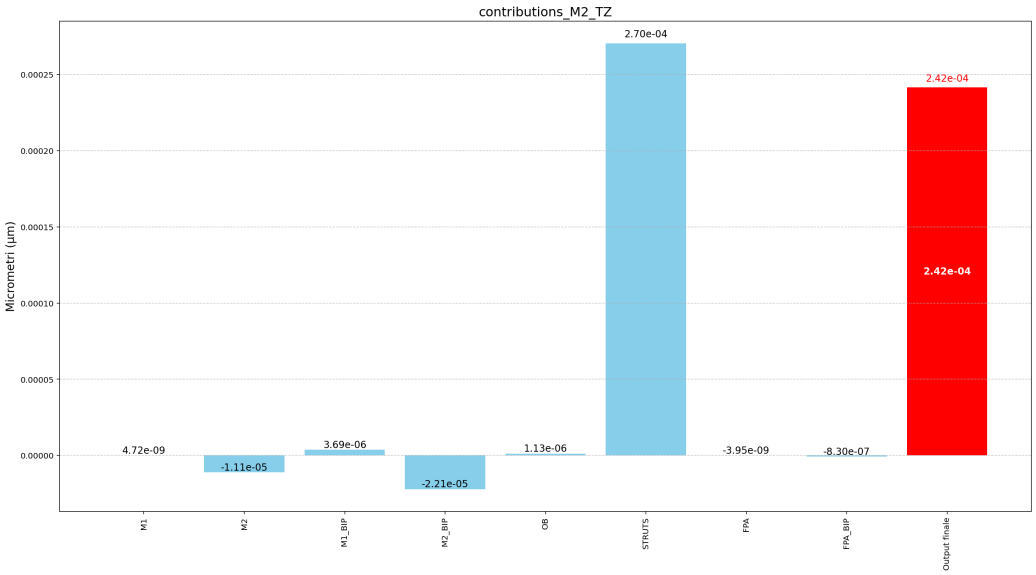

Figure 5.11: DeltaT for M2_TZ.

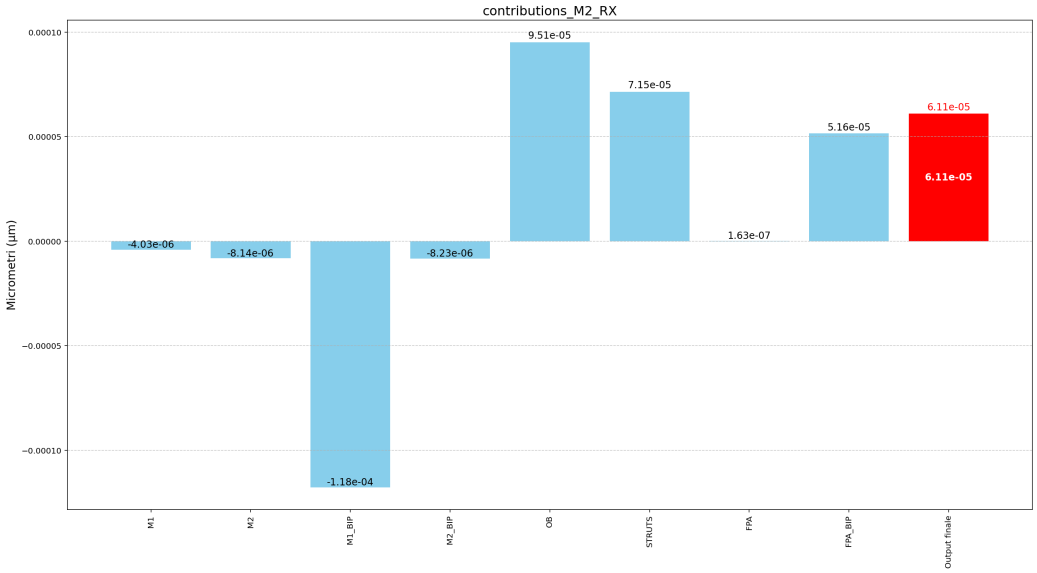

Figure 5.12: DeltaT for M2_RX.

The bar charts corresponding to the deltaT output show the thermo-elastic responses resulted from the application of the real variation in temperature field obtained from the ESATAN-TMS thermal analysis. The main contributing groups for each response variable that were already constant in the UnitT sensitivity analysis still remain the dominant ones. Thus, it can be concluded that the structural regions with the highest intrinsic sensitivity are the ones causing the deformation under the realistic thermal conditions.
The main difference between the UnitT and deltaT results is that the magnitude and sign of the individual contributions are now changing based on the actual temperature distribution predicted for each thermal node group. UnitT is a normalized sensitivity assessment, whereas the deltaT case is the real thermo-elastic deformation state induced by the operational thermal environment.
From examining the graphs, it is apparent that the deformation that should be given the most attention is the axial translation of the second mirror, M2_TZ, which shows the largest absolute displacement among the considered response variables. Thus, the out-of-plane stability of the second mirror seems to represent a crucial factor in terms of performance. For each of the response variables, one needs to compare the calculated displacement with the corresponding design requirement. The values obtained have to be within the allowed limits in order to be compliant with the performance criteria and to ensure that thermo-

elastic deformations do not result in unacceptable degradation of the instrument functionality.

- **groupAverageT** The groupAverageT output results from the real temperature variation field (deltaT) by first calculating, at each time step, the mean temperature change of all the thermal nodes of the group in question. This average temperature then equally represents the whole group, and, at the same time, the rest of the nodes are set to zero. This way, the thermo-elastic response linked with the overall thermal behaviour of each structural region can be obtained by eliminating the local temperature variations and focusing on the impact of the average thermal loading.
  The group average temperature change is formally computed for each time step with [5]:

$$\Delta T_{t,i}^{G_j} = \Delta T_t^{G_j}(\text{groupAverageT}) = \frac{1}{A_j}\int_{A_j} \Delta T_{t,i}^{G_j}\, dA, \quad i = 1, \ldots, n \tag{5.5}$$

  As the analysis is carried out under steady-state conditions, time-dependent outputs are not generated.

- **groupSpatialT** The groupSpatialT result is calculated by first isolating the actual temperature variation field (deltaT) and then subtracting the group average temperature field (groupAverageT) from it. This operation isolates the local temperature variations within each group, thus eliminating the effect of the average temperature level. As such, the temperature field in question reflects the influence of spatial temperature gradients within each area on the total thermo-elastic response [5].

$$\Delta T_{t,i}^{G_j} = \Delta T_{t,i}^{G_j}(\text{deltaT}) - \Delta T_t^{G_j}(\text{groupAverageT}), \quad i = 1, \ldots, n \tag{5.6}$$

- **timeAverageT** The timeAverageT output is mainly intended for the case when the temperature field changes with time. It might be interesting to find out how much the average temperature level contributes to the thermo-elastic response. In this respect, TEV internally, for each thermal node, calculates the mean temperature change over the whole time step range, thus producing a time-averaged temperature field.
  The corresponding thermo-elastic response is then calculated from this

mean temperature field, thus making it possible to evaluate the influence of the average thermal state without its temporal variations. From the overall vector of time-averaged temperature changes also the subgroup temperature change vectors corresponding to each defined thermal node group can be obtained [5].

$$\Delta T_{t,i}^{G_j} = \Delta T_{t,i}^{G_j}(\text{timeAverageT}) = \frac{1}{t_{\text{end}} - t_{\text{start}}} \int_{t_{\text{start}}}^{t_{\text{end}}} \Delta T_{t,i}^{G_j}(t)\, dt, \quad i = 1, \ldots, n \tag{5.7}$$

- **timeVarT** The timeVarT output is figured by taking away the time-average temperature field (timeAverageT) from each actual temperature variation field (deltaT). This is a way to obtain the temporal variations of the temperature field only, without the average temperature over time.
  Thus, this temperature field is the fluctuating part of the temperature load and it is possible to evaluate how the time-varying temperature changes affect the thermo-elastic response. This detailing is very advantageous for transient analyses where the way structural behaviour is influenced by the average as well as the varying components of the temperature field might be different [5].

$$\Delta T_{t,i}^{G_j} = \Delta T_{t,i}^{G_j}(\text{timeVarT}) = \Delta T_{t,i}^{G_j}(\text{deltaT}) - \Delta T_{t}^{G_j}(\text{timeAverageT}), \quad i = 1, \ldots, n \tag{5.8}$$

Chapter 6

Fundamentals of uncertainties

6.1 Uncertainty

Generally, uncertainty can be understood as the absence of full knowledge about a quantity or system. In the case of engineering applications, it is due to the fact that we can not completely describe the physical phenomena and also the parameters which are limited in the models and the knowledge of operating conditions. However, the words error, accuracy, bias, and precision which are frequently linked to uncertainty actually refer to different concepts and should not be confused with one another [9].
An error is the difference between a measurement or a prediction and the true value that corresponds to it. The true value in most cases is not known, although theoretically, it is the exact value of a quantity according to its definition. Therefore, uncertainty is generated not only by the presence of errors but also by the fact that the true value of the quantities involved can never be perfectly determined [9].
When measurements or model assessments can be repeated, one can describe uncertainty by probability distributions which represent the variability of the results. Within this framework, accuracy is connected with how close the expected value is to the true value, while bias stands for the systematic difference between them. Precision, thus, is related to how far the results are spread and can be determined by statistical measures like variance or standard deviation [9].
For thermo-elastic analysis, the idea of uncertainty is not limited to measurements only but includes numerical models as well. Material properties, thermal boundary conditions, environmental loads, and geometric features, as input parameters, are typically only approximately known and vary in a certain range. These uncertainties, thus, travel through the chain of analyses

and impact the prediction of temperature fields, structural responses, and finally the system performance parameters. Hence, accurate characterization and propagation of uncertainties is a prerequisite for trustworthy predictions and proper support for robust design decisions [9].

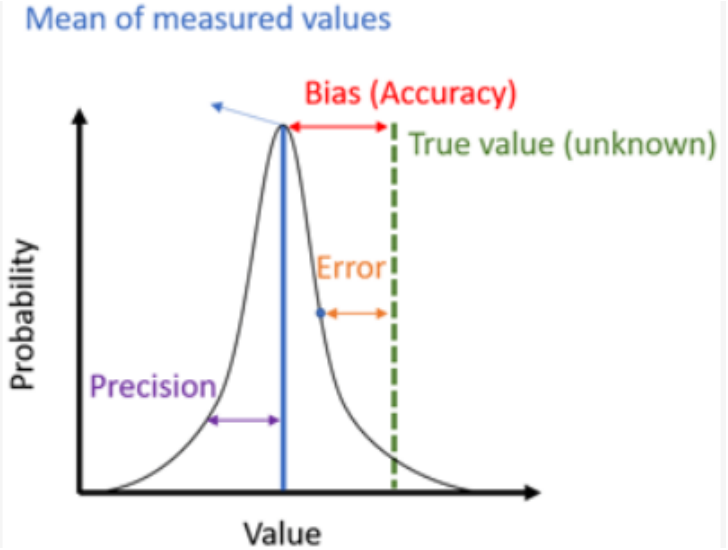

Figure 6.1: Uncertainty as described by the probability distribution of measured values [9].

In order to further characterize the statistical properties of uncertain parameters, additional descriptors of probability distributions are often considered, such as skewness and kurtosis, which provide information about the asymmetry and the shape of the distribution.

- **Skewness** This descriptor is a measure of the probability distributions symmetry.

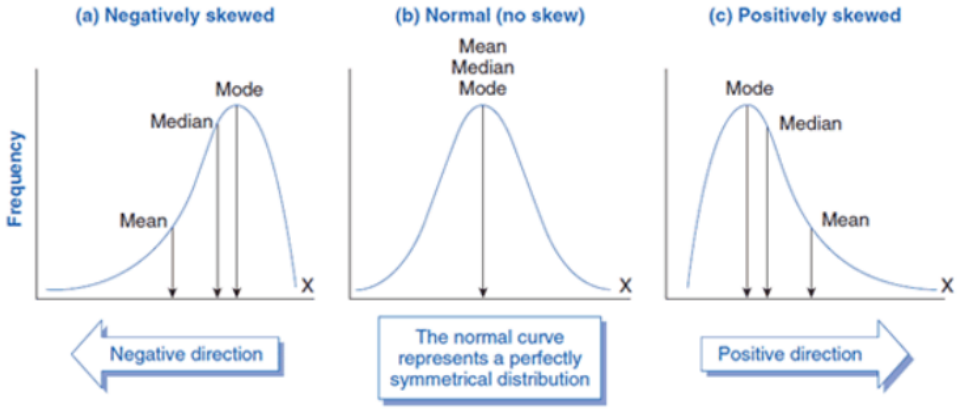

Figure 6.2: Effect of skewness factor [9].

- **Kurtosis** This descriptor is a measure of the tailedness and peakedness relative to a normal distribution.

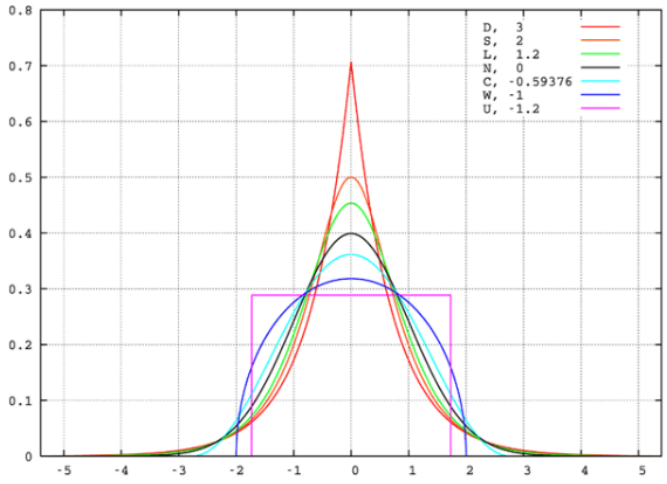

Figure 6.3: Effect of Kurtosis factor [9].

6.2 Uncertainty classification

- **Aleatory Uncertainty** Aleatory uncertainties stem from the fluctuating nature of physical phenomena. Hence, they are linked to the random/stochastic character of the system being studied. Usually, these

uncertainties are considered as non-reducible or irreducible because they result from natural randomness rather than from the lack of knowledge. While the scientific community is still debating whether such variability is due to intrinsic randomness or a limitation of measurement capabilities, aleatory uncertainties are in general non-reducible in engineering practice [24].
The most common way to represent aleatory uncertainties is through probability distributions, which describe the likelihood of different values of a given parameter. Therefore, a key element in uncertainty assessment is the identification of probability distributions that accurately represent the variability of input parameters. This means frequently that the process depends on the use of data obtained by experiments, statistical treatment, or on the judgement of experts if direct measurements are scarce or absent [24].
Aleatory uncertainties in the field of space thermal and thermo-elastic analyses might refer to the environmental conditions such as changes in the intensity of sunlight, reflection from the earths surface or radiation from the planet, besides manufacturing tolerances and operational variability. Accurate characterization of these uncertainties is therefore a prerequisite for realistic prediction of the system behavior and for a proper evaluation of the design robustness [24].

- **Epistemic Uncertainty** Epistemic uncertainties are related to the absence of knowledge about the system being studied and, thus, they result to some extent from an incomplete or imperfect modelling of physical phenomena. On the other hand, epistemic uncertainties, as opposed to aleatory ones, are usually regarded as being reducible because the level of these uncertainties can be lowered by means of enhancing the understanding of the system, carrying out more accurate measuring, or using better modelling methods.
  Apart from aleatory uncertainties, epistemic uncertainties can also be described using probability distributions. However, in this case, the distributions represent uncertainty about the knowledge of the parameter rather than the parameter's intrinsic variability. Normally, such distributions are determined based on the judgement of experts, through the use of simplified assumptions, or by relying on the small amount of data that is available [24].
  Different kinds of epistemic uncertainties can be identified under this heading:

  - **Phenomenological uncertainty** A first category of such uncertainties is related to the phenomenological ones, which are the cases where unknown or unknowable relevant system information gives rise to a problem. Those kinds of situations are very common in the case of innovative or not sufficiently characterized systems, where some factors, for instance, remain completely unidentified. These are some of the system elements that have been so far unrecognized, or whose full extent is still to be discovered, hence, their reference as "unknown unknowns" [24].

  - **Model uncertainty** A second category consists of the model uncertainties that refer to the errors or inaccuracies of the mathematical models adopted for the description of the physical phenomena. Although the primary equations governing a system might be well, known, the model differs from the reality in that it makes use of simplifications, assumptions, and numerical approximations. For instance, in space thermal and thermo-elastic analyses, model uncertainties may refer to the mode of heat transfer, material properties, or boundary conditions. Even the most commonplace modeling tools, which are continuously tested through validation, are a source of some level of uncertainty that needs to be accounted for in the analysis [24].

Besides the difference between aleatory and epistemic uncertainties, the uncertainties in thermo-elastic analyses can be divided into different categories based on how they are characterized and represented within the modelling framework. Mainly, it makes sense to separate explicit and implicit uncertainties, based on whether or not there is quantitative information available that describes their variability [3].

- **Explicit uncertainty** uncertainties that can be derived from measurement-based information or experimental data. These uncertainties can be further divided into [3]:

  - **Quantified uncertainty** Uncertainties for which measurements have been taken on representative samples or test items. Here, the uncertainty may be characterized by statistical quantities such as the average, standard deviation, or probability distribution. Typically, these uncertainties are physical and are frequently associated with material properties or environmental factors.

  - **Quantified uncertainty** Such uncertainties are recognized as existing but cannot be quantified directly because of the absence of representative experimental data. In this way, an approximate figure may be obtained by analogy with similar materials, components, or experience in modelling. This kind of uncertainty can be related not only to the physical properties but also to the modelling aspects, e.g. results of mesh refinement studies or design cases similar to that of the previous analyses.

- **Implicit uncertainty** These are uncertainties that have no direct measurement data or that cannot be readily introduced into a numerical model. Uncertainties of this kind can be due to both physical sources and modelling simplifications. Uncertainties related to manufacturing tolerances, conditions of assembly, or other extremely intricate phenomena which cannot be perfectly represented in the model are the examples of such uncertainties [3].

6.3 Probability Distribution Function

A probability distribution function is a mathematical function used to describe how the probability of a random variable is distributed over its possible values. It provides a quantitative representation of the likelihood that a variable takes certain values within a given range. In the context of uncertainty analysis, probability distributions are used to model the variability of uncertain input parameters and to represent their possible fluctuations. For a random variable X, evaluated at the values x, the cumulative probability that the variable assumes a value less than or equal to x is described by the equation 6.1 [25]:

$$F(x) = P(X \leq x) \tag{6.1}$$

Where $P(\leq x)$ represents the probability that the random variable X takes a value smaller than or equal to x.
Probability distributions can generally be classified into two main categories depending on the nature of the random variable:

- **Discrete probability distribution** This distribution describes the probability associated with the possible outcomes of a discrete random variable. In this case, the variable can only assume a finite or countable number of distinct values, each associated with a specific probability. Only the values that represent physically possible outcomes are included in the distribution.

An important property of this probability distributions is that the sum of the probabilities associated with all possible outcomes is equal to one [25].

- **Continuous probability distribution** This distribution describes a continuous random variable. In this case, the variable can assume any value within a given interval defined by its lower and upper bounds. As a consequence, continuous probability distributions include all real values within the considered range.
  For continuous variables, the probability of observing a single exact value is infinitesimally small and therefore considered to be zero. Instead, probabilities are defined over intervals of values. This means that the probability associated with a continuous variable is expressed as the likelihood that the variable falls within a specified range rather than assuming a specific value [25].
  For continuous variables, probability distributions are described through a mathematical function known as PDF, which defines how probability is distributed over the range of possible values of the variable and provides the probability density associated with each value.
  An important property of the PDF is that probabilities are obtained by integrating the function over a given interval. In other words, the probability that a variable takes a value within a certain range corresponds to the area under the PDF curve over that interval. Consequently, the total area under the curve across the entire domain of the variable is equal to one, representing the certainty that the variable will assume a value within its possible range. The probability that a continuous random variable X takes a value within a given interval $[a, b]$ is obtained by integrating the probability density function over that interval [25].

$$P(a \leq X \leq b) = \int_a^b f(x)\,dx \tag{6.2}$$

6.4 Uncertainty Distribution

The uncertainties may be represented by different types of probability distributions, which characterize the potential variations in the parameter values. These distributions are defined by their corresponding probability density functions (PDFs), which describe the likelihood of different values within the considered range. The decision regarding which distribution to use is influenced by the available data and by the nature of the uncertainty affecting the parameter [10].

- **Normal Distribution** One of the most popular probability distributions for depicting uncertain parameters is the normal distribution. The curve is bell-shaped and symmetrical around the axis passing through the mean. The width of the curve is determined by the standard deviation. In the case of this distribution, the values that are closer to the mean have higher chances of occurring. On the other hand, the probability of getting the values that are at the extreme distance from the mean gradually goes down.
  The normal distribution is the first choice for the representation of measurement uncertainties of the type: repeatability, reproducibility, or stability, which is experimental. In fact, the Central Limit Theorem states that the distribution of the measurement results is a normal one if the number of independent measurements is large enough. It is just a matter of time when, for example, a huge dataset of measurement samples is taken and represented in a histogram, which will have the shape of the Gaussian distribution. Thus, the normal distribution can be used to describe measurement-based uncertainties in engineering analyses [10].

- **Rectangular Distribution** The rectangular distribution is also commonly referred to as the uniform distribution. In such a distribution, any value within a certain range is equally likely to occur. Thus, the probability remains consistent throughout the set of possible values, implying that none of the outcomes within the interval is regarded as more likely than the others.
  When there is not much information about the distribution of a parameter, this kind of distribution is often employed in uncertainty analysis. In these cases, taking a rectangular distribution is a safe move as it shows the parameter can equally probably take any value between the indicated limits [10].

- **Triangle Distribution** The triangular distribution is characterized by three parameters: a minimum, a maximum, and a most probable value which lies in the interval. In contrast to the rectangular distribution which assumes equal probability for all outcomes, the triangular distribution presumes that values near the central estimate have higher probability than those close to the bounds.
  This distribution serves as a good model in a situation when uncertainty is analyzed with only a few data points but the approximate

central value can be guessed. Hence, it is often referred to as a "lack of knowledge" distribution, on the other hand, it shows the notion that the most likely value is located near the centre of the interval [10].

- **U-shaped Distribution** The U-shaped distribution is essentially a probability distribution where the points close to the extreme ends of the range are more likely than the ones near the middle. The probability density function, as indicated by its name, takes the form of a "U" letter, but it does not have to be exactly symmetrical.
  This kind of distribution is suitable for scenarios where results happen more often near the lower or upper limits of the range, rather than around a central value. Therefore, it can be deployed to model uncertainties when the occurrence of extreme values is more likely than that of the middle ones [10].

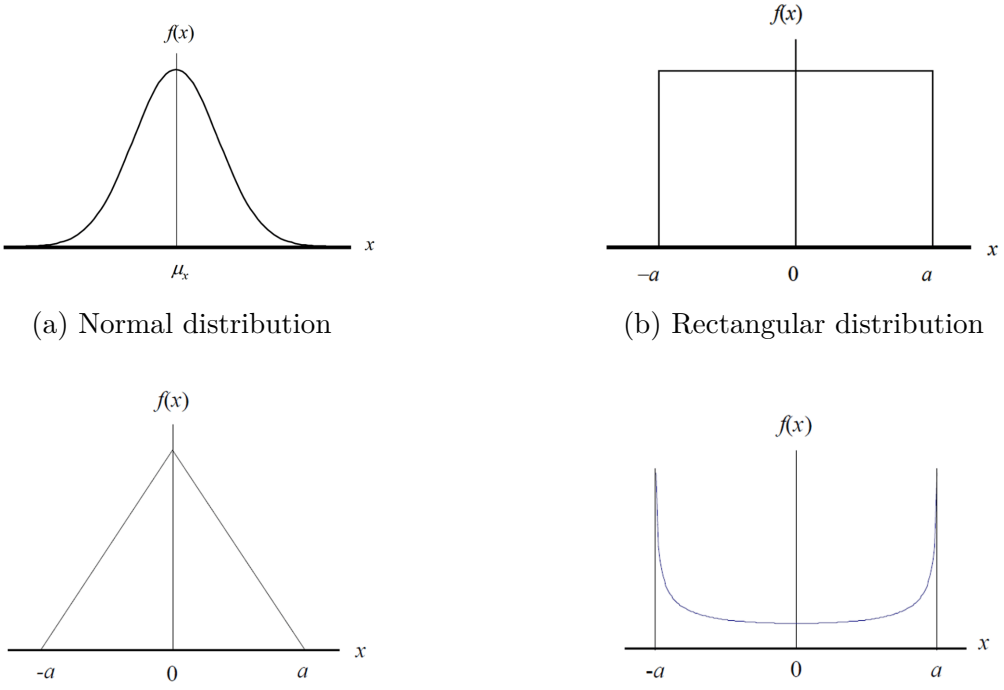

(a) Normal distribution

(b) Rectangular distribution

(c) Triangular distribution

(d) U-shaped distribution

Figure 6.4: Examples of probability distributions used in uncertainty analysis [10]

6.5 Design Parameters

After briefly pointing out different sources of uncertainties that can influence engineering analyses, we first need to specify which input parameters are uncertain in the present work. When looking at thermo-elastic analysis, these parameters are linked to both thermal and structural modelling, and the extent of their fluctuations determines the level of uncertainty in the predicted thermo-elastic behavior of the system.
To carry out the uncertainty analysis, a number of input parameters were chosen from the perspective of their expected impact on the thermo-elastic response. Examples of these parameters are material properties, thermal loads, and interface characteristics, which are influenced by both aleatory and epistemic uncertainties. An uncertainty range or probability distribution is given to each parameter to represent its variability and to authorize the first propagation of uncertainties through the analysis chain.
In the present work, the uncertainties associated with the selected parameters are represented using normal (Gaussian) probability distributions. This choice is motivated by several considerations. First, the normal distribution is widely used in engineering applications to describe uncertainties derived from measurement data and material properties, which are often characterized by mean values and standard deviations. Second, the use of Gaussian distributions allows a straightforward characterization of uncertainties using commonly available statistical parameters, facilitating the implementation of uncertainty propagation methods within the analysis framework.
Furthermore, the use of Gaussian distributions is particularly convenient for the application of stochastic uncertainty propagation methods. In this work, the URQ method is adopted to propagate the uncertainties of the input parameters through the thermo-elastic analysis chain and to quantify their contribution to the variability of the performance parameters.

Name	Mean	Dev	PDF	Units
eps_Black_paint	0.84	0.015	gauss	
alpha_Black_paint	0.93	0.05	gauss	
eps_Mirror	0.03	0.01	gauss	
alpha_Mirror	0.04	0.015	gauss	
eps_Kapton	0.67	0.015	gauss	
alpha_Kapton	0.38	0.05	gauss	
incln	97.4	1	gauss	deg
alt_a	550000	10000	gauss	m
sun_temperature	5778	11	gauss	K
planet_temperature	254.3	10	gauss	K
k_HC	1.36	0.272	gauss	W/mK
k_Ti6Al6Va	7	1.4	gauss	W/mK
k_Zerodur	1.63	0.326	gauss	W/mK
k_Kapton_Bulk	0.2	0.04	gauss	W/mK
lc_IF	0.01	0.002	gauss	W/K
lc_fpa_bip	0.1	0.02	gauss	W/K
lc_m1_bip	0.1	0.02	gauss	W/K
lc_m2_bip	0.1	0.02	gauss	W/K
lc_strut	0.2	0.04	gauss	W/K
lc_detector	0.025	0.005	gauss	W/K
mli_eff	1	0.2	gauss	
q_det	0.5	0.1	gauss	W
T_SC	-5	-1	gauss	

(a) Thermal Parameters

Name	Mean	Dev	PDF	Units
E_Mat1_33_M2Pan_M2_Bipod_Ti	1.15E+11	1.15E+10	gauss	Pa
Dens_Mat1_33_M2Pan_M2_Bipod_Ti	4510	451	gauss	kg/m³
CTE_Mat1_33_M2Pan_M2_Bipod_Ti	8.7E-06	8.7E-07	gauss	1/K
E_Mat1_14_FPA_Bipod_Ti	1.15E+11	1.15E+10	gauss	Pa
Dens_Mat1_14_FPA_Bipod_Ti	4510	451	gauss	kg/m³
CTE_Mat1_14_FPA_Bipod_Ti	8.7E-06	8.7E-07	gauss	1/K
E_Mat1_24_M1_Bipod_Ti	1.15E+11	1.15E+10	gauss	Pa
Dens_Mat1_24_M1_Bipod_Ti	4510	451	gauss	kg/m³
CTE_Mat1_24_M1_Bipod_Ti	8.7E-06	8.7E-07	gauss	1/K
E_Mat1_34_Strut_Ti	1.15E+11	1.15E+10	gauss	Pa
Dens_Mat1_34_Strut_Ti	4510	451	gauss	kg/m³
CTE_Mat1_34_Strut_Ti	8.7E-06	8.7E-07	gauss	1/K
E_Mat1_2_mat1.2	1.02E+11	1.02E+10	gauss	Pa
Dens_Mat1_2_mat1.2	1892	189.2	gauss	kg/m³
CTE_Mat1_2_mat1.2	-2E-07	-2E-08	gauss	1/K
E_Mat1_3_mat1.3	9.03E+10	9.03E+09	gauss	Pa
Dens_Mat1_3_mat1.3	2530	253	gauss	kg/m³
CTE_Mat1_3_mat1.3	1E-07	1E-08	gauss	1/K
t_PShell_5_VPanel_skin	0.001	0.0001	gauss	m
t_PShell_6_M2_Panel_skin	0.0005	5E-05	gauss	m
t_PShell_19_FPA_HC	0.001	0.0001	gauss	m

(b) Structural Parameters

Figure 6.5: Design Parameters

The uncertainty in the chosen input parameters is conveyed by setting suit-

able probability distributions. The decision on the distribution is made based on the information available and the type of parameter being considered. Here, a Gaussian (normal) distribution has been used for all input parameters, on the assumption that their variation is symmetric around the central value and a mean value and a standard deviation can thoroughly characterize their variability. These distributions are subsequently applied in the uncertainty analysis to assess how input variation affects the thermo-elastic performance.
For the uncertainty analysis performed in this study, the Univariate Reduced Quadrature (URQ) method was used. This method enables the propagation of uncertainties by determining the system response at a small number of thoughtfully selected points near each input parameter's nominal value. Besides the nominal value, two more values are taken for each parameter, which represent positive and negative deviations within the set uncertainty range. The obtained responses are then combined to determine the total variation of the performance parameters.

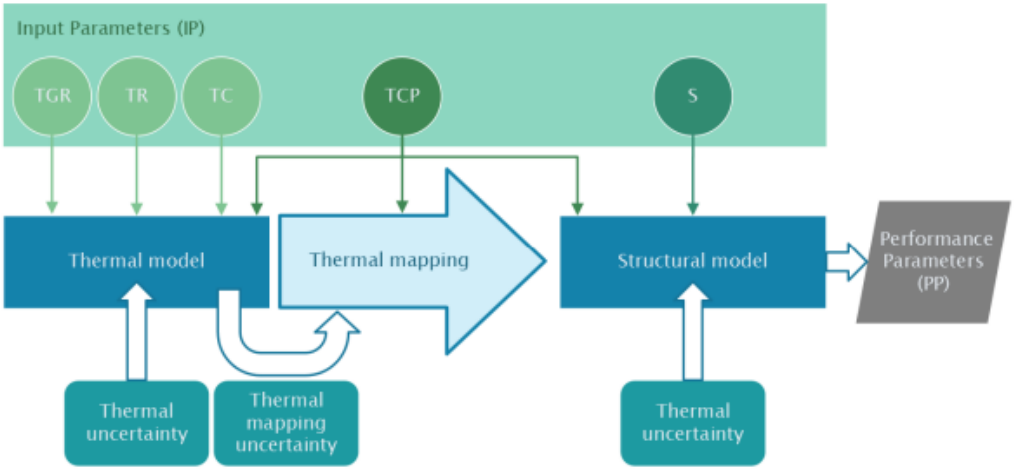

Figure 6.6: Diagram of the methodology proposed for thermo-elastic uncertainty analysis [11].

Chapter 7

Uncertainties Analysis with Simulia Isight

7.1 Simulia Isight

The thermo-elastic analyses for space applications are getting more and more complex and, therefore, often require running a large number of simulations, especially when considering components degradation, uncertainty propagation, and sensitivity studies. Hence, doing the analysis chain by hand becomes not only inefficient but also error-prone. Hence, automation of the processes through the help of software tools drives the quality and quantity of the work both substantially.
SIMULIA Isight is a process integration and design exploration software by Dassault Systmes extensively used in engineering to automate complex simulation workflows. Its functionality encompasses the integration of various analysis software in a single framework thus providing an avenue for the creation of automated processes that can handle data exchange, run simulations, and systematically collect results. Using a graphical interface, Isight offers the ability to direct several programs, for example, thermal solvers, structural solvers, and post-processing scripts, to communicate with one another. When dealing with thermo-elastic analysis, SIMULIA Isight can be a real game changer as it enables smooth automation of the interactions between the thermal model, temperature mapping, and structural analysis. Hence, a user can easily carry out many runs with the variation of input parameters, which is the key for uncertainty propagation and parametric studies. Furthermore, Isight facilitates optimization and design exploration methods that help in unlocking the most influential parameters of the system performance. Through this paper, SIMULIA Isight was leveraged to automate the thermo-

elastic analysis workflow, including running ESATAN-TMS, temperature mapping with pySinas, and structural analysis using NASTRAN, thus drastically lowering the computational load and making sure the simulations are in agreement through repetition.

7.2 Thermo-elastic workflow with Simulia

The thermo-elastic analysis workflow has been broken down into a series of connected blocks, each depicting a distinct stage in the total operation. This methodology describes the assignment of each block to a certain software component used in the te analysis line, e.g. pySinas, ESATAN-TMS, TEV or NASTRAN. Consequently, the whole procedure thus follows the normal pattern of a thermo-elastic analysis operation, but is entirely encompassed in one integrated environment.

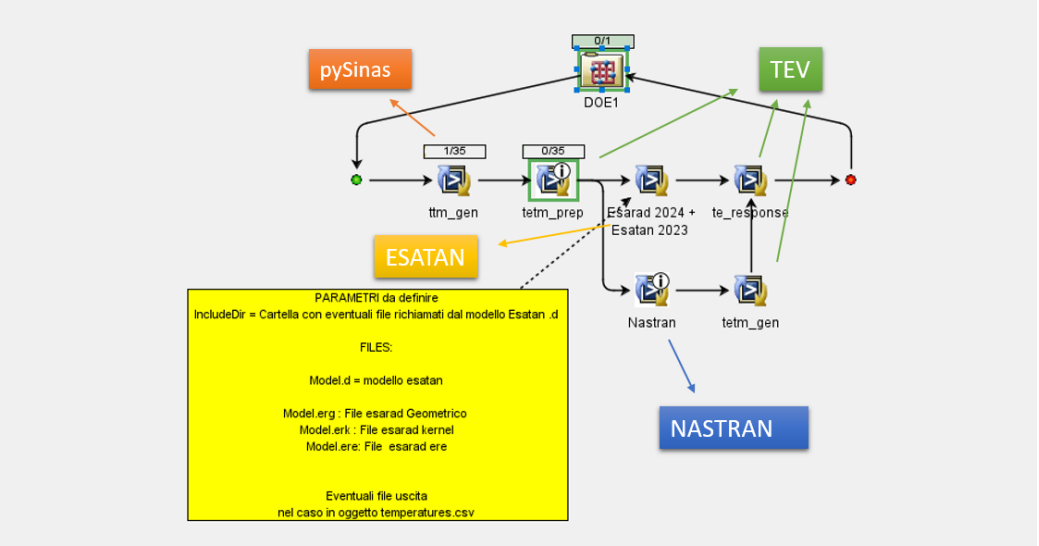

Figure 7.1: Thermo-elastic analysis workflow with Simulia Isight.

For each block, one or several execution commands are stipulated to carry out the necessary functions. Such commands are the same ones that would be used in a manual te analysis. In this way, the developed workflow is very close to the conventional method while at the same time providing elevated levels of consistency, traceability, and repeatability for all the simulations.
Moreover, alongside the execution commands, each block has to define the execution environment, stating if the process is done locally or on a remote

computational resource. With this option, a user can harness the hardware available more efficiently, for instance, computationally heavy simulations can be run on dedicated servers or clusters. The need for such flexibility arises particularly when one has to conduct a large number of analyses, for example, in parametric studies or the propagation of uncertainty.

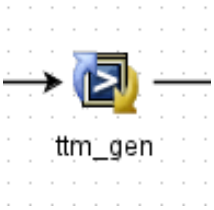

Figure 7.2: Block used for ttm generation.

7.3 Input/Output files and parameters definition

At each step of the workflow, SIMULIA Isight allows the definition of input and output files, which are necessary for managing the data exchange between the different analysis steps. This generally happens by bringing in a reference file, which acts as a template and determines the structure and format of the input and output data. From this template, Isight can recognize the files needed to run each step and the outputs that must be created and handed over to the next components in the workflow.

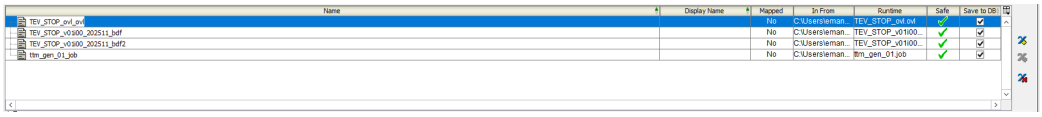

(a) Input Files

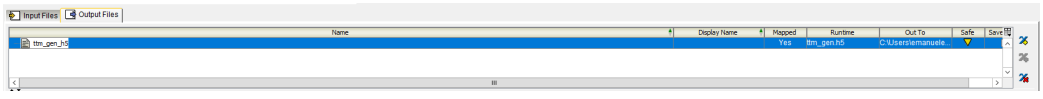

(b) Output Files

Figure 7.3: Input/Output Files of ttm generation

Apart from managing files, you can also set parameters right in these files. Inside the templates, you can pinpoint the exact variables and link them with the design parameters in the Isight environment. In case of uncertainty analyses, a parameter can be given a nominal value and also a range or distribution. The parameters are synchronously updated in the input files during the running of the workflow and therefore the corresponding simulations can be run with different configurations. This feature is a major plus for uncertainty propagation. It allows for the variation of chosen input parameters in a systematic manner over several runs. Consequently, it is possible to assess the effect of each parameter on the thermo-elastic behavior quite rapidly without having to manually change the input files for each simulation.

7.4 DOE used for uncertainty analysis

For the uncertainty analysis, a Design of Experiments (DOE) task has been hybrid within SIMULIA Isight allowing the selected input parameters to be systematically varied. The DOE approach facilitates a parametric study in which only one parameter is changed at each time, all the others remaining at their nominal values. Such a method agrees well with the Univariate Reduced Quadrature (URQ) method utilized here, which involves finding the system response for particular changes of each parameter individually.

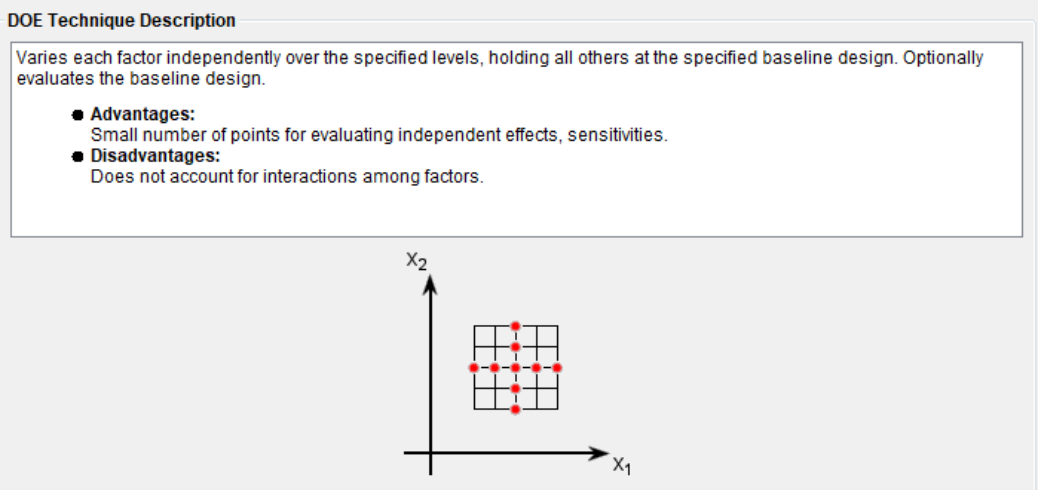

Figure 7.4: Parametric study description.

The DOE workflow hence facilitates an initial run where the parameters are set to their nominal values, so the resulting output serves as the reference.

Next, a new run is made by changing one parameter at a time and keeping the other parameters unchanged. For each parameter, three values are considered: a nominal value, a lower bound, and an upper bound, thus representing the range of uncertainty that has been chosen for the parameter. This procedure enables a highly efficient way of exploring how each parameter affects the thermo-elastic response, without having to run a large number of simulations. Because of this, the DOE approach offers a systematic and computationally effective method to apply the URQ technique and to assess the effect of input uncertainties on the system performance.

7.5 Results of uncertainty analysis

The initial outputs are displayed as tornado charts. To create such charts, the variation in the corresponding response for each input parameter is first calculated by determining the difference between the results obtained at the upper and lower bounds of the parameter. Then, this response variation is divided by the parameter range, thus giving a sensitivity measure that makes it possible to compare directly different parameters. After that, the parameters are ordered by their effect on the output, and the results of this ranking are shown in descending order.

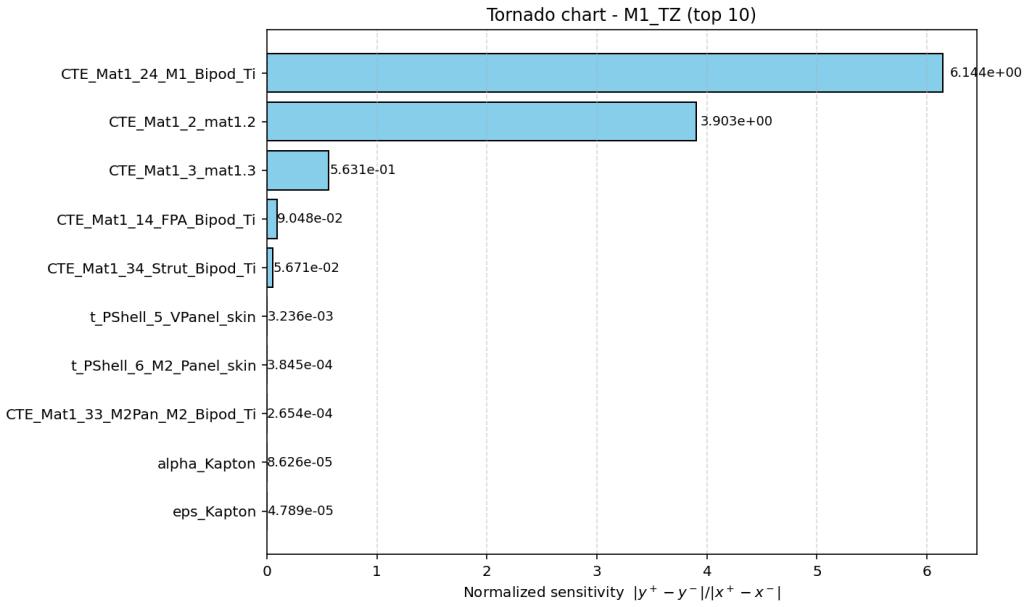

Figure 7.5: M1_TZ Tornato chart.

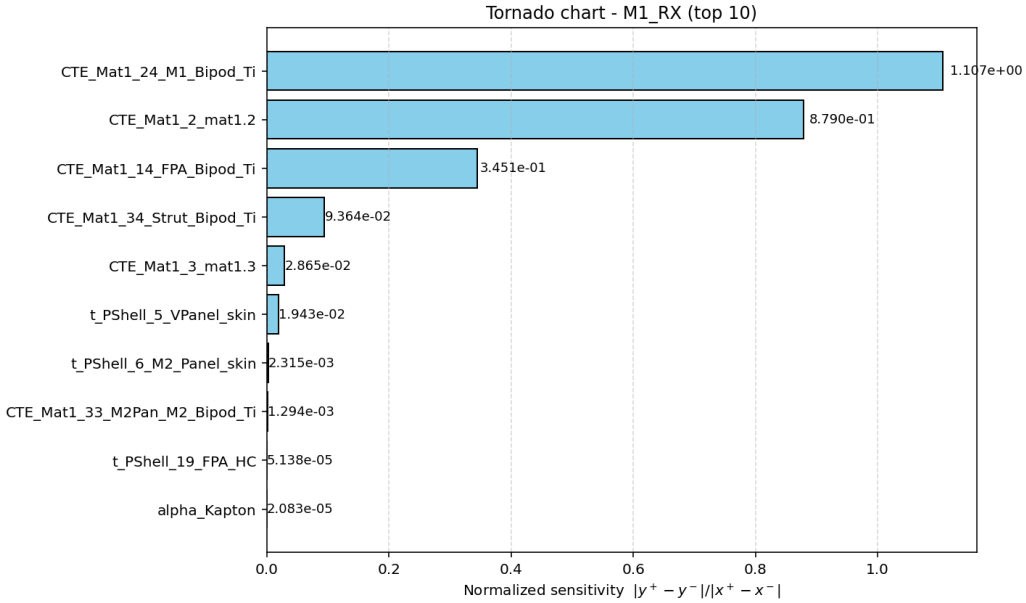

Figure 7.6: M1_RX Tornato chart.

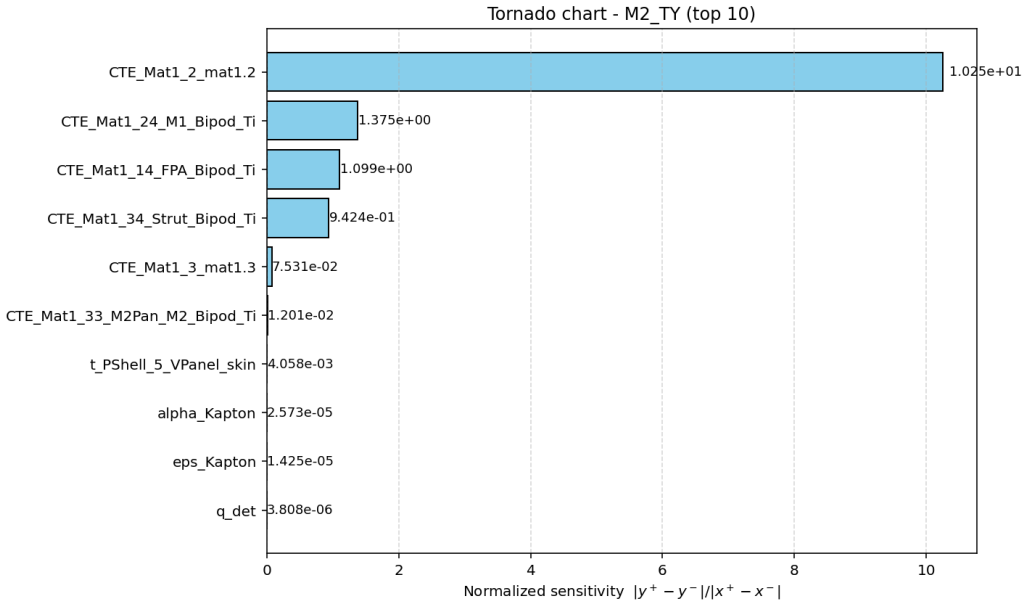

Figure 7.7: M2_TY Tornato chart.

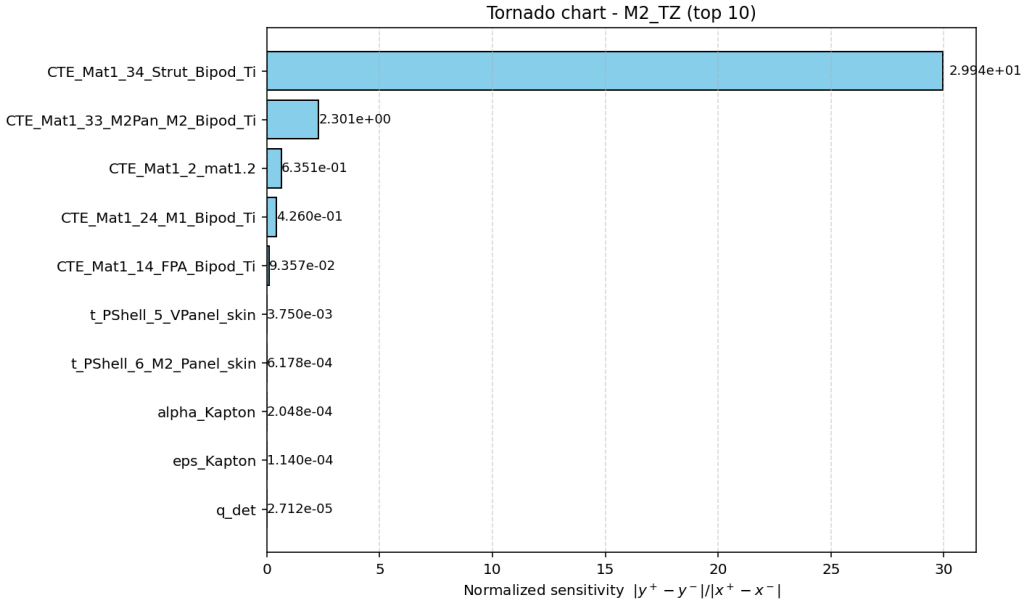

Figure 7.8: M2_TZ Tornato chart.

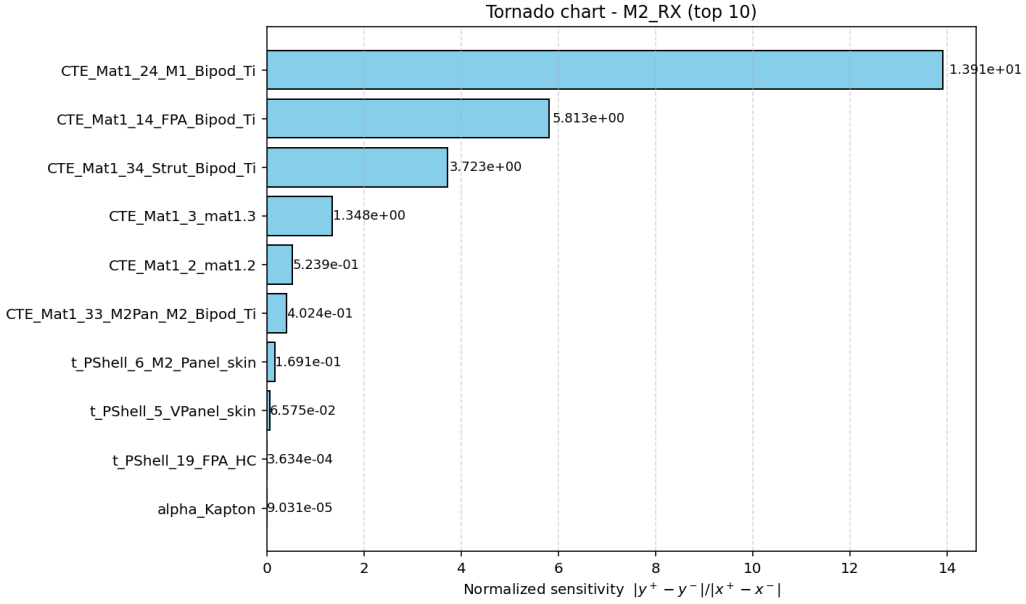

Figure 7.9: M2_RX Tornato chart.

The interpretation of the tornado charts indicates that the parameter that in most cases has the greatest effect on the performance parameters is the coefficient of thermal expansion (CTE) of the titanium structure. This finding is in line with the fact that the major load-carrying elements of the system are made of titanium, and hence their thermal expansion greatly affects the whole thermo-elastic response.
However, translational displacements along the y and z directions of the secondary mirror (M2) are exceptions to the rule, where the parameter influencing the most is the coefficient of thermal expansion of the Zerodur material. This finding underlines the contribution of the optical components to certain performance parameters, in particular those associated with the relative positioning of the mirrors.
First of all, tornado charts give the measure of the output sensitivity with respect to each input parameter, however, they do not consider the size of the corresponding uncertainties. Hence, these charts capture the most sensitive parameters, but not necessarily the ones that are most critical. To be able to figure out the parameters that affect the system performance the most, it is necessary to look into their contribution to the total variance of the output, which is a function of both the sensitivity and the uncertainty of each parameter.
To get a deeper insight into the effect of the input parameters on the system performance, the extent to which each parameter influences the variance of the performance parameters has been assessed. While tornado charts only tell us about the sensitivity of the outputs, this analysis also considers the sensitivity and the size of the uncertainties involved, thus it points out the most important parameters.
The contributions have been figured out by using the results of the uncertainty propagation when determining the fraction of the total output variance that corresponds to each input parameter. The resultant contributions have been visually displayed as pie charts, which makes the relative significance of each parameter very clear and straightforward.

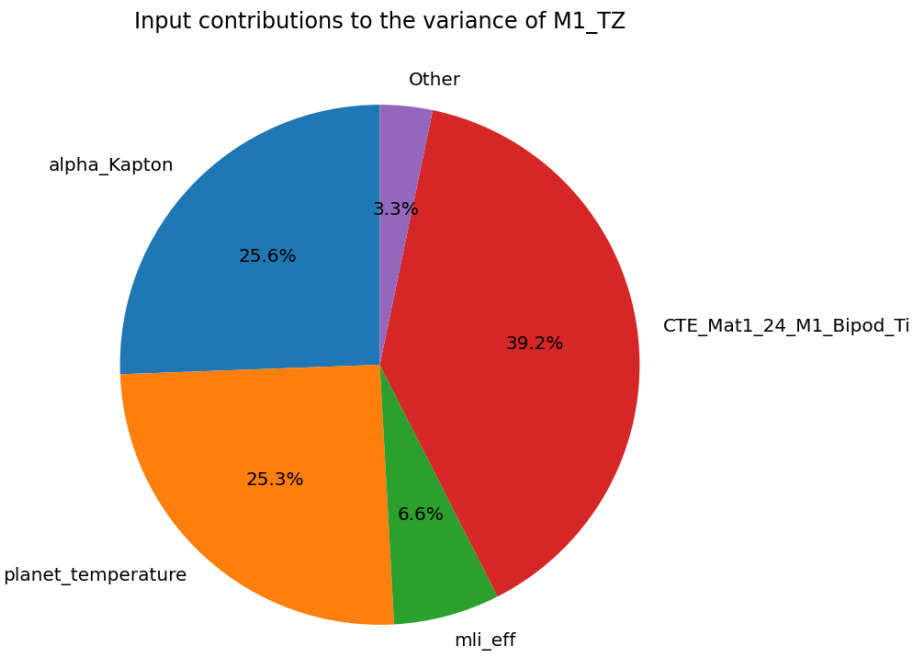

Figure 7.10: M1_TZ chart.

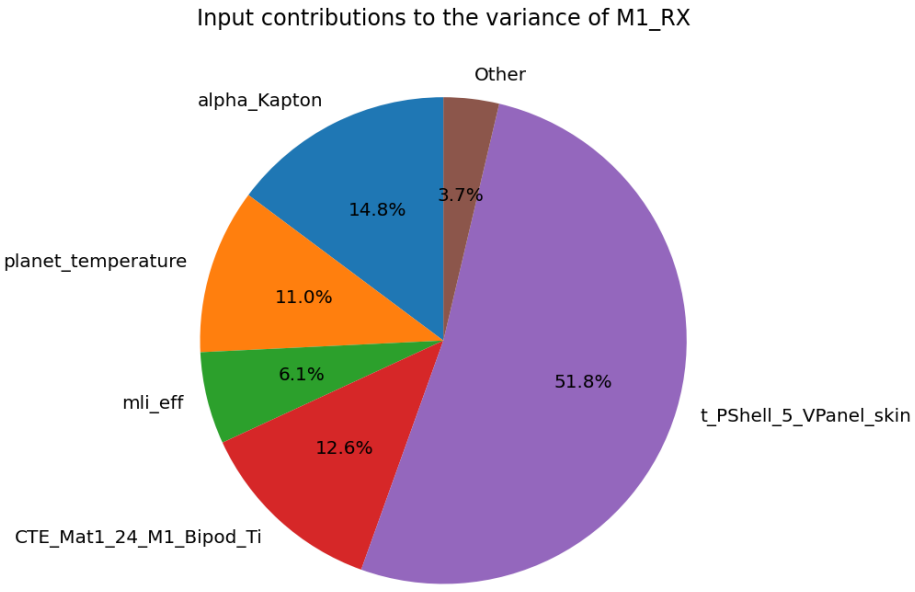

Figure 7.11: M1_RX chart.

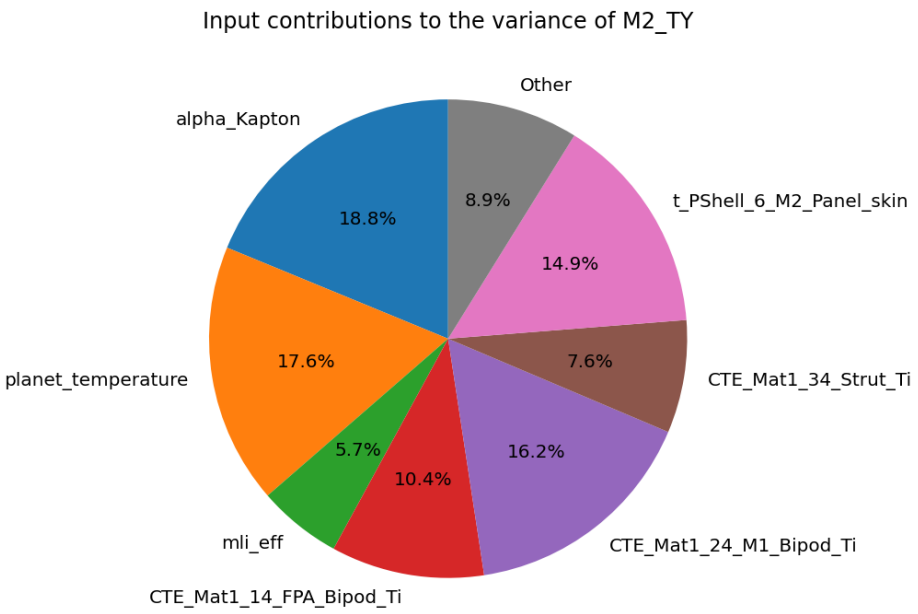

Figure 7.12: M2_TY chart.

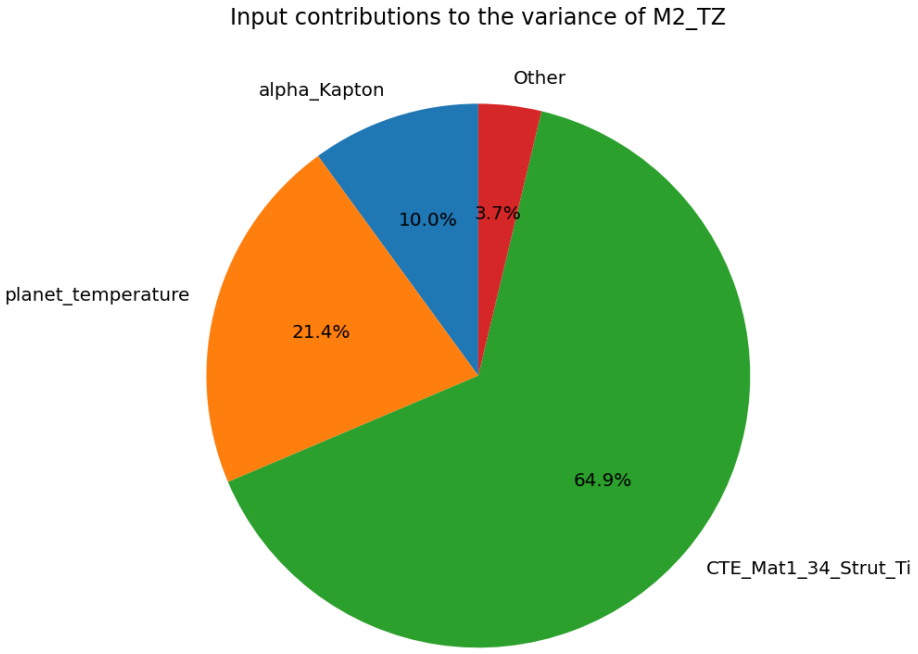

Figure 7.13: M2_TZ chart.

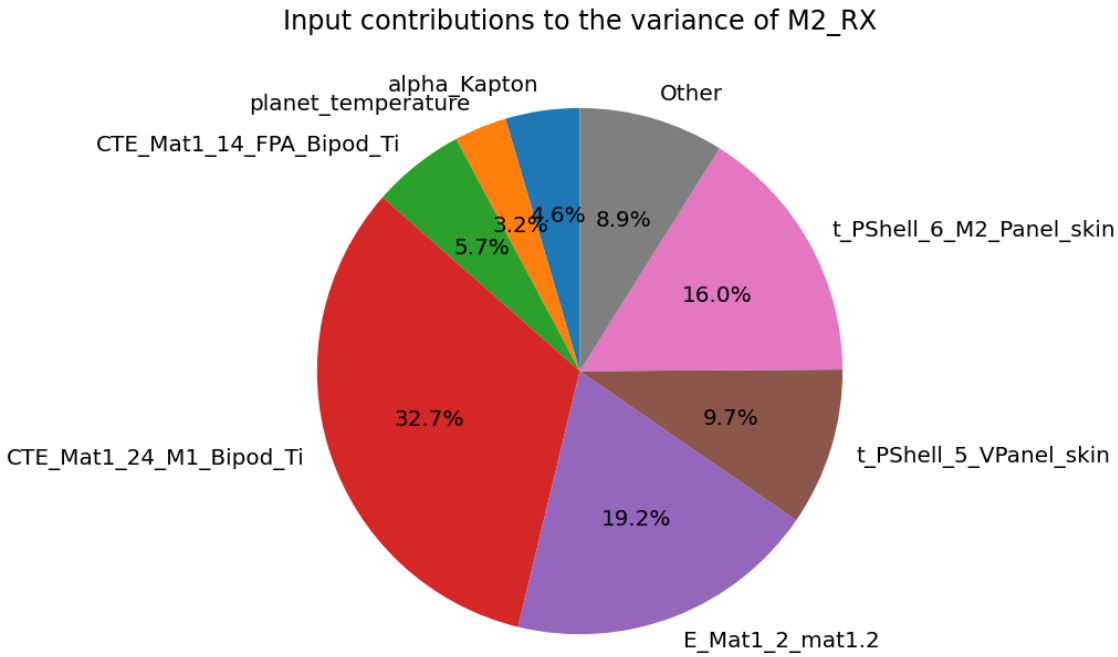

Figure 7.14: M2_RX chart.

The analysis of the variance contribution charts reveals that if both sensitivity and uncertainty are considered, the main parameter for the majority of performance outputs is the coefficient of thermal expansion (CTE) of the titanium structure. This finding reaffirms the crucial role of the structural components in determining the total thermo-elastic response of the system. One exception is the rotation of the primary mirror, where a different parameter seems to be the main contributor, thus implying the existence of specific local effects for some performance parameters.
After the most critical parameter has been determined, finding ways to mitigate its effects on the system performance must be the next step. An initial method is to consider a replacement for the titanium material that would have similar mechanical and thermal properties but with a lower level of uncertainty. To be more specific, this might mean using materials having a coefficient of thermal expansion which is more stable and better characterized, or the variability of the properties for these materials is more tightly controlled during production. Nevertheless, performing such a replacement must be done cautiously since it might bring about compromising aspects like structural stiffness, mass, manufacturability, and the overall system performance. Hence, choosing a different material must be a multidisciplinary

decision-making that takes into account such aspects as the possible detriment of the impact of reduced uncertainty benefits on other design requirements.
A second approach is to reduce the uncertainty associated with the titanium properties themselves. This can be done through a better characterization of the material, for example by carrying out more experimental tests in environmental conditions that are representative. When the data is increased in both amount and quality, the material properties can be quantified more precisely and their statistical variability can be lowered. Besides that, the use of higher, quality manufacturing processes and implementation of stricter quality control procedures can limit variations in material properties for different components. Also, the agreement of numerical models with experimental data can enhance the reliability of the predicted behaviour, thus providing a more precise estimation of the input uncertainties. Hence, by decreasing the uncertainty of the material properties, their impact on the total variance of the thermo-elastic response is lowered.

7.6 Results with Rosenblueth Method

Besides the statistical analysis done with the URQ method, a second statistical analysis was done with the Rosenblueth Point Estimate Method to check the consistency of the two methods. The Rosenblueth technique is largely inspired by the URQ method, because it studies the system response to changes in the input parameters whose values are close to the nominal ones. On the other hand, the perturbed values of each parameter in this case, are just the addition and subtraction of one standard deviation from the nominal value.
For each uncertain parameter, two additional simulations are performed in which the parameters take the values of upper and lower perturbations, respectively, and all the other parameters are fixed at the nominal levels. After all the necessary simulations have been done, the results are used to calculate the sensitivity coefficients, which show how the uncertainty parameters depend on the input variables. These coefficients are calculated using the equations 1.7, which quantitatively measure the effect of each parameter on the thermo-elastic response.

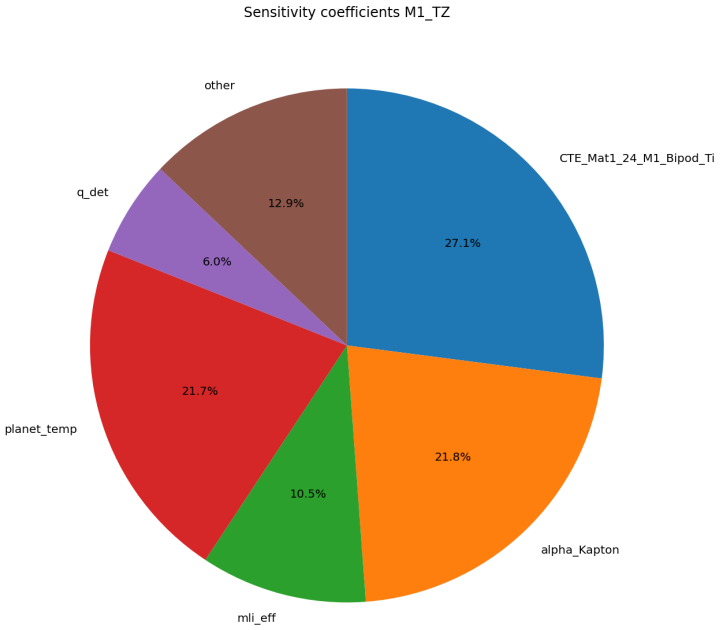

Figure 7.15: M1_TZ with Rosenblueth.

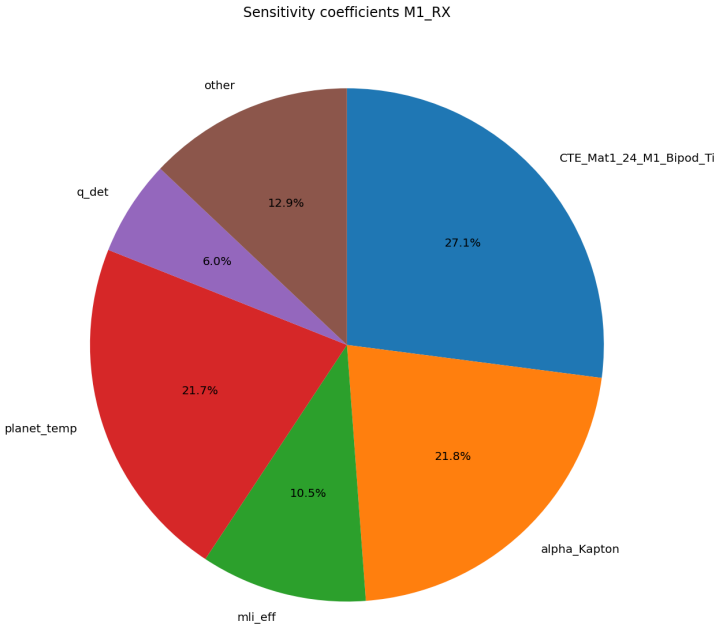

Figure 7.16: M1_RX with Rosenblueth.

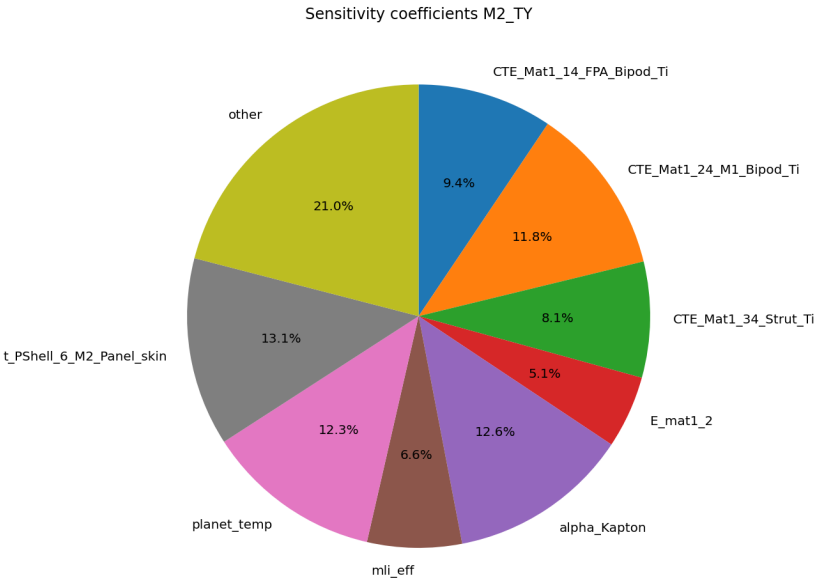

Figure 7.17: M2__TY with Rosenblueth.

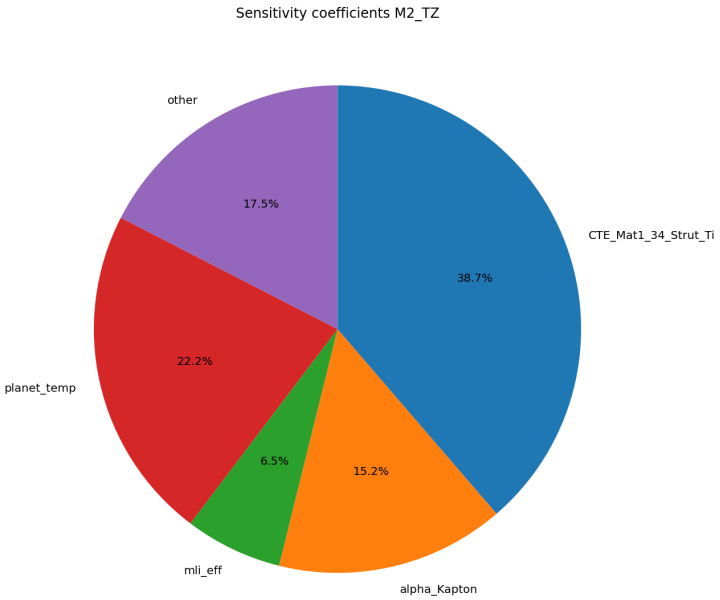

Figure 7.18: M2__TZ with Rosenblueth.

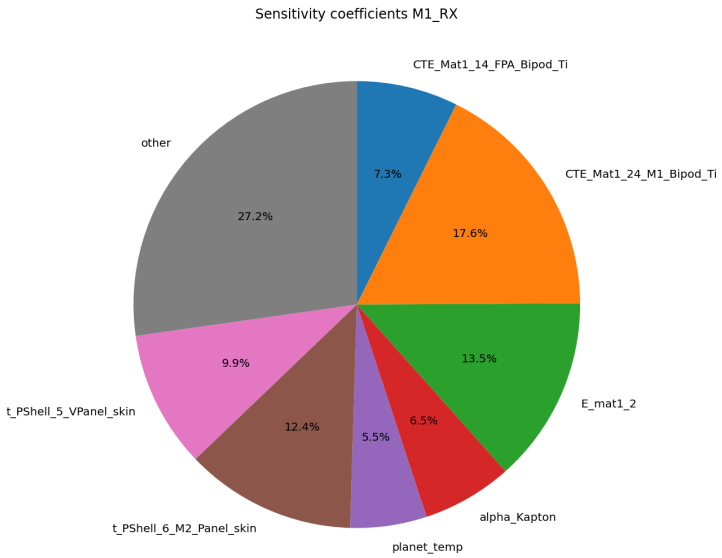

Figure 7.19: M2_RX with Rosenblueth.

The comparison of results obtained by URQ method and by Rosenblueth point estimate method revealed that, in general, the two methods are in good agreement. More specifically, the main factors influencing the performance metrics are identical in both studies. This agreement serves as a proof that the uncertainty analysis is properly performed and that the identification of the parameters with the strongest influence is not affected by the choice of the uncertainty propagation method.
While the ordering of the most impactful parameters has not been altered, slight variations in the size of the contributions estimated by the two methods can be noticed. Such differences are quite natural, since the URQ method makes use of weighted quadrature points whereas the Rosenblueth approach obtains the system response by making symmetric perturbations of the parameter values around the nominal ones. However, the major patterns for all performance metrics remain intact.
The fact that the results are so close to each other also indicates that, in the uncertainty range considered, the thermo-elastic response is linear or close to linear, at least to a first approximation. In such a scenario, both methods can produce good and trustworthy estimates about how the uncertain parameters impact the system's behavior. Moreover, analyzing the two becoming methods side-by-side manifests that they have differences when it comes to computational efficiency. Rosenblueth point estimate method is an option that is quite easy to implement and, in addition, it gives you results regarding parameter sensitivities in a very direct way. However, it can lose

efficiency if the number of uncertain parameters increases.
Then there is the URQ method, which is a method latently designed to mimic the flow of uncertainties in the space by making the least number of simulations. On top of that, it succeeds in keeping the quality of the outputs in identifying the different statistical moments way up. Selecting between these two, the URQ method might be a better and more favourable choice due to lower simulation numbers and result similarity. As a result, URQ can be viewed as a feasible method for the propagation of uncertainties in highly thermo-elastic complex models where a number of uncertain parameters have to be evaluated.

7.7 Conclusions

The thermo-elastic results can be interpreted in light of the deformation mechanisms discussed in section2.6. The secondary mirror's movement along the z-axis is the most significant deformation observed. This motion, known as $M2\_TZ$, occurs directly along the satellites optical axis. Other rigid, body motions remain at around 10^{-5}, but this one reaches about 10^{-4}. That difference suggests thermal expansion is the main cause of structural response in this case. The titanium frame holding the optical components contributes the most to this movement. Because the shift is mainly translational and lacks bending or twisting, it likely results from titanium's coefficient of thermal expansion and local temperature changes. Temperature remains stable across the horizontal plane but changes significantly along the z-axis. The deformation pattern follows the direction of heat flow, leading to a consistent axial displacement of the secondary mirror.
The CTE of titanium is the most influential material property in this analysis. It accounts for the greatest amount of variation in output values. This sensitivity shows the thermo-elastic response reacts strongly to changes in this parameter. The largest deformations in the system come from this property. It is also the main source of uncertainty in structural predictions. Optical performance can be affected if the secondary mirror shifts axially. Changes in path length may cause defocus in the system. Accurately measuring the supporting structures behavior and material properties is essential. And ensuring these values are precise improves prediction reliability. This focus helps maintain system performance under temperature changes.

Bibliography

[1] A. Pagani, "Slides from "design termico di strutture aerospaziali"," 2023. Cited on pp. 5.

[2] S. Appel and J. Wijker, *Simulation of Thermoelastic Behaviour of Spacecraft Structures: Fundamentals and Recommendations*. Springer Aerospace Technology, 2021. Cited on pp. 16–19, 26, 27, 38.

[3] M. De Cillia, A. Van Oostrum, R. Peman, T. Gonzalez-Llana, D. Rapp, T. Meschenmoser, G. Mareschi, L. De Palo, G. Perachino, and S. Appel, "European guidelines for thermoelastic verification," *ESA*, Mar. 2023. Cited on pp. 14–16.

[4] R. Daniele, "Thermo-elastic verification: evaluation of the new esa guidelines and software with application to a scientific satellite," 2025.

[5] S. Appel, "Slides from "thermo-elastic verification tool getting started"," 2023.

[6] A. García-Pérez, A. Fernández-Soler, G. Morgante, J. Pérez-Álvarez, G. Alonso, L. García-Moreno, A. Scippa, D. Gottini, and R. Lilli, "Temperature mapping methods for thermoelastic analyses of the ariel spacecraft payload module," *Acta Astronautica*, vol. 223, pp. 77–97, 2024.

[7] ESA, *Using Pysinas*, 2024.

[8] ESA, *Using TEV*, 2024.

[9] B. N. Tran, J. van der Kwast, S. Seyoum, R. Uijlenhoet, G. Jewitt, and M. Mul, "Uncertainty assessment of satellite remote-sensing-based evapotranspiration estimates: a systematic review of methods and gaps," 2023.

[10] R. Hogan, "Probability distributions for measurement uncertainty," 2024. ISOBudgets, accessed: 2026-03-04.

[11] U. García Luis, *Thermo-elastic study of the pointing platform for space telescopes*. Phd thesis, Universidad de Vigo, 2023.

[12] D. G. Gilmore, *Spacecraft Thermal Control Handbook: Fundamental Technologies*. The Aerospace Press, 2002.

[13] K. J. Bathe, *Finite Element Procedures*. Prentice Hall, 1996.

[14] W. Nowacki, *Thermoelasticity*. Pergamon Press, 1986.

[15] K. Jenkins and D. Hershfeld, "Thermal/dynamic characterization test of the solar array panel for the hubble space telescope," tech. rep., NASA Goddard Space Flight Center, 1999.

[16] U. Garcia-Luis, A. M. Gomez-San-Juan, A. E. Pelaez Santos, F. Navarro-Medina, P. Gonzalez De Chaves Fernandez, A. Ynigo-Rivera, and F. Aguado-Agelet, "Evaluation of the thermo-elastic response of space telescopes using uncertainty assessment," *ESA*, 2024. University of Vigo.

[17] E. Rosenblueth, "Point estimates for probability moments," *Proceedings of the National Academy of Sciences*, vol. 72, no. 10, pp. 3812–3814, 1975.

[18] H. Xu and S. Rahman, "A generalized dimension-reduction method for multi-dimensional integration in stochastic mechanics," *International Journal for Numerical Methods in Engineering*, vol. 61, pp. 1992–2019, 2004.

[19] A. Pagani, "Slides from "analisi termoelastiche di strutture aerospaziali"," 2023. Cited on pp. 4, 5.

[20] J. Pérez *et al.*, "Temperature mapping techniques for thermo-elastic analysis of spacecraft structures," *Acta Astronautica*, vol. 158, pp. 1–14, 2019.

[21] S. e. a. Shah, "Structural-thermal-optical performance analysis of space systems," *Journal of Spacecraft and Rockets*, vol. 53, no. 4, pp. 721–735, 2016.

[22] A. M. Gómez-San-Juan *et al.*, "Thermo-elastic analysis methodologies for stop applications," *Acta Astronautica*, vol. 170, pp. 399–412, 2020.

[23] U. García-Luis, A. M. Gómez-San-Juan, A. E. Peláez Santos, *et al.*, "Temperature mapping methods for thermoelastic analysis of spacecraft structures," *Acta Astronautica*, vol. 219, pp. 77–97, 2024.

[24] A. M. Gómez San Juan, *Análisis de incertidumbres en sistemas de control térmico en ambientes espaciales*. Phd thesis, Universidad, 2018.

[25] S. Turney, "Probability distribution: Formula, types, and examples," 2022. Revised January 24, 2025.